ABSTRACT

Title of Dissertation: REGULATION OF THE INHIBITORY DRIVE IN THE OLFACTORY BULB

Alexia Nunez-Parra, Doctor of Philosophy, 2013

Dissertation directed by: Dr. Ricardo C. Araneda, Assistant Professor
Department of Biology

Animals are exposed to a variety of odor cues that serve as environmental guides for their exploratory and social behaviors. Two distinct but complementing pathways process chemosensory cues: the Main and the Accessory olfactory System (AOS). Sensory neurons send their axons to the olfactory bulb (OB), specifically to the main and the accessory olfactory bulb (MOB and AOB, respectively) where they synapse onto principal neurons, the mitral (MCs). The OB is the only relay center between sensory neurons and cortical and limbic structures and therefore important aspects of odor processing occur in this region. Specifically, a distinctive mechanism used for olfactory processing is a strict regulation of MCs output by inhibitory neurons called granule cells (GCs).

Importantly, inhibition of MCs is a dynamic process; it is regulated by the constant addition of new GCs to the OB circuit throughout life, in a process

known as adult neurogenesis. Little is known, however, about the contribution of adult born neurons to the processing of olfactory cues, known as pheromones. Detection of pheromones by the AOS is critical for proper display of social behaviors such as hierarchical dominance and mate recognition. Here, we studied how the integration of new-born neurons could be regulated. We found that the arrival of new neurons into the adult AOB increases after animals are exposed to aggression and mate cues, suggesting that these newly arrived neurons can add important plasticity to the AOB circuitry and modify olfactory processing under different behavioral contexts.

In addition, GCs mediated inhibition in the OB is precisely controlled by an extensive centrifugal innervation. For example, cortical feedback projections and neuromodulatory afferents originating in the midbrain and basal forebrain excite GC, inhibiting MCs' and decreasing their output. Regulation of of GCs by inhibition has also been reported, however, the source of this inhibition and its relevance to olfactory processing is not known. Here we characterized inhibitory inputs onto GCs and show that GCs receive extensive inhibition from GABAergic neurons in the HDB/MCPO and from neighboring GCs. Moreover, we show, for the first time, that inhibition onto GCs is required for proper olfactory discrimination.

REGULATION OF THE INHIBITORY DRIVE IN THE OLFACTORY BULB

by

Alexia Nunez-Parra

Thesis submitted to the Faculty of the Graduate School of the
University of Maryland, College Park in partial fulfillment
of the requirements for the degree of
Doctor of Philosophy
2013

Advisory committee:

Professor Ricardo C. Araneda, Chair
Professor Robert Dooling
Professor Jens Herberholz
Professor Elizabeth Quinlan
Professor Matthew Roesh

PREFACE

All electrophysiological experiments were performed by Alexia Nunez-Parra. Behavioral data and cell counting in Chapter 1, were obtained in collaboration with Victoria Pugh. Behavioral data summarized in Chapter 2 was obtained in collaboration with Robert Maurer.

One publication resulted from this work has been published so far:

Alexia Nunez-Parra, Victoria Pugh and Ricardo C. Araneda

Regulation of adult neurogenesis by behavior and age in the accessory olfactory bulb. *Mol Cell Neurosci*. 2011 Aug;47(4):274-85. The (VNS) participates in the detection and processing of pheromonal information related to social and sexual behaviors. Within the VNS, two different populations of sensory neurons, with a distinct pattern of distribution, line the epithelium of the vomeronasal organ (VNO) and give rise to segregated sensory projections to the accessory olfactory bulb (AOB). Apical sensory neurons in the VNO project to the anterior AOB (aAOB), while basal neurons project to the posterior AOB (pAOB). Several studies indicate that the segregation of projections into the AOB serves an important role in pheromonal processing, including the ability to discriminate different blends of odor stimuli. In the AOB, the largest population of neurons are inhibitory, the granule and periglomerular cells (GCs and PGs). Remarkably, these neurons are continuously born and functionally integrated in the adult brain, underscoring their role on olfactory function. Here we explore the possibility that behaviors mediated by the VNS differentially regulate adult neurogenesis across the anterior-posterior axis of the AOB. We used immunohistochemical labeling of newly born cells under different behavioral conditions in mice. Using a resident-intruder aggression paradigm, we found that subordinate mice exhibited increased neurogenesis in the aAOB. In addition, in sexually naive adult females exposed to soiled bedding odorized by adult males, the number of newly born cells was significantly increased in the pAOB; however, neurogenesis was not affected in females exposed to female odors. Furthermore, we found that at two months of age adult neurogenesis was sexually dimorphic, with male mice exhibiting higher levels of newly born cells than females. However, this difference was not observed in older mice, which instead exhibited a decrease in the levels of neurogenesis. The age-dependent decrease in neurogenesis was not due to an increase in cell death but to a decrease in progenitor cell survival. These results indicate that the physiological regulation of adult neurogenesis in the AOB by behaviors is both sex and age dependent.

This work is described in Chapter 2. In my dissertation the term accessory olfactory system (AOS) was used instead of VNS.

Two publications are currently being prepared from data presented in Chapter 3.

Alexia Nunez-Parra, Richard Smith, Robert Maurer and Ricardo C. Araneda

Basal forebrain inhibiton onto granule cells is required for olfactory discrimination in the olfactory bulb. *In preparation.*

Alexia Nunez-Parra and Ricardo C. Araneda

Intrinsic and extrinsic inhibition regulates granule cells' activity in the accessory olfactory bulb. *In preparation.*

To Christian, my greatest source of inspiration

ACKNOLEDGEMENTS

First and foremost, I would like to sincerely thank my advisor and mentor, Dr. Ricardo Araneda. Throughout my graduate studies he has been incredibly supportive and challenging at the same time. Dr. Araneda empowered me to uncover my true scientific potential by promoting a laboratory environment of critical thinking, innovation and thorough experimentation. In addition, I would like to thank my committee members, Dr. Quinlan, Dr. Herberholz, Dr. Roesch, and Dr. Dooling, whose insights and advice were incredibly helpful in the development of this research.

Second, I would like to acknowledge the Araneda Lab. All of the members contributed to create an intellectually stimulating and comfortable work environment. Special thanks to Richard Smith, Krista Krahe, Robert Maurer and Victoria Pugh, for their assistance and feedback in the completion of this project.

Third, I would like to thank my family and friends. My parents, who provided an example of hard work and academic achievements, encouraged me to always follow my dreams. My siblings motivated me to believe in a greater good and work for a better tomorrow.

Finally, I would like to express my deepest gratitude to my wonderful husband, Dr. Christian Cea-Del Rio. His constant emotional support and encouragement made possible to go through these 5 years of intense work. He inspires every aspect of my life. I will be forever grateful for his support.

TABLE OF CONTENTS

LIST OF FIGURES

LIST OF ABBREVIATIONS

ACh	acetylcholine
aAOB	anterior accessory olfactory bulb
aGCL	anterior granule cell layer
AMPA	2-amino-3-(3-hydroxy-5-methyl-isoxazol-4-yl) propanoic acid
AOB	accessory olfactory bulb
AON	accessory olfactory nucleus
APV	(2R)-amino-5-phosphonopentanoate
BrdU	5-bromo-2'-deoxyuridine
C7	ethyl heptanoate
C8	ethyl octanoate
CC	current clamp
ChR	channelrhodopsin
CNQX	6-cyano-7-nitroquinoxaline-2
CNO	clozapine-N-oxide
DDI	dendrodendritic inhibition
DDS	dendrodendritic synapse
d.p.i.	days post injection
DREADD	Designed Receptors Exclusively Activated by a Designed Drug
dSAC	deep short axon cell
E/I	excitation/inhibition
eIPSC	evoked inhibitory postsynaptic current
EPL	external plexiform layer
EPSC	excitatory postsynaptic current

GABA	gamma-aminobutyric acid
GAD	glutamate decarboxylase
GC	granule cell
GCL	granule cell layer
GFP	green fluorescent protein
GL	glomerular layer
GLU	glutamate
HDB	horizontal limb of the diagonal band of Brocca
h.p.i.	hours post injection
IPL	internal plexiform layer
IPSC	inhibitory postsynaptic current
LightStim	light stimulation
LOT	lateral olfactory tract
MC	mitral cell
MCL	mitral cell layer
MCPO	magnocellular preoptic area
MeA	medial amygdala
mGLUR	metabotropic glutamatergic receptor
mIPSC	miniature inhibitory postsynaptic current
MOB	main olfactory bulb
MOE	main olfactory epithelium
MOS	main olfactory system
M/T	mitral/tufted cells
NA	noradrenaline
NMDA	N-methyl-D-aspartate

OB	olfactory bulb
OSN	olfactory sensory neurons
pAOB	posterior accessory olfactory bulb
PFA	paraformaldehyde
PG	periglomerular cell
pGCL	posterior granule cell layer
RMS	rostral migratory stream
sIPSC	spontaneous inhibitory postsynaptic current
SVZ	subventricular zone
TC	tufted cell
TTX	tetrodotoxin
TRPC2	transient receptor potential channel type 2
TUNEL	deoxynucleotidyl transferase-mediated dUTP nick end-labeling
VC	voltage clamp
VNO	Vomeronasal organ
w.p.i.	weeks post injection

CHAPTER 1: BACKGROUND/INTRODUCTION

1.1 Sensory perception and olfaction

A main task of the nervous system is to produce an internal representation of the environment where the animal is immersed in. Information from the external world gates decision making, necessary to elicit behaviors related to survival and reproduction. Sensory cues of the five modalities relevant to mammals (vision, audition, touch, olfaction and taste) activate specialized neurons that transform sensory information into an electric signal. This signal is then relayed by various neurons before it reaches higher processing centers in the cortex. In each step, from the periphery to the final relay station, information is highly modified by feedforward and feedback control mechanisms to produce an accurate sensory perception (Dulac, 2000; Louie & Glimcher, 2012).

The olfactory system is highly tuned to process a complex signal that can consist of a tantalizing number of odor molecules. These odor molecules have diverse physicochemical properties related to their structure; including functional groups, size and volatility, and are found in the environment at concentrations within several orders of magnitude (Buck, 1996). Olfaction is also one of the most ancestral senses and a sophisticated neural circuit has evolved to extract accurate information from odors. The identity of these odor molecules is incredible complex and proper olfactory coding is key to elicit behaviors such as, mating, aggression, parenting, predator identification and food location, among others (Su *et al.*, 2009). Olfactory cues can generally be divided into two different types: common olfactory odors and pheromones. Common volatile

olfactory molecules are usually small and lipophilic (Buck, 1996) and vary in structure ranging from organic (aldehydes, esters, etc.) to non-organic (i.e. ammonia and hydrogen sulfide) compounds. They are present in almost all organic matter found in the environment, including food sources. On the other hand, pheromones are molecules released by an individual to coordinate communication among members of the same species (conspecifics). They are found in urine, saliva, tears and preputial gland secretions, among others (Loebel *et al.*, 2000; Chamero *et al.*, 2007). Pheromones can be small volatile molecules or peptides and proteins, differences that relate to their specific functions. Alarm pheromones, for instance, are volatile to ensure wide dispersion (Lin *et al.*, 2005), while in other scenarios, such as territorial marking, pheromones need to be constricted to one place in space and therefore are more likely to consist of of peptide and proteins (Hurst & Beynon, 2004).

1.2 Functional role of the main and accessory olfactory systems

Humans rely on the main olfactory system (MOS) to process olfactory information, while most mammals, fish and reptiles, exhibit an additional and complimentary system called the accessory olfactory system (AOS). In the MOS and AOS, olfactory molecules interact with olfactory sensory neurons (OSN) in the main olfactory epithelium (MOE) and in the vomeronasal organ (VNO), respectively. Neurons from both epithelial sheets send their axons to specific non-overlapping regions of the olfactory bulb (OB), the main and the accessory olfactory bulb (MOB and AOB, respectively), where they synapse onto principal neurons, the mitral and tufted cells (Fig 1). Unlike other sensory modalities these

principal cells, which provide the only output to the OB, send their axons to higher processing systems, bypassing the thalamus. From the MOB, olfactory information is relayed to the olfactory cortex and brain areas related to olfactory perception and learning (i.e. amygdala).

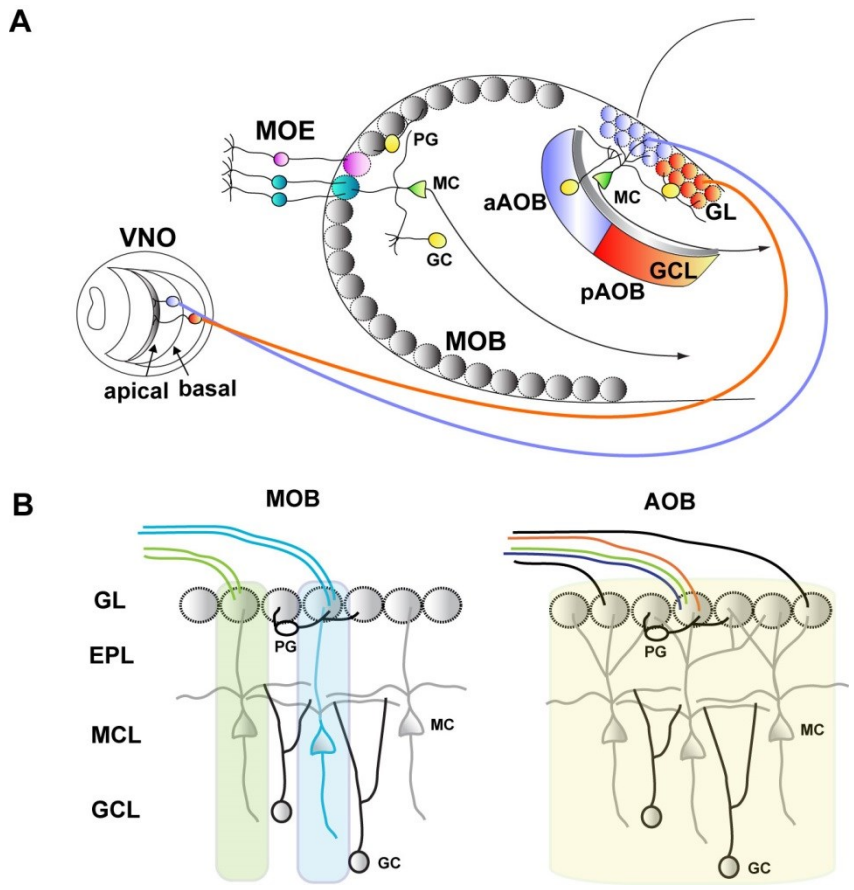

Fig1: **Synaptic organization in the OB**. (**A**) Sensory neurons in the main olfactory epithelium (MOE) project to the glomerular layer (GL) of the main olfactory bulb (MOB). Apical sensory neurons in the Vomeronasal organ (VNO) project to the anterior AOB (aAOB), while neurons in the basal layer of the VNO project to the posterior AOB (pAOB). In both regions, axons of sensory neurons synapse onto mitral cells (MC). Inhibitory neurons, granule cells (GCs) and peroglomerular cells (PGs) are shown in yellow (**B**) In the MOB, information flows in parallel columns; one glomerulus receives synaptic inputs from sensory neurons expressing the same odorant receptor and MCs send their single apical dendrite to only one glomerulus. In contrast, in the AOB, sensory neurons expressing the same receptor project to multiple glomeruli and MCs project their primary dendrites to several glomeruli.

On the other hand, sensory information passing through the AOB is sent directly to the vomeronasal amygdala and from there to the hypothalamus and other areas of the limbic system (Bartoshuk & Beauchamp, 1994; Dulac & Torello, 2003; Keverne, 2004).

Due to their anatomical and central projection differences, for many years the dogma in the field was that the MOS and AOS where functionally distinct. The MOS was thought to interact with volatile odorants conveying information about common odors food, predator location and mate recognition. On the other hand, the AOS, due to its direct link to the reproductive hypothalamus, was associated with pheromonal detection necessary for social communication among conspecifics (maternal and defensive behaviors) and endocrine changes related to reproductive behaviors (Keverne, 2004). This classical view was supported by a series of studies that tested the behavioral output of animals after disruption of either system, or their components (Bartoshuk & Beauchamp, 1994). For instance, ablation of the VNO, but not of the MOE, abolished pregnancy block in female mice. This pregnancy block results when a recently mated female is exposed to odors of a male different to the stud (Bruce, 1959; Rajendren & Dominic, 1985). Removing the VNO also disrupts puberty acceleration of pre-pubertal female mice exposed to male odors (Vandenbergh, 1973; Lomas & Keverne, 1982). In addition, VNO function disruption also reduces lordosis behavior and sexual receptivity in female mice (Rajendren *et al.*, 1990; Keller *et al.*, 2009). In the case of the MOS, lesions of the MOE, have corroborated its role in mate identification (discrimination) and attraction. Intranasal application of

zinc sulfate, which selectively lesions the MOE leaving the VNO intact, abolishes the preference of male and female mice for olfactory cues from the opposite sex. On the other hand, VNO ablation, or lesions in the projections to the AOB, are not effective in eliminating this preference (Keller *et al.*, 2006; Jakupovic *et al.*, 2008). However, challenging this traditional view, more recent data, using genetic ablation of specific genes to the olfactory system has given rise to the notion that the MOS and AOS play a complimentary role in olfactory processing. An elegant approach was taken by Dulac and collaborators, which genetically ablated the TRPC2 channel in mice (Leypold *et al.*, 2002; Stowers *et al.*, 2002). This channel is exclusively expressed in VNO sensory neurons and is hypothesized to mediate sensory transduction in these cells. Interestingly, TRPC2-/- animals failed to display aggressive behavior towards other males and instead engaged sexually with male and females indiscriminately. This evidence suggested that TRPC2 transduction signal is necessary for gender identification but not necessary for the display of sexual behaviors. Albeit, it is worth to mentioning, that TRPC2-/- mice did not exhibit pregnancy block (Kelliher *et al.*, 2006), a behavior for which overwhelming evidence indicates mediation by the AOS, suggesting that other transduction pathways might be activated in the constitutive TRPC2-/- k.o. mice.

Further evidence supporting a complementary role of both systems is the observation that sensory neurons in the MOS can be activated by pheromones. For instance, pheromones secreted by glands in the mother's nipple are crucial to elicit the nipple-search and nipple-attachment behavior in newborn rabbits. Removal of the MOE, but not the VNO abruptly disrupts this stereotyped

behavior (Hudson & Distel, 1986). In addition, androstenone, a pheromone released by male pigs, facilitates the sexual receptivity in sows. This behavior is also mediated by the MOS, as blocking the passage of the pheromones to the VNO had no effect in adrostenone sensitivity (Dorries *et al.*, 1997).

More importantly, the MOS and AOS are interconnected at the level of their central projections. The MOB principal neurons project to several areas in the brain that constitute the primary olfactory cortex, which includes the piriform cortex, olfactory tubercle, anterior olfactory nuclei, entorhinal cortex and lateral part of the cortical amygdala. Tertiary projections in the MOS reach the medial amygdala (MeA) and posteromedial cortical amygdala. The AOB in turn, projects directly to the MeA and posteromedial cortical amygdala, with tertiary projections to the bed nucleus of the stria terminalis, the medial preoptic area and the hypothalamus. Therefore, unlike in the MOS, the AOS bypasses cortical areas (Dulac & Torello, 2003). Interestingly, areas of the MOB that are thought to be activated by volatile pheromones project to the MeA (Kang *et al.*, 2009), suggesting that the amygdala is a site of information convergence for the AOB and MOB. This idea is further supported by evidence showing that the AOB receives feedback projections from the MeA. Thus, some pheromones can activate a MOB-MeA-AOB pathway and regulate MC's activity in the AOB. This synergistic action of the MOS and AOS is thought to increase the salience of cues from the opposite sex and motivate the animal to maintain proximity to the stimulus source (Martel & Baum, 2009). Information processed by both systems also converges at the level of the hypothalamus, specifically, onto gonadotropin

releasing hormone neurons. These neurons also send feedback projections to the MOB and AOB, modulating the excitability of neurons in both regions of the bulb (Keller *et al.*, 2009).

To recapitulate, the evidence discussed above suggests that the MOS and AOS have complimentary roles decoding olfactory information. This does not necessarily mean that there is a redundancy in information processing. Instead, since both olfactory pathways connect to distinct regions of the OB (Fig 1) the signal transmitted from each region (i.e. AOB and MOB) might supply a distinct combinatorial coding to higher brain areas.

1.3 Synaptic organization of the olfactory bulb

Several neuroanatomical and electrophysiological studies have led to the elucidation of the synaptic organization of the OB, the first site where olfactory processing occurs. More than a century ago, Santiago Ramón y Cajal described the exquisite organization of the OB, with well-defined cellular layers and a clear relationship between sensory input and output. The organized neuronal network of the OB has made this region of the brain an ideal model to study neuronal circuitry and connectivity in the context of sensory processing.

Axons from sensory neurons innervate a functional unit called the glomerulus (Fig 1B), an spherical structure formed by the neuropils of the sensory axons and the dendritic tufts of primary dendrites of mitral and tufted cells. Glomeruli are located in the most apical layer of the OB (glomerular layer, GL) and are defined anatomically and functionally by a surrounding group of small inhibitory

interneurons, the periglomerular cells (PGs). This heterogeneous group of cells can release GABA (gamma-aminobutyric acid) or dopamine. PGs project their dendrites to one or two glomeruli and have an axon that can extend laterally, reaching neighboring glomeruli. Another cell type found surrounding the glomeruli are short axons cells (SAs), which are GABAergic and upon activation they can inhibit several glomeruli simultaneously. Together, due to their connectivity within the GL, PG and SA cells are thought to regulate the flow of incoming sensory information accessing downstream circuits.

Mitral and tufted cells provide the sole output of sensory information to higher cognitive brain areas upon activation by glutamate (GLU) released by the OSN axons. Both types of output neurons are glutamatergic and diverge in their synaptic connectivity within the bulb, as well as, in their output projection pattern. In the MOB, mitral cells (MC), are located in a well-defined layer (MCL), and extend a single apical dendrite to the GL and a couple of, radially pointing, lateral or secondary dendrites, into the external plexiform layer (EPL). This regional separation between the apical and secondary dendrites of the MCs, suggests that different type of regulations can occur in the EPL and the GL. On the other hand, the somas of tufted cells (TC) are found scattered through the EPL and MCL. TCs project to distinct regions of the olfactory cortex, different to the main targets of MCs, and are thought to participate in the integration of information from each bilateral OB. In the AOB, the principal neurons cannot be classified as MC or TCs, therefore they are usually referred as M/Ts. These M/Ts are intermingled in a region that resembles the EPL of the MOB (Farbman, 1992).

Nonetheless, for the remaining of this dissertation we will refer to both types of principal neurons, in the MOB and AOB, as MCs. Below the MCL, the internal plexiform layer (IPL) separates MCs from granule cells (GCs). The IPL is a thin layer devoid of cells and filled with axon collaterals and centrifugal feedback fibers. The GCs are the most abundant cell type in the OB. They are axonless GABAergic neurons that extend their dendritic arbor into the EPL, where they establish ubiquitous dendrodendritc synapse with secondary dendrites of MCs (Shepherd, 1972; Levine & Marcillo, 2008). In the GC layer (GCL) an additional interneuron type with a short axon can be found. Some of these interneurons, described as “Blane cells,” are known to produce feedfoward inhibtion of GCs through their axonal projections into the GCL (Pressler & Strowbridge, 2006; Eyre *et al.*, 2008).

1.4 Olfactory coding

As mentioned above, the olfactory system has a remarkable ability to detect and discriminate a large number of odor molecules. While for most sensory modalities the stimulus is arranged along an easily identifiable dimension such a wavelength or spatial orientation, odor molecules are defined by a seemingly dimensionless space. An estimate of this "space" can only be obtained by using multiple variables, including chemical structure and physicochemical properties, such as volatility and solubility. Therefore, to solve the incredible difficult computation necessary for odor processing, the olfactory system has evolved the use of a combinatorial code, which is analyzed at different stages of processing.

OSN in the MOS express olfactory receptors encoded by approximately 1,000 genes, the largest family of G protein coupled receptors known, which can recognize an almost infinite amount of odor mixtures (Buck & Axel, 1991). Interestingly, each OSN expresses only one type of odorant receptor and olfactory neurons expressing the same receptor, project to one or two glomeruli in the MOB (Ressler *et al.*, 1994; Mombaerts *et al.*, 1996). This particular arrangement creates a map in the MOB that corresponds to a neuronal type activated in the MOE by a particular odor (Fig 1B). Moreover MCs in the MOB extend their apical dendrite to only one glomerulus maintaining this map downstream. Therefore, glomerular activity, corresponding to the activity of each type of receptor, must be then integrated in other brain areas, such as the olfactory cortex (Belluscio *et al.*, 1999).

In the VNO, sensory neurons also express one type of odor receptor. VNO receptors, however, belong to two different families of G protein coupled receptors, known as V1R and V2R, which are unrelated to the those found in the MOE (Dulac & Axel, 1995). The VNO epithelium exhibits differences in pheromone receptor expression and segregated axonal projection to the AOB, give rise to anatomical and functional subdivisions of the AOB (Halpern *et al.*, 1995; Jia & Halpern, 1996; Sugai *et al.*, 2006). Sensory neurons in the apical layer of the VNO express V1R receptors and project to the anterior AOB (aAOB), while neurons in the basal layer express V2R receptors and project to the posterior AOB (pAOB) (Herrada & Dulac, 1997; Rodriguez *et al.*, 1999). This particular arrangement of sensory inputs into the AOB suggests that these

subdivisions participate in the processing of pheromonal information related to specific behaviors. For instance, presentation of a diestrus female to a male mice activates neurons in the aAOB (Kumar *et al.*, 1999), whereas male aggressive behavior, exposure of males to female's volatile odors, and the exposure of females to male major urinary proteins induces activation of cells in the pAOB (Brennan *et al.*, 1999; Kumar *et al.*, 1999; Yoshikage *et al.*, 2007). Unlike olfactory receptors in the MOS, VNO receptors are encoded by a much smaller family of about 300 genes (Dulac & Axel, 1995).Therefore, small differences in perception are thought to arise from a more complex spatial interconnection in the first relay of information of the AOS, the AOB. In the AOB, MCs project dendrites to multiple glomeruli and one glomerulus can receive inputs from sensory neurons expressing different type of receptors (Takami & Graziadei, 1990; Belluscio *et al.*, 1999; Wagner *et al.*, 2006). Interestingly, MC dendritic projections are constraint to either the anterior or posterior portion of the AOB, in agreement with the segregated projections from the VNO (Jia & Halpern, 1997). Thus, in the AOS, sensory integration already occurs at the level of the AOB, a task believed to occur in higher cognitive centers (like the cortex) in the MOS (Belluscio *et al.*, 1999).

In addition, neurons in the VNO, unlike other sensory neurons, and sensory neurons in the MOE, do not rapidly adapt to a sensory stimulus, in fact they can spike for about 40 seconds before entering into a silenced state. Recordings in AOB MCs, in freely moving animals, showed that the peak activity responses occurred slower than MC responses in the MOB, and that physical contact was

necessary to trigger MC spiking (Luo *et al.*, 2003). This evidence suggests that the VNO is not suited to detect rapid changes in environmental olfactory information, but rather to identify the more prolonged cues associated with reproductive and sexual behaviors (Keverne, 2004). In general, the cellular organization of the AOB might be primed to identify complex mixture of pheromones, while the MOS could be specialized to be highly sensitive and precise to differentiate between very similar odorant molecule structures (Keverne, 2004).

1.5 Olfactory processing in the OB

Unlikely other sensory systems, such as vision and audition, olfactory information is transmitted from the OB directly to cortical and subcortical structures bypassing the thalamus. This arrangement suggests that processing of information in the OB is necessary for proper sensory representation in higher brain areas (Kay & Sherman, 2007).

The most salient physiological mechanism in olfactory processing in the OB is the precise regulation of MCs' activity by inhibitory interneurons through dendrodendritic synapses (DDS). As mentioned above GCs are the most abundant cell types in the OB, with an estimated proportion 200 GCs for each MC (Shepherd, 1972). Dendrodendritic inhibition (DDI) takes place in the EPL, at DDS between the apical dendrites of GCs and the lateral dendrites of MCs (Fig 2). Activation of a MC by an olfactory stimulus, produces an action potential that propagates to lateral (or secondary) dendrites (Rall & Shepherd, 1968). Activation of MC dendrites releases GLU onto the dendritic spines of a GC,

causing the GC to release GABA back onto the MC. This recurrent or feedback inhibition is mediated by the activation of NMDA (*N*-methyl-D-aspartate) and AMPA (2-amino-3-(3-hydroxy-5-methyl-isoxazol-4-yl) propanoic acid) receptors in GCs and $GABA_A$ receptors in MCs (Jahr & Nicoll, 1982; Isaacson & Strowbridge, 1998; Schoppa *et al.*, 1998). Supporting the notion that DDI occurs solely by local activation of ionotropic glutamate receptors, the blockage of Na^+ gated channels and action potential generation, does not block dendrodendritic inhibition (Jahr & Nicoll, 1982). Furthermore, calcium entry through voltage gated Ca^{+2} channels or NMDA channels has been suggested to trigger GABA release from GCs spines (Chen *et al.*, 2000; Halabisky *et al.*, 2000). In addition, activation of metabotropic glutamatergic receptors (mGLURs) has been shown to also facilitate GABA release from GCs at DDS. In the AOB, for instance, activation of mGLUR1 is critical to the generations of recurrent inhibition (Castro *et al.*, 2007). In the MOB, mGLUR1 expressed in MCs and mGLUR5 expressed in GCs, are known to modulate GCs and MCs excitability facilitating DDI (Dong *et al.*, 2009).

Dendrodendritic communication between MC and GCs can be graded, and this level of complexity is an important component of the neuronal computation required for odor processing. In addition to recurrent inhibition just described, communication between MC and GCs can involve more components of the circuit, in a process known as lateral inhibition.

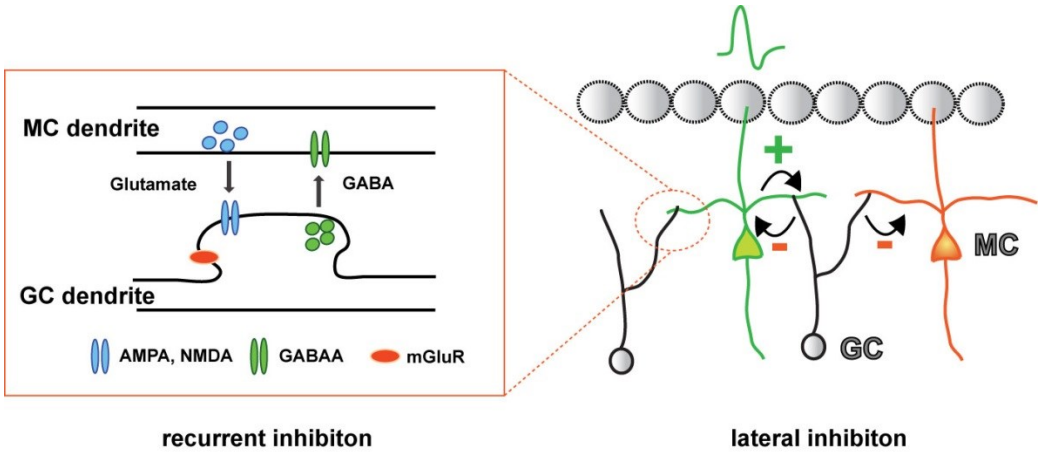

Fig2: **Diagram of a GC-MC dendrodendritic synapse (DDS)**. Glutamate released from a MC acting on metabotropic and ionotropic glutamate receptors (AMPA, NMDA and mGluR) induce release of GABA from GCs. Since a GC project to multiple MCs, the activation of one MC (green) can inhibit other MC (orange) in a process called lateral inhibition.

The degree and extent of DDI between MCs and GCs, will depend on how far an action potential spreads through the secondary dendrite of a MC. It has been shown that these dendrites can extend as far as 1 mm away from the soma of MCs (Shepherd *et al.*, 2007). More importantly, a GC apical dendrite can make DDS with more than one MC; thus, a high level of activation of a GC by a MC can promote extensive depolarization in the GC and release GABA onto neighboring MCs leading to lateral inhibition (Imamura *et al.*, 1992; Shepherd *et al.*, 2007). In each glomerulus, axonal projections of ~5,000 OSN, expressing the same type of odorant receptor synapse onto ~50 MCs (Schoppa & Urban, 2003). This connectivity creates an olfactory code in the OB retained in column-like structures, similar to the ocular dominance columns found in the visual cortex. Due to this arrangement MC's lateral inhibition is believed to play an important role sharpening olfactory signals necessary for fine olfactory discrimination. In a

set of experiments using simple aldehydes of different carbon lengths (2 to 8 carbons), Imamura and collaborators (1992), showed that MCs preferentially responded to one or two molecules of the aldehyde series. Moreover, the same MC exhibited a weaker response to aldehydes with lengths immediately flanking the ones that strongly activated it (Imamura *et al.*, 1992). The weak response to a particular odor in a MC will be overridden by the response of other MCs, in a glomerular-column, that are strongly activated by the same odor. The reduction obtained in the network background noise is thought to sharpen olfactory information coding (Imamura *et al.*, 1992; Yokoi *et al.*, 1995).

1.6 Regulation of OB inhibitory drive

Behavioral and physiological experiments support the idea that modulation of DDI can trigger different forms of olfactory learning (Brennan & Keverne, 1997). It can transform olfactory information, sharpen signals and increase olfactory discrimination by modifying MCs' output (Devore & Linster, 2012). Therefore, to maintain a precise control of odor coding, the inhibitory drive of GCs onto MCs is under extensive regulation. Remarkably, the OB is one of the few regions in the brain that receives a continuous supply of inhibitory neurons throughout life, in a process known as adult neurogenesis (Altman & Das, 1965b; Lois & Alvarez-Buylla, 1993; 1994). Most of the newly born cells arriving into the OB become GCs and only 5% mature into PGs (Petreanu & Alvarez-Buylla, 2002). This amazing feature allows the OB circuit to remain plastic and to be able to modify inhibition of MCs by the addition of new neurons, a process that can be further regulated by learning and experience. Neurons born during development and in

the adult originate from progenitor cells located in the subventricular zone (SVZ) of the brain, from where they migrate to the OB through the rostral migratory stream (RMS), and become functionally integrated within the OB network. However, more than 50% of the interneurons reaching the bulb died before they are successfully incorporated into the GC and GL layer suggesting that integration is a highly regulated process. One possibility is that the integration of this surplus of arriving neurons can be increased or decreased under different physiological conditions (Petreanu & Alvarez-Buylla, 2002).

Functional integration of newborn neurons has been studied using immunofluorescence and electrophysiological techniques. Double immunolabelling for 5-bromo-2'-deoxyuridine (BrdU), a marker of adult born neurons, and the immediate early gene c-FOS, a marker of neuronal activity, has shown that neurons generated in the adult can become active after the animal is exposed to olfactory cues (Magavi *et al.*, 2005). More recenty, other groups have selectively stimulated adult born GCs using optogenetic techniques and showed that they form functional and mature synaptic connections with MCs, but also with neighboring GCs (Bardy *et al.*, 2010). Importantly, the degree of neuronal recruitment of these adult born neurons can be greatly modulated by a number of factors including olfactory stimuli and the activity of afferent modulatory systems, suggesting that adult neurogenesis is regulated in the context of behavioral experience (Lledo & Lazarini, 2007). Some of these factors are also know to regulate adult neurogenesis at other levels, including the proliferation of

progenitor cells in the SVZ and the migration rate of neuroblasts through the RMS.

In addition to a constant supply of interneurons, the OB receives abundant centrifugal projections that regulate GC excitability (Matsutani & Yamamoto, 2008). These afferents include projections from neuromodulatory nuclei and feedback projections from regions of the brain that receive direct inputs from the OB like the olfactory cortex. Our laboratory and others have extensively studied the role of neuromodulation on GCs and has shown that noradrenaline and acetylcholine influence GC excitability (Smith *et al.*, 2009; Devore & Linster, 2012; Zimnik *et al.*, 2013). Moreover, acetylcholine modulation of the olfactory neuronal network facilitates olfactory discrimination (Chaudhury *et al.*, 2009; Hellier *et al.*, 2010; Devore & Linster, 2012). Additionally, the OB receives "feedback projections" from the olfactory cortex and other areas, such as the accessory olfactory nucleus (AON) and the amygdala (Matsutani & Yamamoto, 2008). Most of these cortical projections preferentially target GCs, suggesting that inhibitory the drive in the OB is under important the control of central inputs. Feedback projections from the piriform cortex and AON, for instance, excite GCs increasing DDI between GCs and MCs (Balu *et al.*, 2007; Boyd *et al.*, 2012; Markopoulos *et al.*, 2012).

In addition to excitation, recent studies have suggested that GCs may be under centrifugal inhibitory control. In particular, GABAergic neurons in the basal forebrain, specifically the horizontal limb of the diagonal band of Brocca (HDB) and mangocellular preoptic area (MCPO) have extensive projections to the GC of

the OB (Gracia-Llanes *et al.*, 2010). The HDB/MCPO has been implicated in several physiological functions such as learning and attention, sleep homeostasis and generation of theta rhythms in the hippocampus (Easaw *et al.*, 1997; Sotty *et al.*, 2003; Colom, 2006; Kalinchuk *et al.*, 2008; Zhang *et al.*, 2010; Hasselmo & Sarter, 2011). The electrophysiological and neurochemical properties of neurons in this brain area is very diverse, including cells that exhibit slow, fast and regular spiking, in agreement with the involvement of this region in the regulation of diverse brain functions (Sotty *et al.*, 2003). Two main neuronal types from the HDB/MCPO project to OB: cholinergic and GABAergic neurons (Zaborszky *et al.*, 1986). Direct electrical stimulation of the HDB/MCPO has been shown to either increase or decrease MCs activity (Nickell & Shipley, 1988; Kunze *et al.*, 1992b). Furthermore, it has been suggested that excitation of MCs is mediated by inhibition onto GCs by these centrifugal inputs (Kunze *et al.*, 1992a; Paolini & McKenzie, 1997). Interestingly only 5% of the total neuronal population in the basal forebrain corresponds to cholinergic neurons, while 35% correspond to GABAergic neurons (Gritti *et al.*, 2006). This evidence raises the exciting possibility that GC activity may not only be regulated by excitatory afferent inputs but by afferent inhibitory inputs as well. Thus, GC activity may require a precise balance between excitatory and inhibitory centrifugal inputs that could affect olfactory perception depending on the animal internal state. This has been the historical role associated with other centrifugal inputs to the OB, such as the cholinergic and noradrenergic systems. Here we challenge this view by showing that inhibition can also serve this purpose.

1.7 Specific aims

GC-mediated inhibition onto MCs is essential for proper coding, perception and learning of olfactory information. Therefore, regulation of the inhibition of the OB is strictly orchestrated by a number of factors, which include the unique constant arrival of inhibitory neurons (adult neurogenesis) and modulation of GC activity by centrifugal fibers.

1.7.1 Regulation of adult neurogenesis by behavior and age in the accessory olfactory bulb

The AOS plays an important facilitating role for the execution of several social behaviors including mating and aggression. Notably, chemosensory information associated with these behaviors recruits the activity of GCs in the AOB, suggesting that these behaviors can regulate adult neurogenesis. In the MOS network activity, hence, olfactory stimuli, promotes newborn neurons survival and integration. Yet, despite the important role of the AOS in social communication, little was known about inhibitory recruitment in the AOB and the factors that regulated adult neurogenesis. In the first chapter, I a) characterized adult neurogenesis in the AOB across gender and age and b) studied how behaviors known to be greatly mediated by the VNO could regulate newborn neurons integration.

1.7.2 Inhibitory regulation of inhibitory neurons in the OB

Centrifugal fibers, from neuromodulatory systems and cortical afferents, regulate GC excitability and therefore olfactory processing. Most of these fibers promote excitation of GCs, enhancing inhibition at DDS. Recent evidence

indicates that GABAergic fibers arising from the HDB/MCPO primarily target the GCL of the OB, suggesting that centrifugal inputs inhibit GCs. Moreover, GCs born in the adult brain can also inhibit neighboring GCs, adding an additional source for GC inhibition. In the second chapter of my dissertation, I first characterized GABA inhibitory inputs onto GCs in the MOB. Then, I selectively stimulated, using optogenetic techniques, GABAergic fibers from the HDB/MCPO and adult born GCs, and studied their impact and contribution to GC inhibition. Behavioral studies were performed in which inhibition arising from the HDB/MCPO was silenced to test the role that inhibition of GCs has in decoding olfactory information. Finally, the impact of GABA release from the HDB/MCPO was also studied in GCs of the AOB to detrmine the impact of centrigugal inhibition on AOS mediated chemosensory processing.

CHAPTER 2: REGULATION OF ADULT NEUROGENESIS BY BEHAVIOR AND AGE

2.1 Introduction

The ability to find potential mates and properly identify social status among conspecifics is essential for species survival and largely relies on the detection and recognition of social chemosensory cues by the concerted activity of the main olfactory and vomeronasal systems (Baum & Kelliher, 2009). OSN in the MOE and in the VNO send their axons to specific regions of the OB, the MOB and AOB where they establish their first synapse onto principal neurons, the MCs. In addition, in the VNO, sensory neurons exhibit differences in pheromone receptor expression and segregated axonal projection to the AOB, giving rise to anatomical and functional subdivisions in the AOB (Halpern *et al.*, 1995; Jia & Halpern, 1996; Sugai *et al.*, 2006). Thus, neurons in the apical layer of the VNO express V1R receptors and project to the aAOB, while neurons in the basal layer express V2R receptors and project to the pAOB, (Fig 2A) (Herrada & Dulac, 1997; Rodriguez *et al.*, 1999). This particular arrangement of sensory inputs into the AOB has suggested that these functional subdivisions are involved in the processing of pheromonal information related to species-specific behaviors. For instance, in male mice, presentation of a diestrus female activates neurons in the aAOB (Kumar *et al.*, 1999), whereas male aggressive behavior, exposure of males to female's volatile odors, and the exposure of females to male major urinary proteins induces activation of cells in the pAOB (Brennan *et al.*, 1999; Kumar *et al.*, 1999; Yoshikage *et al.*, 2007).

The most salient physiological mechanism in olfactory processing in the OB is the precise regulation of MCs' activity by inhibitory interneurons. These inhibitory neurons are broadly classified as PGs and GCs. A large population of these neurons correspond to GCs, which produce recurrent and lateral inhibition of MCs through dendrodendritic synapses, shaping their output and thereby playing a fundamental role in olfactory processing (Schoppa & Urban, 2003; Arevian *et al.*, 2008). Remarkably, unlike most neurons in the adult mammalian brain, these inhibitory neurons are continuously born throughout life in a process known as adult neurogenesis (Altman & Das, 1965a; Lois & Alvarez-Buylla, 1993; 1994). Neurons born during development and in the adult originate from progenitor cells located in the SVZ of the brain, from where they migrate to the OB and become functionally integrated within the OB neuronal network. More importantly, the rate of adult neurogenesis can be greatly regulated by a number of factors including olfactory stimuli and the activity of afferent modulatory systems, suggesting that adult neurogenesis is regulated in the context of olfactory behavioral experience (for review see Lledo & Lazarini, 2007).

The AOS plays an important facilitating role in several social behaviors including mating and aggression (Mugford & Nowell, 1970; Bean, 1982; Clancy *et al.*, 1984; Maruniak *et al.*, 1986; Leypold *et al.*, 2002; Stowers *et al.*, 2002;

Norlin *et al.*, 2003). Notably, chemosensory information associated with these behaviors recruits the activity of inhibitory neurons in the AOB, suggesting that these behaviors can regulate adult neurogenesis (Sugai *et al.*, 2006; Yoshikage *et al.*, 2007). Here, we use immunohistochemical labeling of newly born cells to show that social behaviors relying on the activation of the AOS regulate adult neurogenesis in the mouse AOB. We found that adult neurogenesis can be differentially modulated across the anterior-posterior axis of the AOB depending of the type of social stimulus. The induction of aggressive behavior in males, via a resident-intruder paradigm, significantly increased neurogenesis in the aAOB of the intruder. In contrast, naive females exposed to male urine exhibited increased adult neurogenesis in the pAOB. Interestingly, we found that the generation of new neurons in the AOB is sexually dimorphic at one month of age, with males having greater numbers of newly born neurons compared to females. However, this sexual difference is not maintained at later ages and adult neurogenesis dramatically decreases with age in both sexes.

2.2 Methods

Animals. All experiments were performed on C57/BL6 female and male mice (1-6 months old) obtained from breeding pairs housed in the animal colony of the Biology Department of the University of Maryland or obtained from Jackson Laboratories (Bar Harbor, MA). For behavioral experiments, male and female mice were housed either singly or in groups of 3-4 and allowed to acclimate for at least one week prior to the behavioral experiments. Animals were kept on a 12 hr light/dark cycle with food and water *ad libitum* and all experiments were conducted following the guidelines of the IACUC of the University of Maryland, College Park.

Bromodeoxyuridine (BrdU) injection and fixation. To visualize mature newly born cells in the OB, adult mice were injected three times intraperitoneally, every two hours, with BrdU (100 mg/kg) prepared in phosphate-buffered saline (PBS, 10 mg/ml). One month after the BrdU injections, mice were deeply anesthetized with isofluorane (Halocarbon) and the brains fixed by transcardial perfusion with cold PBS, followed by a 4% paraformaldehyde solution (PFA, Electron Microscopy Science) in PBS pH 7.4. To study neuronal proliferation in the SVZ, animals received a single dose of BrdU and were sacrificed 2 hours later. The brains were dissected carefully to avoid any damage to the olfactory bulbs, post fixed in PFA 4% for 4 hrs at 4 °C, and then cryoprotected overnight with a solution of 30% sucrose in PBS. The brains were then embedded in Tissue-Tek O.C.T. (Electron Microscopy Science) and sagittal sections (20 µm) from a randomly chosen hemisphere were obtained using a Leica CM1850 cryostat. The

sections were mounted on frozen tissue slides (Fisher) and stored at –20 °C until use.

Double labeling immunofluorescence. Sagittal sections of the olfactory bulb containing the AOB and MOB were used for immunolabeling. First, the slides were warmed at 55 °C for 10 min, hydrated in PBS for 5 min (two times), and rinsed quickly with ddH_2O. To denature the DNA, the sections were treated with HCl 2N at 37 °C for 1 hr, followed by neutralization with three washes of Na^+ tetraborate buffer (0.1 M, pH 8.5) for 10 minutes. The slides were then washed with PBS, two times for 10 min, and one time with 0.1% Triton X-100 (Sigma Aldrich) in PBS (PBS-T) for 10 minutes. Nonspecific sites were blocked with 10% donkey serum (Sigma Aldrich) in PBS-T for 2 hrs at room temperature (RT). The slices were then incubated with rat anti-BrdU at a dilution of 1:30 (ABD Serotec, MCA2060) or 1:50 (Abcam, ab6325), and mouse anti-NeuN diluted 1:200 (Chemicon International, MAB377) prepared in PBS-T with 2.5% of donkey serum overnight at 4°C. After the incubation with antibodies the samples were washed with PBS-T four times for 10 min and incubated with the secondary antibodies; donkey anti-Rat Alexa-594 (Invitrogen, A-21209) and donkey anti-Mouse Alexa-488 (Invitrogen, A-21202) both diluted at 1:750 in PBS-T with 2.5% of donkey serum, for 2 hrs at RT. The sections were then washed with PBS-T for 10 min followed with three washes with PBS for 10 min. The samples were mounted with Vectashield (Vector Laboratories), visualized with a Leica SP5 X confocal microscope and the images analyzed offline.

TUNEL Staining. To detect cell apoptosis we performed deoxynucleotidyl transferase-mediated dUTP nick end-labeling (TUNEL) assay using the Apoptag fluorescein in situ apoptosis detection kit, following standard protocols (S7110, Millipore, Billerica, MA). The same brains used to quantify the number of BrdU positive cells in the AOB and MOB were used in the TUNEL assay.

Resident-intruder paradigm. To determine the effect of male aggression on adult neurogenesis we used the resident-intruder paradigm. The resident and control groups of male mice were housed individually, while subordinate mice were housed in groups of four. At day 1, residents and subordinates were injected with BrdU. The bedding of the resident's cage was not changed for at least one week prior to the first presentation of the intruder. Fifteen days after the BrdU injection, a randomly chosen intruder was placed into the resident's cage for 15 min, for five consecutive days. Each day, the intruder was exposed to two different residents within an hour period. A group of control mice was housed individually throughout the 30-day period. The interaction was videotaped and analyzed offline blindly. Biting, tail rattling, chasing, cornering, and tumbling were considered as aggressive behaviors while crouching, retreating and freezing were considered submissive behaviors. The aggressive behavior was quantified using different parameters such as attack and defensive posture frequency. The values reported are the average of the data analyzed by at least two different people.

Stress by restraint. To determine the effects of stress on adult neurogenesis, male mice were housed individually for at least one week before the BrdU

injection. Two weeks after the BrdU injection, a cylindrical acrylic tube was placed in the cage and the animal was allowed to walk inside. Once the mouse was inside, the tube's gate was closed and the animal was confined inside the restrainer for 15 min, once a day, for 5 days. After the 15 min period, the mouse was allowed to back out of the tube. The restrainer allowed back and forth movement but not head to tail turns. As a control we used the same individually housed animals as in the resident-intruder paradigm. Mice exposed to restraint showed increased values of serum corticosterone, which has been shown to correlate with stress (control, 106 ± 17 ng/ml, n = 6; restraint, 208 ± 5 ng/ml, n = 3; t-test, $p < 0.006$) (Heinrichs & Koob, 2006).

Exposure of males to social odors. To determine the effect of male social odors in the integration of new neurons, we exposed males to male social odors (urine and bedding). Similar to the resident intruder paradigm (see above) mice were housed individually ("resident group") or in a group of four ("intruder group"). The resident group was exposed to urine extracted from a group of four different males housed also in a group; this was the urine donor group. A cotton swab was embedded in urine from a different male every day and hung from the lid of the cage during 15 min each day for 5 days. Mice from the intruder group, were place alone for 15 min twice a day (for 5 days) in a cage previously soiled by a mouse housed in isolation for at least one week. Every time subordinate mice were exposed to a cage soiled by a different male.

Exposure of female to social odors. To determine the effect of social odor exposure on adult neurogenesis, a group of female mice was exposed to male

odors for 7 days through the use of soiled bedding (Mak *et al.*, 2007). Briefly, two days prior to the beginning of the experiments a male mouse was placed into a cage with clean bedding and the cage bedding was changed every two days. To expose females to male pheromones, on day 1 the female group was placed into a cage that contained the soiled bedding that had been previously odorized for two days by a male as described above (Fig 4A). Every other day the bedding of the cage housing the females was replaced by the bedding soiled by the same male and this procedure was repeated until the end of day 7; on this day, control and experimental mice were injected with BrdU. The control group consisted of females exposed to clean cage bedding (i.e. not odorized) that was replaced every other day as in the experimental group. Another group of females was exposed to cage bedding soiled by a female, following the same schedule of exposure as the one used for the male odor exposure. Only females that presented regular estrous cycles were chosen for these experiments (18 out of 19 females). The estrus cycle was determined by microscopic inspection of vaginal smears obtained daily between 9 and 11 am.

Quantitative and Statistical analysis. One in six serial sagittal sections containing the AOB were used for quantification and three to six sections were counted per animal. The numerical density was calculated using the optical dissector method (Mayhew & Gundersen, 1996). Confocal Z-stack images were captured at 3 μm optical steps using a 63X oil immersion objective. For each section we obtained 2 to 4 Z-stack images of the granule cell and glomerular layers (GCL and GL, respectively) in the AOB and MOB. All images were blindly

analyzed and only BrdU positive (BrdU+) cells in which the nucleus was clearly labeled were included in our analysis. For TUNEL quantification, the sections were co-stained with anti-Dioxigenenin-Fluorescein antibody and the nuclear staining TOPRO, and only the cells that exhibited colocalized labeling were considered for analysis. For each region (total and subdivisions of the AOB) data are expressed as the mean number of BrdU+ cells normalized to the area of the Z-stack in mm^3 (BrdU+ cells/ mm^3) ± S.E. (standard error). Total cell density was calculated manually using sections stained with the nuclear dye TOPRO-3 (Invitrogen). The AOB volume was estimated through the Cavalieri principle using the following formulas; $Vol(i)=T*\sum Ai$ with $A(i)=\sum P*d^2$, where T= number of slices*t (Mandarim-de-Lacerda, 2003). For these calculations we used low magnification sections (10X) with a thickness (t) of 20 μm. The area (A) was measured by placing over the sections a grid of squares with distance (d) between lines and then counting the total number of points (P, intersections) that fell inside the region of interest. To quantify proliferation in the subventricular zone, four coronal sections were collected from a region of 1420 μm that started at the opening of the left ventricle and continued towards the caudal end. Values shown correspond to the average of all the BrdU+ cells counted in all four sections. To test for statistical significance, we used the t-test and one-way ANOVA, followed by the Bonferroni and Tukey's multiple comparison tests (SPSS 18.0 software). One animal (out of 84) was excluded from the analysis as the value of BrdU+ cells/ mm^3 exceeded the value of the mean ± 2SD (standard deviation) of its respective group.

2.3 Results

2.3.1 Adult neurogenesis in the accessory olfactory bulb in juvenile mice is sexually dimorphic.

Anatomical and physiological evidence indicate that in several species the AOS is sexually dimorphic (Dawley & Crowder, 1995; Herrada & Dulac, 1997; Segovia *et al.*, 1999; Peretto *et al.*, 2001; Segovia *et al.*, 2006), suggesting that adult neurogenesis could be differentially regulated in the AOB of male and female mice. To address this possibility we first determined the level of adult neurogenesis in the AOB of sexually mature and juvenile mice. To this end, one-month old mice were injected with BrdU, a marker that is incorporated into the DNA of dividing cells, and labeled neurons in the AOB were quantified 30 days after the BrdU injection. Previous studies have indicated that after one month, newly born neurons have already differentiated into mature GCs and PGs within the MOB (Petreanu & Alvarez-Buylla, 2002; Belluzzi *et al.*, 2003; Carleton *et al.*, 2003; Lledo *et al.*, 2006).

In sagittal sections of the mouse brain, the AOB is located in the dorso-posterior region of the OB and can be clearly distinguished from the MOB (Fig 1A). In the AOB, the MC and the GCL are separated by fibers of the lateral olfactory tract (LOT), whereas the GL faces the ventral prefrontal cortex (Fig 1A, top right). Mature neurons were recognized by detecting the presence of NeuN, a nuclear marker that is present in post-mitotic and terminally differentiated neurons (Mullen *et al.*, 1992)

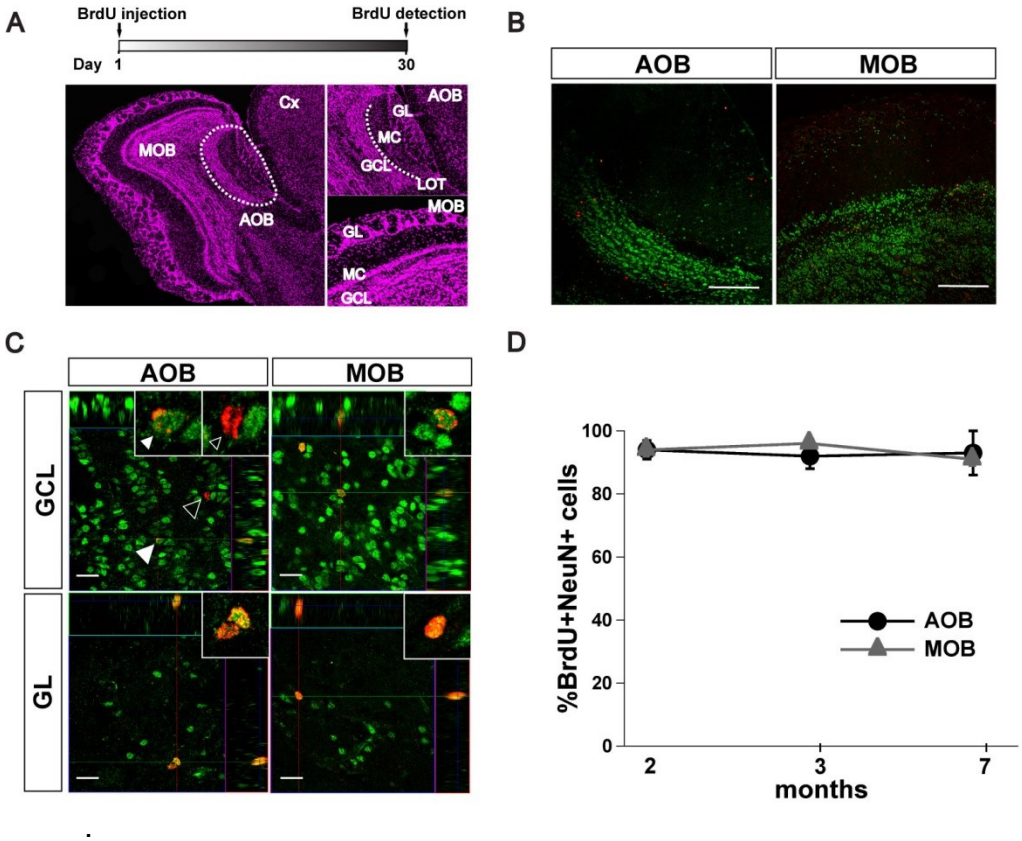

Fig 1: **Adult neurogenesis in the AOB.** (**A**) Top, experimental design used to quantify adult neurogenesis; immunoreactive cells were counted in sagittal sections of the OB one month after the BrdU injections (see methods). Left picture, reconstruction of an OB slice stained with TOPRO-3 nuclear staining to show the cellular distribution in the AOB and MOB, using low magnification confocal images (10x). The AOB is located in the dorso-posterior region of the OB (dotted line). Right pictures, higher magnification of the AOB (top) and MOB (bottom) showing the distinct cellular layers analyzed for the presence of BrdU positive (BrdU+) cells. In the AOB the LOT separates the MCL from the GCL (dotted line). (**B**) Low magnification confocal image (10x) of a section double labeled with BrdU (red) and NeuN (green) antibodies (scale bar, 100µm). The AOB and MOB exhibit abundant NeuN labeling in the GCL with scattered BrdU labeling. (**C**) Orthogonal view of higher magnification images of the GCL and GL in the AOB (left) and in the MOB (right) in double stained sections (63x; scale bar, 20 µm). Left top panel, representative section of the GCL in the AOB showing a cell positive for both BrdU and NeuN (filled white arrow) and a cell positive for BrdU only (empty arrow, see also inset). Similar labeling pattern is observed in the MOB (right panels). (**D**) Summary graph showing the quantification of the total number of BrdU+ cells that were also positive for NeuN in the AOB and MOB at difference. At all ages tested, most of the BrdU+ cells are also NeuN positive.

As shown in Fig 1B we found abundant NeuN staining in the AOB and MOB, especially in the dense GCL. Confocal imaging analysis revealed abundant BrdU positive (BrdU+) cells throughout the GCL and GL in the AOB and MOB (Fig 1C). The pattern of nuclear staining with BrdU was variable; some cells exhibited a punctuated pattern while other cells exhibited a more uniform staining pattern (Fig 1C). Nevertheless, confocal analysis revealed that at all ages the majority of the new cells present in the adult AOB were indeed neurons, since most of the cells that were BrdU+ also stained for NeuN (2, 3 and 7 months; 94 ± 3%; 92 ± 4%, 93± 8%, respectively; n=3 per group, Fig. 1D). Similarly, as previously described most cells in the MOB also exhibited an overlapping staining pattern for BrdU and NeuN at all ages tested (2, 3 and 7 months; 94 ± 2%; 96 ± 1%, 91± 2%, respectively; n=3 per group) as previously reported (Rochefort *et al.*, 2002; Alonso *et al.*, 2006; Mak *et al.*, 2007; Mouret *et al.*, 2009; Veyrac *et al.*, 2009).

Interestingly, at two months of age the level of adult neurogenesis was significantly different between male and females (Fig 2B). We found that the total number of BrdU+ cells in the AOB was ~40 % higher in males than in females (males, 2782 ± 373, n = 5; females 1704 ± 186, BrdU+ cells/mm^3, n = 6; t-test, $p < 0.03$). Sensory projections from the VNO exhibit a divergent pattern of distribution across the anterior-posterior axis of the AOB, suggesting that these regions may process different chemosensory information (Fig 2A). Therefore, we determined whether the sexual dimorphism in adult neurogenesis observed at this age was also expressed along the anterior-posterior axis. As shown in Fig

2B, two-month old male mice exhibited a significantly higher number of BrdU+ cells in the pAOB compared to females (males, 2748 ± 406, n = 6; females, 1493 ± 135 BrdU+ cells/mm^3, n = 6; t-test, $p < 0.02$). The number of newborn neurons found in the aAOB was also higher in males compared to females, but this difference did not reach statistical significance within our sample (males, 2817 ± 507; females, 1914 ± 307 BrdU+ cells/mm^3; t-test, $p > 0.15$). In contrast, we did not observe gender differences in the number of BrdU+ cells in the MOB (males, 6171 ± 406, n = 5; females, 5965 ± 380 BrdU+ cells/mm^3, n = 6; Fig 2B). The observed gender difference in neurogenesis along the anterior-posterior axis of the AOB could be due to other factors including differences in the number of cells or volume in these two regions. However, as shown in Fig 2C, the total number of cells was not different between males and females (males, aAOB, $529x10^3$ ± $18x10^3$, pAOB, $517x10^3$ ± $32x10^3$ cells/mm^3; females, aAOB, $614x10^3$ ± $47x10^3$; pAOB, $564x10^3$ ± $27x10^3$ cells/mm^3, n = 3 both). Likewise, the sexual dimorphism in adult neurogenesis is not due to differences in volume between the anterior and posterior subdivisions of the AOB (males, aAOB, $58x10^6$ ± $2x10^6$, pAOB, $52.7x10^6$ ± $2x10^6$; females, aAOB, $57.7x10^6$ ± $12x10^6$; pAOB, $57.7x10^6$ ± $11x10^6$ μm^3; n = 3 both).

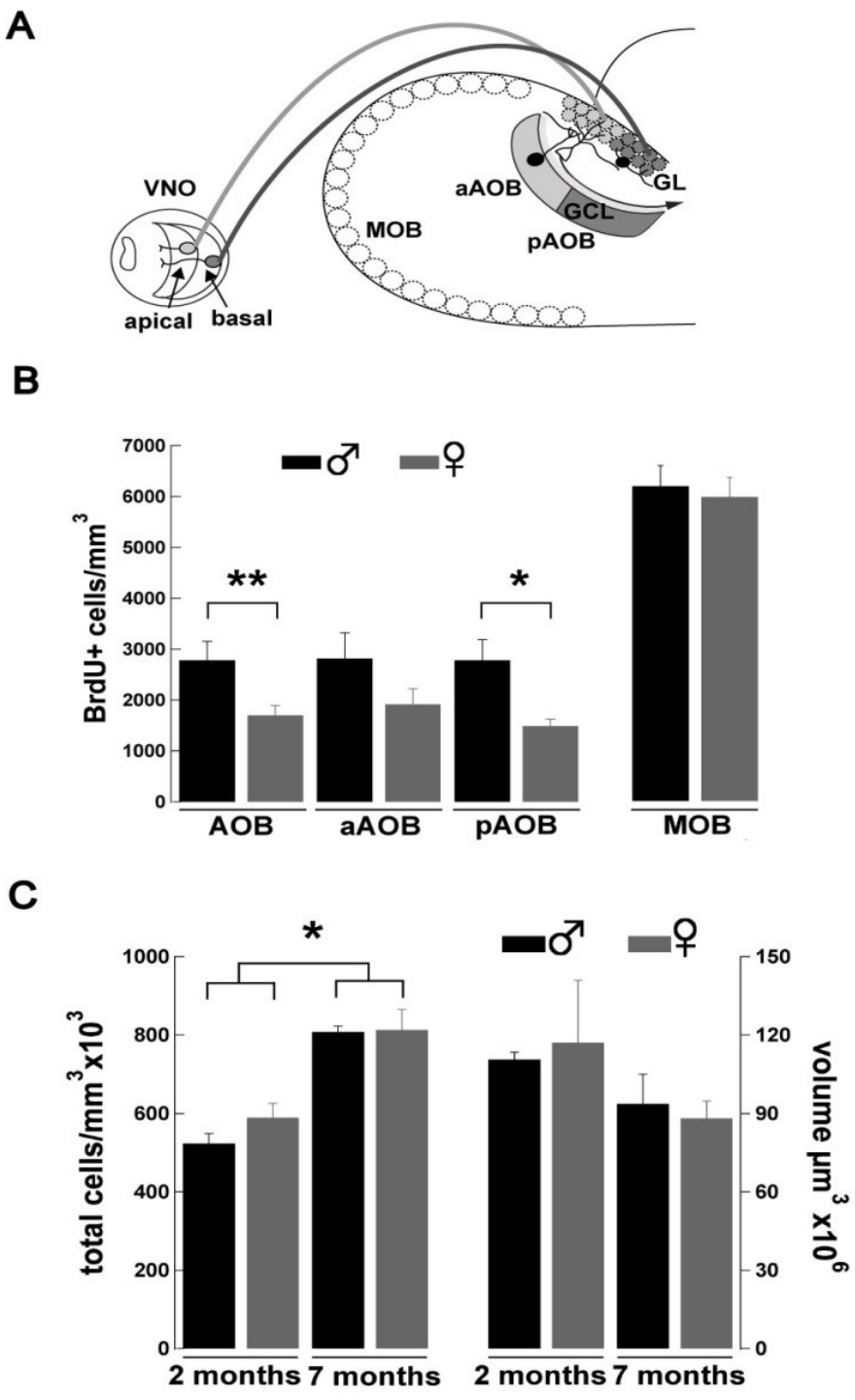

Fig2: **Adult neurogenesis in the AOB is sexually dimorphic.** (**A**) Diagram showing the sensory projections from the VNO to the AOB. Apical sensory neurons in the VNO (light gray) project their axons to the aAOB while basal sensory neurons project their axons to the pAOB (dark gray); in the AOB sensory neurons make their first synapse onto dendrites of MCs (unfilled cell). Adult-born neurons are found in the GCL and in the GL and they are shown in black. (**B**) Graph bar showing the total number of BrdU+ cells in the AOB, and its subdivisions, in two-months old male (black) and female (grey) mice. The number of BrdU+ cells is significantly higher in the pAOB of males compared to female mice (t-test,*,$p<0.03$,**,$p<0.02$). The total number of BrdU+ cells in the MOB is not different between male and female mice. (**C**) The total number of cells (cells/mm^3) and total tissue volume (μm^3) is not different between genders or in the anterior-posterior axis of the AOB.

2.3.2 Adult neurogenesis in the AOB decreases with age.

Olfactory dysfunction is a common pathology reported by the elderly population and is one of the first symptoms manifested by people suffering from neurodegenerative diseases (Kovacs, 2004). The decline in the number of new neurons arriving to the MOB has been suggested as a possible mechanism underlying the decrease in olfactory discrimination related with aging (Enwere *et al.*, 2004), yet a similar age-dependent decrease in adult neurogenesis in the AOB has not been examined. Accordingly, we determined the number of BrdU labeled cells at two, three and seven months of age, in male and female mice, injected one-month earlier. As shown in Fig 3A, we found a significant decrease in the number of BrdU+ cells at three and seven months compared to the number of cells at two months. At three months the number of BrdU+ cells in males was decreased by 70%, while at seven months it was decreased by 90% (two months, 2782 ± 373, n = 5; three months, 825 ± 194, n = 6; seven months, 258 ± 102 BrdU+ cells/mm^3, n = 5; ANOVA, $F_{(2,13)}$= 27.9 $p < 0.001$; Tukey HSD 'two vs. three months' and 'two vs. seven month' $p < 0.001$). In females, at three months the number of BrdU+ cells was decreased by 63%, while at seven months it was decreased by 99% (two months, 1704 ± 186, n = 6; three months, 640 ± 140, n = 6; seven months, 22 ± 22 BrdU+ cells/mm^3, n = 5; ANOVA, $F_{(2,14)}$= 34.6 $p < 0.001$; Tukey HSD 'two vs. three months' and 'two vs. seven month' $p < 0.001$). Nevertheless, despite this age-dependent decrease in neurogenesis, the total cell density in the AOB was higher at seven months than at two months in both males and females (male, two months, $523x10^3 \pm 25x10^3$; seven months,

$808x10^3 \pm 14x10^3$ cells/mm^3; female, two months $589x10^3 \pm 36x10^3$; seven months, $813x10^3 \pm 52x10^3$ cells/mm^3, n = 3 both; t-test, $p < 0.025$, see methods). However, we did not observe sex differences in the total number of cells at these ages. Similarly, the volume in the AOB was not different at these ages or between sexes (males, two months, $111x10^6 \pm 3x10^6$; seven months, $94x10^6 \pm 11x10^6$ μm^3; females, one month, $117\ x10^6 \pm 24x10^6$ μm^3; seven months, $88x10^6 \pm 7x10^6$ μm^3). Interestingly, the sexual dimorphism in adult neurogenesis at two months was not preserved in older animals (Fig 3A), suggesting that sexual dimorphism in juvenile mice could arise from an age-dependent physiological process rather than simple anatomical differences among sexes. Furthermore, in agreement with previous studies, we found an age-dependent decrease in adult neurogenesis in the MOB which affected both genders (males, two months, 6171 ± 406, n = 5, three months, 2796 ± 503, n = 6, seven months, 1041 ± 306 BrdU+ cells/mm^3, n = 5, ANOVA, $F_{(2,13)}= 34.7$ $p < 0.001$; Tukey HSD 'two vs. three months' and 'two vs. seven month' $p < 0.001$; females, two months, 5965 ± 380, n = 5, three months, 2848 ± 459, n = 6, seven months, 1036 ± 261 BrdU+ cells/ mm^3, n = 5; ANOVA, $F_{(2,14)}= 40.3$ $p < 0.001$; Tukey HSD 'two vs. three months' and 'two vs. seven month' $p < 0.001$).

To determine whether the decline in the number of new neurons in the adult AOB was due to a decrease in neuronal integration or a diminished number of neuroblasts being generated in the SVZ, we studied neuronal proliferation at 2 and 6 month of age, which coincides with the time when the animals used in our studies received the BrdU injections. As shown in figure 4A (top panel), we found

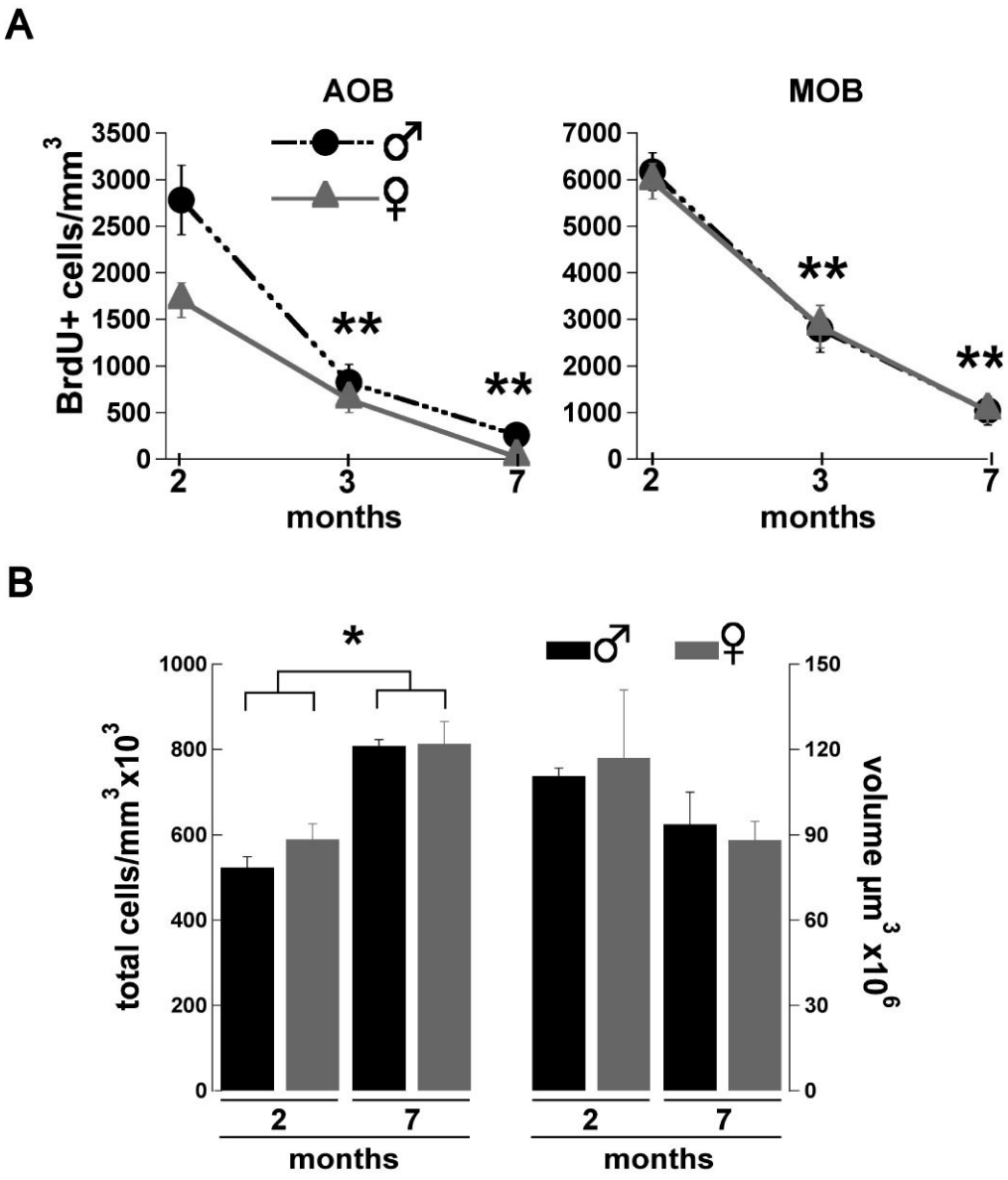

Fig3: **Adult neurogenesis in the AOB decreases with age**. (**A**) Number of new neurons in the AOB and MOB in mice injected at one, two or six months of age and analyzed one month post-injection. In male (black circles) and female (grey triangles) mice the number of BrdU+ cells is significantly decreased at 3 and 7 months compared with 2 months (Females, one-way ANOVA, $F_{(2,14)}$=34.6 p<0.001; Tukey HSD 'two vs. three months' and 'two vs. seven month'; males, ANOVA, $F_{(2,13)}$= 27.9 p<0.001; Tukey HSD 'two vs. three months' and 'two vs. seven month';**, P< 0.001). In the MOB the number of BrdU+ cells is not different between male and female mice at any age group. (**B**) Total number of cells (cells/mm^3) and total tissue volume (µm^3) in the AOB of male (black bars) and female (gray bars) at 2 and 7 months. The number of cells at 7 months is significantly higher in both male and females (t-test; *, p<0.025) but there is no difference in AOB volume.

that the SVZ of 6-month-old mice exhibited a decrease in the number of BrdU+ cells compared to the 2 month-old animals. The quantification (Figure 4A, bottom panel) showed a significant decreased in the number of BrdU+ cells in both males (two months, 521 ± 27; six months 352 ± 45 BrdU+ cells; n=4, t-test, $p<0.03$) and females (two months, 597 ± 80; six months 367 ± 50 BrdU+ cells; n=4, t-test, $p<0.05$).

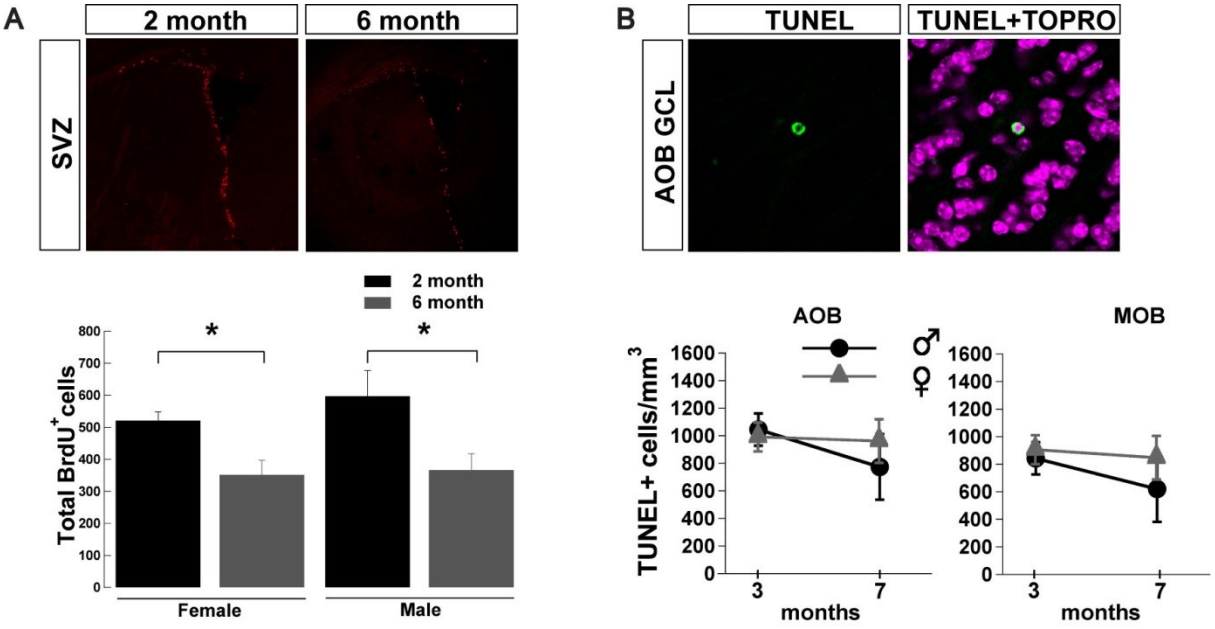

Fig4: **The age-dependent decline in adult neurogenesis is due to a decrease in SVZ proliferation and not an increase cell death in the OB**. (**A**) Top panel, coronal sections immunolabeled with BrdU antibody. The SVZ of older mice (left) exhibited significantly fewer BrdU+ cells than younger mice (right). Bottom panel, the decline in BrdU+ cells was significant in females and males (* $p<0.05$). (**B**) Top panel, TUNEL staining of an apoptotic cell in the GCL of the AOB. Bottom panel, number of TUNEL+ cells/mm^3 in male and female mice at different ages in the AOB and MOB; there was not a significant difference between ages in the OB.

This age-dependent decreased in adult neurogenesis could be due to an increase in cell death of cells arriving into the AOB in older mice. To explore this possibility, we quantified the number of apoptotic cells in the OB one month after BrdU injection using the TUNEL assay (Figure 4B, top panel). We found no difference in the number of apoptotic cells between males and females at 3 and 7 months of age in the AOB (males, three months, 1045 ± 118, n = 4, seven months, 774 ± 238, n = 4; females, two months, 992 ± 105, n = 4, seven months, 962 ± 158 TUNEL+ cells, n = 4) or in the MOB (males, three months, 843 ± 114 cells, n = 4, seven months, 620 ± 261, n = 4; females, two months, 906 ± 334, n = 4, seven months, 847 ± 339 TUNEL+ cells, n = 4).

2.3.3 Adult neurogenesis in the AOB can be differentially regulated by behavior.

The activity of the AOS is crucial for social behaviors such as identifying and attracting mates and discerning the social status of conspecifics (Dulac & Torello, 2003). Several of these behaviors involve olfactory learning, which is thought to result from synaptic plasticity within the neuronal network of the OB, and adult neurogenesis provides an exciting mechanism for this plasticity (Keverne, 1995; Lledo & Lazarini, 2007). To explore the possibility that activation of the AOB circuitry during aggressive behaviors could regulate integration of adult-born neurons, we subjected male mice to a resident-intruder paradigm two weeks post injection of BrdU (Figure 5A, top panel). Offline analysis of the videotaped interactions indicated that all mice exhibited the expected dominant (resident) and subordinate (intruder) behavior throughout the entire experiment.

However, as previously described (Mitra *et al.*, 2006; Rodriguez-Alarcon *et al.*, 2007), resident mice showed a significant decrease in the attack frequency over the 5 days of the trials (day 1, 13 ± 2; day 5, 8 ± 2; n = 6, t-test, $p < 0.05$), while the intruders showed a decrease in defensive posture frequency (day 1, 13 ± 3. s; day 5, 6 ± 2 s; n = 4, t-test, $p < 0.05$). Nevertheless, we found that male mice exposed to aggression exhibited a region-specific increase in neurogenesis that was limited to the aAOB. As shown in Fig 5A, male intruders had a significant increase in the number of new neurons in the aGCL compared to individually-housed controls (intruder, 2594 ± 209, n = 4; control, 1210 ± 346, BrdU+ cells/ mm^3, n = 4; t-test, $p<0.015$). The number of new neurons in the aGCL of the residents was higher than in control mice, but within the sample analyzed this difference was not statistically significant (resident, 2289 ± 365 BrdU+ cells/ mm^3, n = 6; t-test $p < 0.08$). Surprisingly, the resident-intruder paradigm also induced changes in neurogenesis in the MOB (Fig 5C). Likewise the AOB, the increase in neurogenesis was circumscribed to the GCL, however, unlike the AOB, both subordinates and dominant males exhibited a significant increase in neurogenesis (control, 5340 ± 268, n = 4; resident, 7158 ± 595, n = 6; intruder, 7448 ± 409 BrdU+ cells/ mm^3, n = 4; t-test 'control vs. intruder' $p < 0.05$, 'control vs. resident' $p < 0.05$). Recently it has been shown that a protein component in urine promotes male-male aggression (Chamero *et al.*, 2007), therefore we wondered whether the exposure of males to male odors such as male bedding or urine would be a sufficient stimulus to promote adult neurogenesis in the AOB. To examine this possibility we exposed intruders to bedding soiled by a dominant

male and resident males to urine collected from group-housed males. Interestingly, we found that in the intruder mice, but not the resident, these odor stimuli increased the integration of new neurons in both regions of the AOB GCL compared to controls (intruder, aGC, 3835 ± 980;n=3, t-test, $p<0.04$; pGC, 3286 ± 534 BrdU+ cells/ mm^3; n=3, t-test, $p<0.009$; resident, aGC 1070 ± 837; n=3, t-test, p=0.87; pGC, 1301 ± 163 BrdU+ cells/ mm^3, n=3; t-test, p=0.78). Surprisingly, the same stimulus did not affect the integration of newly born neurons in the MOB of the resident or the intruder mice (intruder, 5955 ± 2146;n=3, t-test, p=0.075; resident, 5613± 1775 BrdU+ cells/ mm^3; n=3, t-test, p=0.87).

The resident-intruder paradigm has also been used to elicit stress in mice (Yap *et al.*, 2006), therefore stress could have affected adult neurogenesis in our aggressive behavior paradigm. To explore this possibility, male mice were exposed to stress by restraint, using a similar exposure regime as was used in the aggression protocol (Fig 5B, top panel).

Noticeably, the stress paradigm did not influence adult neurogenesis in the GCL of the AOB (Fig 5B bottom; control, aGCL, 1210 ± 346, pGCL, 1228 ± 173 BrdU+ cells/ mm^3, n = 4; stressed, aGCL, 1502 ± 329, pGCL, 730 ± 204 BrdU+ cells/ mm^3, n = 6). Similarly, there was no difference in adult neurogenesis in the GCL of the MOB in mice subjected to the stress paradigm (Fig 5C; control, 5340 ± 268, n = 4; stressed, 4241 ± 397 BrdU+ cells/ mm^3, n = 6).

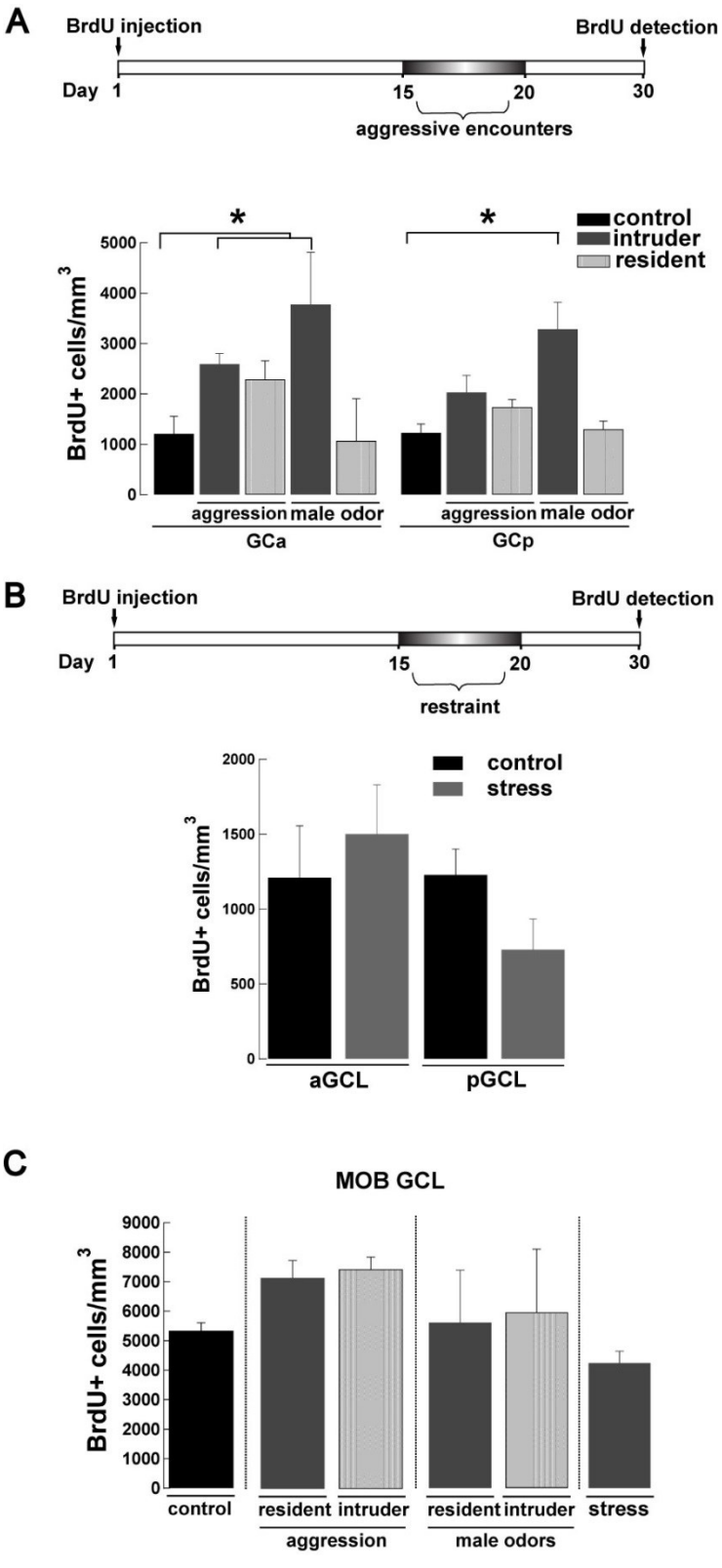

Fig5: **Aggression, but not stress increases adult neurogenesis in the AOB of male mice.** (**A**) Top panel, experimental design used for the resident-intruder aggression paradigm. Male mice are injected with BrdU at day 0 and from day 15 to day 20 the resident is exposed to a daily encounter of 15 minutes with an intruder. Neurogenesis is quantified 10 days later. A control group of male mice is singly housed but not exposed to any intruder. Bottom panel, number of BrdU+ cells in the GCL of the AOB in control (black), resident (dark grey) and intruder males. The intruder showed a significant higher number of BrdU+ cells in the anterior GCL (aGCL) when exposed to aggression and throughout the GCL when exposed to bedding soiled by a male (t-test,* $p<0.05$). (**B**) Top panel, experimental design used for the stress by restraint paradigm. At day 0 male mice were injected with BrdU and from day 15 to day 20, each animal was restrained daily for 15 min and neurogenesis was quantified at day 30. Bottom panel, stress by restraint did not produce a significant change in the number of BrdU+ cells in the GCL of the AOB (anterior and posterior). (**C**) Males exposed to aggression (resident and intruders) showed an increased number of BrdU+ cells in the GCL of the MOB (t-test,* $p<0.05$). This increase in BrdU+ cells was not observed in resident or intruders exposed to male odors. As in the AOB animals exposed to stress showed no significant difference between the control and treated group.

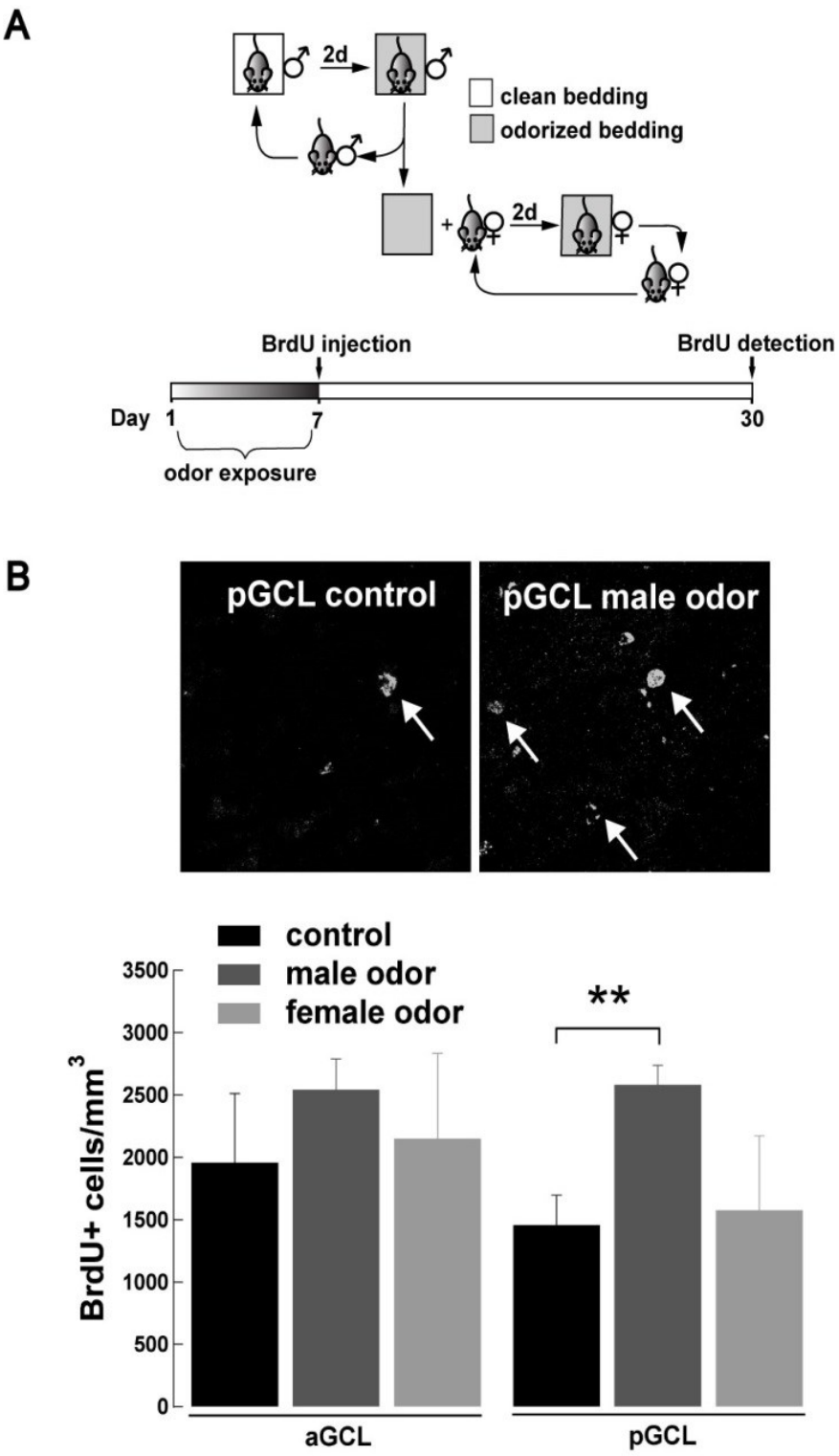

Fig6: **Adult neurogenesis in the AOB increases in females exposed to male odors**. (**A**) Diagram of the experimental paradigm used for odor exposure. Female mice are placed for seven days in a cage containing bedding previously soiled by a male. Every other day the soiled bedding is changed for new soiled bedding from the same male to continuously expose females to male odors. Mice are injected with BrdU on the last day of the odor exposure (day 7) and neurogenesis quantified at day 30. (**B**) Representative confocal images of BrdU+ cells in the GCL of the pAOB. Female mice exposed to male odors (right) show a larger number of BrdU+ cells in the GCL of the pAOB (white arrows) than control females that were exposed only to clean bedding (left). (**C**) Number of BrdU+ cells in the GCL of the aAOB and pAOB in female exposed to male (dark grey) or female odors (light gray). A group of control females was exposed only to clean bedding (back). Female mice exposed to male-soiled bedding exhibit a significantly greater number of BrdU+ cells in the anterior GCL (ANOVA 'pGCL' $F_{(2,15)}$=8.23 p<0.005; Dunnett,**, p<0.004).

Hormonal changes associated with pregnancy and male odor exposure, regulate the proliferation of new neurons in the SVZ (Segovia *et al.*, 1999; Mak *et al.*, 2007; Larsen *et al.*, 2008). Thus, to further support our hypothesis that social odors known to influence the activity of the AOB can regulate adult neurogenesis, by increasing proliferation, we exposed naïve females to male odors. Females were exposed soiled bedding odorized by a male (Fig 6A, top) for seven days, and subsequently injected with BrdU. A group of control females was exposed only to clean bedding. After the odor-exposure paradigm, animals were injected with BrdU and BrdU+ cells were quantified at day 30 (Fig 6A, bottom). We found that a seven days exposure to male odors greatly enhanced neurogenesis in the AOB of females in a region specific manner. As shown in Fig 6B, females exposed to male odors exhibited a differential increase in the number of new neurons in the GCL of the pAOB compared to control females (odor-exposed, 2583 ± 154, n = 8; control, 1456 ± 240 BrdU+ cells/ mm^3, n = 7; ANOVA 'pGCL' $F_{(2,15)}$= 8.23 $p < 0.005$; Dunnett $p < 0.004$). In contrast, the increase in neurogenesis was not present in females exposed to female odors, suggesting that this effect was gender specific (Fig 5B; 1576 ± 597 BrdU+ cells/ mm^3, n = 3). Interestingly, as previously shown (Mak *et al.*, 2007) a similar effect was observed in the MOB, where females exposed to male but not to female odors exhibited an increase in the number of BrdU+ cells in the GCL (control, 6563 ± 574, n = 7; females exposed to male odors, 8463 ± 252, n = 8; females exposed to female odors, 7710 ± 1213 BrdU+ cells/ mm^3, n = 3; one-way ANOVA 'MOB GCL' $F_{(2,15)}$= 4.99 $p < 0.03$; Dunnett $p < 0.02$).

2.4 DISCUSSION

The generation of new neurons in the adult persists throughout life in two areas of the brain, the OB and the hippocampus (Altman & Das, 1965b; Lois & Alvarez-Buylla, 1994; Ming & Song, 2005; Lledo *et al.*, 2006). In the MOB, the generation of neurons in the adult plays an important role in olfactory-dependent behaviors, although the mechanisms underlying the replacement of neurons has not been fully elucidated (Lledo & Saghatelyan, 2005; Lledo *et al.*, 2008; Zhao *et al.*, 2008; Gheusi *et al.*, 2009). Adult neurogenesis is regulated by several physiological conditions and behaviors, including odor enrichment, mate choice, pregnancy and aging (Rochefort *et al.*, 2002; Shingo *et al.*, 2003; Lemasson *et al.*, 2005; Mak *et al.*, 2007; Bovetti *et al.*, 2009). Here we show that adult neurogenesis is regulated by social behaviors in the AOB, a region of the OB involved in pheromonal communication. Aggressive behavior in males and exposure of females to male odors increased adult neurogenesis in a zone-specific pattern in the AOB. In addition, we found that neurogenesis is sexually dimorphic in juvenile mice; male mice exhibit higher levels of newly born cells in the AOB than females. However, in addition to a gradual age-dependent decrease in neurogenesis, this sexual dimorphism was not maintained in older animals. These results indicate that adult neurogenesis in the AOB is influenced by behaviors and it can be differentially regulated in a sex and age-dependent manner.

Neuroblasts born in the SVZ migrate tangentially and reach the OB within a week, where they begin to migrate radially to specific layers within the OB.

Within a month they have already matured into GC and PG neurons (Petreanu & Alvarez-Buylla, 2002). Accordingly, four weeks after the BrdU injections we identified abundant labeled cells in the GCL and GL of the AOB and most of these cells corresponded to mature GCs and PGs as they were also positive for NeuN. Furthermore, two-month old male mice exhibited a larger number of adult born cells than females in the AOB, and this difference was mainly attributed to increased neurogenesis in the pAOB. The observed difference in neurogenesis was not due to differences in cell density or volume along the anterior axis of the AOB ruling out the possibility that these factors contributed to the sex differences observed. Thus, it is possible that the difference in the number of BrdU+ cells between male and female might not be large enough to significantly alter the much larger number of total cells in the AOB. The physiological relevance of this sexual dimorphism is unknown but it is tempting to speculate that a larger availability of newly born neurons in juvenile males may correlate with an increase in neuronal activity in the AOB. For example, at this age male mice begin to establish dominance hierarchy and engage in sexual activity for which the circuitry of the AOB is actively recruited. The sexual dimorphism in neurogenesis reported here is in agreement with previous studies showing anatomical sexual dimorphism in the AOB and other regions of the AOS (Segovia *et al.*, 1999; Segovia *et al.*, 2006; Suarez & Mpodozis, 2009) and with a study showing sexual dimorphism in neurogenesis in rat AOB (Peretto *et al.*, 2001). Interestingly, a recent report by the latter group failed to find significant differences in neurogenesis between sexes in mice (Oboti *et al.*, 2009). The

nature of the difference between the present work and that of Oboti et al (2009) is not known; however, we note that the strain of mice used in these versus the present study is different (BL/C57 vs. CD-1), and significant differences in adult neurogenesis have been reported for different strains of mice in the adult hippocampus (Kempermann & Gage, 2002). Nevertheless, the density of newly born neurons in the adult AOB reported here is comparable to those recently reported for mice and rat (Peretto *et al.*, 2001; Oboti *et al.*, 2009). Intriguingly, the sexual dimorphism in neurogenesis observed in younger mice was not preserved in older animals; instead we observed a steady decline in neurogenesis with age (see below). Thus, the hormonal and/or behavioral influences that lead to marked differences in basal neurogenesis in juvenile mice of different sex are not pronounced at later ages.

We found a consistent decline, with similar time course, in the number of newly born neurons in the AOB and MOB with aging. Furthermore, this decline in OB neurogenesis corresponded with a reduction in the number of proliferating neuroblasts in the SVZ as we found a significant decrease in the number of labeled cells in the SVZ of older mice after an acute injection of BrdU. In addition, the decline in adult neurogenesis was not due to an increase in cell death, since no difference in the number of apoptotic cells was found between sexes and, more importantly, across ages. The latter results are in agreement with studies showing that the number of newly born neurons in the MOB greatly decreases within the first two months postnatally and at older ages, resulting mainly from a

decrease in SVZ proliferation and not from an increase in cell death (Mirich *et al.*, 2002; Enwere *et al.*, 2004; Lemasson *et al.*, 2005; Ahlenius *et al.*, 2009).

The decline in MOB neurogenesis has been correlated with the decline in olfactory function with aging, suggesting that a similar decline in function may occur in the AOB (Enwere *et al.*, 2004). In the MOB, newly arrived neurons integrate into the existing neuronal network and participate in inhibition, an essential component of olfactory processing (Belluzzi *et al.*, 2003; Carleton *et al.*, 2003; Schoppa & Urban, 2003). Consequently, the generation of new neurons and their programmed death in the MOB greatly influences olfactory processes, including odor discrimination and odor learning (Alonso *et al.*, 2006; Mouret *et al.*, 2008; Moreno *et al.*, 2009; Mouret *et al.*, 2009). Further studies are necessary to determine if the decline in neurogenesis affects these processes in the AOB.

Interestingly, and in accordance with other studies (Peretto *et al.*, 2001; Oboti *et al.*, 2009), the density of adult born neurons in the AOB was lower than in the MOB at all ages tested. The lower number of new cells in the AOB is not due to differences in total number of cells compared to the MOB, suggesting that adult neurogenesis of inhibitory neurons in these two regions is under different regulation and/or has a different physiological role. In the AOS, sensory axons synapse onto multiple glomeruli and MCs send primary dendrites to multiple glomeruli and have shorter lateral dendrites. This anatomical arrangement suggests that lateral and recurrent inhibition by GCs and PGs in the AOB may have a different function. For example, it has been proposed that the connectivity in the AOB is more suited for the analysis of blends of social odors (Wagner *et*

al., 2006). Thus, neurogenesis of inhibitory neurons in these two regions could be under different regulatory mechanisms of proliferation and/or integration, resulting in different turnover rates. In agreement with this possibility, recent studies indicated that the neurogenic pool in the SVZ that gives rise to cells in the MOB is heterogeneous (for review see Lledo *et al.*, 2008). For example, neuronal stem cells located in the dorsal regions of the SVZ give rise to PGs that contain tyrosine hydroxylase and to GCs that integrate into the superficial layers of the MOB. On the other hand, neuronal progenitors located in the ventral SVZ give rise to PGs that contain calbindin and to GCs that integrate within deep layers of the GCL (Merkle *et al.*, 2007). In addition, the complexity of the neurogenic pool is greater than expected because it can give rise to excitatory cells as has recently been described in the MOB (Brill *et al.*, 2009). Thus, different pool of neuronal progenitors in the SVZ could give rise to neurons to the AOB and MOB.

The detection and recognition of pheromones by the AOS is crucial for the proper execution of aggressive behaviors in mice. Removal of the VNO dramatically abolishes aggressive behavior in males (Clancy *et al.*, 1984; Maruniak *et al.*, 1986). Mice lacking the TRPC2 channel, which is thought to be a critical component of signal transduction in the VNO, show impaired male-male aggression (Leypold *et al.*, 2002; Stowers *et al.*, 2002). The proliferation of progenitor cells in the SVZ and the differentiation and integration into the circuitry of the MOB are regulated by social behaviors or social stimuli in several species, suggesting that the activity of newly integrated neurons is recruited in the

processing of relevant odors that mediate these social encounters (Gheusi *et al.*, 2009). Aggressive behavior in male mice increased the number of new neurons in the aAOB of the intruder in a resident-intruder behavioral assay. Similarly, the number of cells in the aAOB was also higher in the resident, although this value did not reach significance; therefore, we cannot rule out the possibility that both groups of mice, if exposed for longer times to aggression, could exhibit increased neurogenesis in the AOB. Nevertheless, the localized increase in newly born neurons in the aAOB suggests the involvement of activity of sensory neurons in the apical layer of the VNO, which projects to this region. Aggression in males is triggered mainly by cues present in urine, which are detected by the VNO. Two fractions of urine, one of low and one of high molecular weight (LMW and HMW), can be isolated and produce localized activation in the AOB. Noteworthy, the HMW fraction has been recently identified as a member of the major urinary protein (MUP) family, for a long time suspected to mediate pheromonal effects in the AOS (Mugford & Nowell, 1970; Chamero *et al.*, 2007). Surprisingly, both the HMW and LMW fractions activate the aAOB, while the pAOB is activated by the HMW fractions only (Brennan *et al.*, 1999; Papes *et al.*, 2010), however, these observations are in agreement with previous studies showing that chemosensory cues hastening aggression can activate either of these two regions of the AOB (Kumar *et al.*, 1999; Sugai *et al.*, 2006). Furthermore, in agreement with our findings, mice lacking Gαi2, a G protein subunit expressed by apical neurons in the VNO which project to the aAOB, also show diminished aggressive behavior (Norlin *et al.*, 2003). Together, these findings suggest that complementary

chemosensory cues (i.e. of LMW and HMW) can trigger the expression of aggressive behaviors by producing activation of both subdivisions of the AOB, which in turn could promote the integration of newly born neurons. Interestingly, we found that exposure to only the bedding soiled by the resident was sufficient to increase integration of neurons in the intruder, suggesting that that physical contact or the presence of the antagonistic male was not necessary and that the resident odor was sufficient stimulus. Moreover, this stimulus increased in integration throughout the whole GCL of the AOB. This can be beneficial in the wild, where subordinate males needs to detect dominant males perimeters even when they are not physically present in a determine area. Resident mice on the other hand, failed to show upregulation of adult neurogenesis when they were presented with male urine, indicating that perhaps this stimulus needs a physical contact. These findings indicate that the regulation of adult neurogenesis in the resident AOB requires the physical act of aggression, perhaps acute hormonal changes triggered by aggression. It is also possible that pheromones from other secretions (i.e. anal or salivary gland) might also add to promote neurogenesis in the context of aggressive behaviors (Thompson *et al.*, 2007).

Our results also indicate that the increase in the integration of new neurons induced in the resident-intruder assay was not due to the stress resulting from social conflict generated between the males (Koolhaas *et al.*, 1997; Heinrichs & Koob, 2006). Mice subjected to stress did not exhibit a significant change in adult neurogenesis in the AOB or in the MOB. These results are in contrast to observations in the hippocampus where social stress,

induced by a similar paradigm to that used in our studies, decreased the rate of adult neurogenesis (Mitra *et al.*, 2006; Yap *et al.*, 2006). Thus, our data provides further evidence to the notion that neurogenesis can be differentially regulated by behavior and/or physiological conditions in different parts of the brain (Fowler *et al.*, 2002; Kaneko *et al.*, 2006; Larsen *et al.*, 2008).

Several studies have indicated that pheromonal cues from males can influence adult neurogenesis in females. For example, estrous induction in females by exposure to males increases cell proliferation in the SVZ of prairie voles (Smith *et al.*, 2001). In female mice, exposure for 7 days to male odors prior to BrdU injections (Mak *et al.*, 2007; Larsen *et al.*, 2008), also promotes an increase in the number if BrdU+ cells in the SVZ and in the MOB. In agreement with these observations, we found that exposure to social odors for the same period of time increased adult neurogenesis in the AOB; females exposed to male but not female odors had a greater density of labeled cells in the pAOB. Interestingly, exposure to male odors produce changes in prolactin levels in the female mice, and these changes in prolactin can be related to an increase in neuronal proliferation in the SVZ (Mak *et al.*, 2007; Larsen *et al.*, 2008). Thus, hormonal changes driven by a particular social stimulus, could affect the proliferation rate of a specific neurogenic pool in the SVZ (see above), which may lead to the integration of neurons in a particular region of the AOB. Alternatively, selective activation of sensory neurons in the basal layer of VNO, during the stimulation period by the signals from the male, could induce hormonal changes that induce a delayed increase in the number of newly born neurons in the

pAOB. Future experiments are needed to determine the mechanisms by which male odors induce differential increases in the anterior-posterior axis of the AOB.

The differential increase in neurogenesis between the AOB sub-regions observed with male aggression and male odor exposure in females are consistent with the prevalent notion that segregated projections from the sensory neurons in the VNO allow for chemosensory stimuli to differentially regulate the activity of the aAOB and pAOB in the AOS pathway (Tirindelli *et al.*, 2009). However, the primary region of the AOB activated by sexual stimuli remains controversial; activation of the aAOB, pAOB or both has been described in rodents (Brennan *et al.*, 1999; Dudley & Moss, 1999; Inamura *et al.*, 1999; Kumar *et al.*, 1999; Yamaguchi *et al.*, 2000; Halem *et al.*, 2001; Kimoto & Touhara, 2005; Sugai *et al.*, 2006; Yoshikage *et al.*, 2007). In addition, a recent study indicated that exposure of female mice to male odors increased the number of new neurons in both subdivisions of the AOB (Oboti *et al.*, 2009). As suggested above, the differences between these and our studies could be due to differences in the strain, age and/or BrdU injection protocol. In addition, a recent report indicated that behavior can be greatly influenced by environmental conditions, making comparison across behavioral studies more difficult (Oliva *et al.*, 2010). Nevertheless, further studies are necessary to determine whether activation of V2R sensory neurons in the VNO by social odors and concomitant activation of the pAOB promotes neurogenesis. It should be noted, however, that an increase in the number of new neurons in a particular region does not need to result from a local increase in neuronal activity; instead, other regulatory

mechanisms can trigger the increase in integration/survival of new neurons, a possibility that needs to be further explored.

Surprisingly, in addition to changes in the level of neurogenesis in the AOB, induced by behavior, adult neurogenesis was also increased in the MOB of males, irrespective of the hierarchical status in the resident-intruder assay, and in females exposed to male odors. One possibility is that the large quantity of chemicals found in urine may provoke a general activation in the MOB leading to increased neurogenesis, which has been extensively shown to be affected by olfactory enrichment in the MOB (Rochefort *et al.*, 2002; Bovetti *et al.*, 2009; Moreno *et al.*, 2009; Veyrac *et al.*, 2009). The dual activation of these regions of the bulb during olfactory-guided behaviors has been only occasionally described (Fiber & Swann, 1996; Guo *et al.*, 1997; Huang & Bittman, 2002; Xu *et al.*, 2005; Martel & Baum, 2007); however, our results are in agreement with several pieces of evidence that support the emerging notion of a complementary role for the main olfactory system (MOS) and the AOS in mate recognition and aggression in rodents (Baum & Kelliher, 2009; Keller *et al.*, 2009; Tirindelli *et al.*, 2009). In females, activation of the AOS is necessary for the proper execution of behaviors elicited by pheromonal cues such as acceleration of puberty (Vandenbergh, 1975), estrous induction (Whitten, 1959) and pregnancy block (Bruce, 1959), while activation of the MOS is necessary for the processing of chemosensory information that conveys social attraction and social recognition (Spehr *et al.*, 2006; Baum & Kelliher, 2009; Keller *et al.*, 2009). Thus, removal of the VNO in male mice elicited normal sexual discrimination among conspecifics but

decreased male preference for the urine of estrous females (Pankevich *et al.*, 2004), while ablation of the MOE reduced females' sexual behavior and olfactory investigation (Keller *et al.*, 2006). Similarly, genetic modifications of sensory neurons in the MOE also support the critical role of the MOS in social behaviors. Mice deficient in CNGA2, a cyclic nucleotide-gated channel that participates in signal transduction, exhibit impaired individual recognition (Mandiyan *et al.*, 2005). In addition, male mice lacking the adenylate cyclase type 3 (AC3), another component of the canonical transduction pathway in the MOS, exhibit impaired sexual and male-male aggressive behaviors (Wang *et al.*, 2006). Furthermore, integration of olfactory information at the level of the amygdala, principally through reciprocal connections with olfactory cortices, greatly contributes to the complementary role between the MOS and AOS (Dulac & Torello, 2003; Kang *et al.*, 2009; Keller *et al.*, 2009). Further studies are necessary to determine the function of newborn neurons in the adult OB within the context of complementary olfactory cues and the contribution of adult neurogenesis in the generation, maintenance and extinction of olfactory-guided social behaviors. Differential regulation of adult neurogenesis in the AOB along the anterior-posterior axis may be crucial for social and sexual behaviors that require the generation of selective odor memories that are necessary to maintain an adequate social behavior.

CHAPTER 3: INHIBITORY REGULATION OF INHIBITORY NEURONS IN THE OB

3.1 Introduction

Sensory information about the external environment is integrated through a series of feedforward stages towards high cognitive areas like the cortex. Sensory perception can be, however, regulated by an individual's internal state, enhancing valuable or suppressing invaluable information depending on the behavioral task (Dani & Bertrand, 2007; Hasselmo & Sarter, 2011; Palmer & Kristan, 2011; Lee & Dan, 2012). The regulation of sensory processing occurs through feedback connections between cortical integration centers and early sites of sensory coding, such as cortico-thalamic connections. In the olfactory pathway, the OB is the first and only rely of sensory information. Principal neurons in this region, which receive information from sensory neurons, project directly into the olfactory cortex bypassing the thalamus, unlike other sensory systems (Kay & Sherman, 2007). Odor encoding in sensory neurons is therefore only one synapse away from cortex, suggesting that the extensive fine-tuning and regulation of olfactory information that occurs before transmission to cortex occurs in the OB. Indeed, sensory processing in the OB is highly dynamic; in addition to integrate incoming odor information it also integrates information from diverse brain regions through centrifugal projections, which can affect behavioral output (Balu *et al.*, 2007; Matsutani & Yamamoto, 2008; Boyd *et al.*, 2012; Markopoulos *et al.*, 2012)

A main integrator of bottom up and top down information in the OB is thought to be its most abundant cell type: the inhibitory GC. As mentioned above, GCs are axonless neurons, which establish connection with other intrinsic neurons in the OB, including MC and local interneurons. DDS between MC-GCs have been extensively studied and show to play a major role on olfactory processing (Jahr & Nicoll, 1982; Isaacson & Strowbridge, 1998; Schoppa *et al.*, 1998; Chen *et al.*, 2000; Schoppa & Urban, 2003; Shepherd *et al.*, 2007). For example, GCs can form synapses with several MCs, whereby robust excitation of one GC by one MC affects a large number of neighboring MCs, in a process called lateral inhibition (Imamura *et al.*, 1992; Isaacson & Strowbridge, 1998; Shepherd *et al.*, 2007). In analogy, with other sensory systems, lateral inhibition is proposed to enhance the salience of strong odor stimuli and therefore to enhance odor discrimination. Importantly, the interaction between MCs and GCs is thought to give rise to network oscillations in the OB, which are associated with MC firing synchronization, adding an important time component to olfactory processing. Specifically, oscillations in the theta (4-12 Hz), beta (15-28) and gamma range (40-70Hz) have been proposed to mediate olfactory learning (Nusser *et al.*, 2001; Ravel *et al.*, 2003; Kay, 2005; Beshel *et al.*, 2007; Lagier *et al.*, 2007).

In addition, several studies have indicated the important feedback regulation of GCs by centrifugal afferents, proposed to play a similar role that the regulation of cortical inputs has on thalamic neurons (Kay & Sherman, 2007). For instance, excitatory feedback projections from the anterior piriform cortex,

which primarily target the cell bodies of GCs, is thought to produce a global depolarization in GCs and release the Mg^{2+} block of NMDA glutamate receptors at DDS enhancing lateral inhibition (Balu *et al.*, 2007). Moreover, GABA release from GCs, elicited by stimulation of excitatory feedback projections is sufficient to reduce MCs firing during odor presentation (Boyd *et al.*, 2012).

Similarly several neuromodulatory systems, including afferent noradrenergic fibers from the locus coeruleus and cholinergic fibers from the basal forebrain regulate GC excitability (Matsutani & Yamamoto, 2008). In particular, behavioral recruitment of these neuromdulatory systems and subsequent regulation of OB neurons is required for olfactory learning and odor discrimination. For example noradrenaline (NA) release increases in the AOB after mating and promotes the formation of the memory in the stud for a recently mated female (Bruce, 1959; Rajendren & Dominic, 1985; Brennan *et al.*, 1995). Similarly, in the MOB, NA is crucial for odor learning in newborn pups. At this early age, odor learning triggers important stereotyped behavior, such as nipple attachment and approach responses (Sullivan, 2001; Raineki *et al.*, 2010). In the MOB acetylcholine (ACh) and NA promotes contrast enhancement and odor learning by sharpening MC output and increasing the oscillatory power of the bulbar circuit (Mandairon *et al.*, 2006; Guerin *et al.*, 2008; Chaudhury *et al.*, 2009; Escanilla *et al.*, 2010; Devore & Linster, 2012). Work in our lab has shown that both ACh and NA increase the excitability of GCs and that excitation of GCs increases the inhibitory tone onto MCs through DDS (Araneda & Firestein, 2006; Smith *et al.*, 2009; Smith & Araneda, 2010; Zimnik *et al.*, 2013). These findings

have led us to put forward a model in which the enhanced inhibition of MCs promoted by NA and ACh increases the signal-to-noise ratio of incoming sensory input. This could explain the increase in olfactory discrimination promoted by the activation of these neuromodulatory systems.

Although mechanisms that promote excitation of GCs have been extensively studied, the mechanisms that promote inhibition onto these cells have received little attention. In fact, direct inhibition of GCs, has been sparsely described and the source of this inhibition is not fully understood. The largest population of neurons in the OB are inhibitory neurons, therefore, inhibition could potentially arise from neighboring GCs or other local inhibitory neurons. Accordingly, recent studies suggest that inhibition of GCs is mediated by local inhibitory neurons located in the GCL termed deep short axon cells (dSACs). dSACs form axo-dendritic synapses with GCs, thereby promoting a decrease in bulbar inhibition and a net increase in MC firing (Pressler & Strowbridge, 2006; Eyre *et al.*, 2008). Recent data indicated that dSACs are activated by excitatory cortical feedback projections, suggesting that inhibition of GCs, via dSACs, can be also be indirectly controlled by cortical feedback (Boyd *et al.*, 2012). In general, the limited information available about inhibition of GCs indicates that in the MOB, this inhibition is required to maintain synchronous oscillation and olfactory discrimination (Nusser *et al.*, 2001; Lagier *et al.*, 2007). Finally, unlike the majority of other brain areas, neurogenesis supplies a constant supply of inhibitory neurons to the OB that integrate into the bulbar network (Altman & Das, 1965b; Lois & Alvarez-Buylla, 1993; 1994). Most of these cells differentiate into

GCs. The continuous supply of GCs is particularly important, given recent evidence suggesting that inhibition from GCs is required for the plasticity necessary to induce olfactory learning (Nissant & Pallotto, 2011; Alonso *et al.*, 2012).

Another potential source of inhibition of GCs are afferent fibers from the basal forebrain, specifically from the horizontal limb of the diagonal band of Brocca and the magnocellular preoptic nucleus. (HDB/MCPO). Neurons in this region project GABAergic, as well as cholinergic, fibers into the OB (Zaborszky *et al.*, 1986). Moreover, recent studies have shown that the GABAergic fibers mainly innervate the GCL, suggesting that they can have an important function inhibiting GCs (Gracia-Llanes *et al.*, 2010). Importantely, a few studies have addressed the role of this region in OB function, but mostly from the perspective of the cholinergic system (Kunze *et al.*, 1992b; Paolini & McKenzie, 1993; Ma & Luo, 2012). In vivo stimulation of the HDB produces an inhibitory response in GCs that could be important to enhance MC activity and olfactory response under different behavioral tasks (Kunze *et al.*, 1992b; Paolini & McKenzie, 1997; Ma & Luo, 2012). Thus, despite their prominence, the function of these afferent inhibitory inputs onto GCs in olfactory processing remain unknown.

Here, we studied the contribution of afferent inhibitory inputs onto GCs to olfactory processing. We focused on the role of this inhibition in the MOB, where we have a better understanding of how regulation of GCs by excitation affects olfactory behavior, allowing for an accessible behavioral correlate to our findings. Using the whole cell patch clamp technique in OB slices, we first characterized

inhibitory postsynaptic currents (IPSCs) in GCs. Then, using selective expression of channerlrhodopsin (ChR), we stimulated GABA release from GABAergic neurons of the HDB/MCPO. We found that activation of GABAergic projections produces a robust inhibition of GCs. More importantly, silencing these HDB/MCPO GABergic inhibitory inputs, using selective targeting of genetically engineered inhibitory receptors, has a profound effect in olfactory discrimination. In addition, we studied the contribution of local interneurons by selectively expressing ChR in GCs. We found that GCs also receive inhibition from neighboring GCs to a much greater extent than previously described and through a mechanism that does not require excitatory input from cortical feedback.

3.2 Methods

Animals. All experiments were performed on C57/BL6 or GAD65-Cre female and male mice (p21-p180) obtained from breeding pairs housed in the animal colony of the Biology Department of the University of Maryland or obtained from Jackson Laboratories (Bar Harbor, MA). Animals were kept on a 12 hr light/dark cycle with access to food and water *ad libitum* and all experiments were conducted following the guidelines of the IACUC of the University of Maryland, College Park.

Slice preparation. We performed brain slices recordings as previously described (Araneda & Firestein, 2006). Briefly, we used sagittal sections (250-300 μm) of the olfactory bulb. After sectioning the slices were placed in normal ACSF (see

below) and left to recuperate for 30-45 min. The extracellular solution used had the following composition (in mM); 125 NaCl, 25 NaHCO3, 1.25 NaH2PO4, 3 KCl, 2 CaCl2, 1 MgCl2,3 myo-inositol, 0.3 ascorbic acid, 2 Na-pyruvate and 15 glucose, continuously oxygenated (95% O2 and 5% CO2).

Electrophysiological recordings. The slices were placed in a submerged recording chamber mounted on a fixed-stage upright Olympus microscope equipped with differential interference contrast (DIC) optics. The recording chamber was continuously perfused with ACSF (~2 mL/min rate). Whole-cell patch-clamp recordings were performed on granule cells visualized using a water-immersion 40X objective and DIC. Cells were recorded in current-clamp mode using a dual EPC10 amplifier. Recording electrodes had a final resistance of 6-8MΩ when filled with an intracellular solution containing (in mM) 125 K-gluconate, 10 Na-gluconate, 4 NaCl, 10 K-HEPES, 4 Mg-ATP, 2 Na-ATP 0.3 Na-GTP, 10 Na-creatine phosphate (300 ± 10 mOsm; pH 7.3). For voltage clamp, the internal solution had the following composition (in mM): 125 Cs-gluconate, 4 NaCl, 2 MgCl2, 2 CaCl2, 2 EGTA, 10 HEPES, 2 Na-ATP, 4 Mg-ATP, and 0.3 GTP adjusted to pH 7.3 with CsOH. The following drugs were bath applied: 6-cyano-7-nitroquinoxaline-2,3-dione (CNQX, 10μM), (2R)-amino-5-phosphonovaleric acid; (2R)-amino-5-phosphonopentanoate (APV, 100μM), LY 367385 (100μM), GABAzine (10μM) and tetrodotoxin (TTX, 0.5 μM). The following drugs were puff applied: GABA (100μM), muscimol (100μM) and GBAzine (10 μM). For data analysis we used the Igor Pro software.

Analysis of inhibitory postsynaptic currents (IPSCs). Spontaneous (sIPSCs) and miniature (mIPSCs) IPSCs were recorded at a holding potential of 0 mV and analyzed offline using the Synaptasoft Mini analysis program. Events were detected using 5-6 pA amplitude threshold. Only events with fast kinetics were considered for the analysis; for animals from p20 to p30, events with a rise time >3 ms where not considered for analysis, and for older animals (ChR2 injected animals) the cutoff was 4.5 ms.

Viral injections. GAD65-Cre mice were anesthetized with isofluorane and mounted in a stereotaxic apparatus. One µL of the adenovirus AAV2/5.CAGGS.flex.ChR2tdTomato, (generously provided by Dr. Karl Deisseroth) was injected unilaterally into the HDB using the following coordinates: AP +0.14mm, ML -1.625mm and DV -5.4. For injections into the RMS the following coordinates were used: AP +3.310mm, ML -0.82mm and DV -2.85mm. Animals used for behavior were injected bilaterally into the HDB with 0.5 µL of the adenovirus AAV8-hSyn-HA-hM4D(Gi)-IRES-mCitrine (UNC vector core).The virus was injected using a microsyringe pump comptroller (WPI) at a rate of 100nL/min. Animals were left to recover and used for electrophysiological recordings at least 2 weeks post-injection. For light stimulation (LightStim), 10 pulses of 10 ms at 5 or 10 Hz were delivered through the 40x objective, using a Lambda LS Xenon Lamp (Sutter) controlled by a Lambda SC Smart Shutter. The area of infection was visually assessed using confocal microscopy at 3 w.p.i. to confirm that the injection was restricted to the HDB/MCPO (see Fig 4B)

Confocal imaging and double labeling immunofluorescence. Mice were perfused intracardially with 4%PFA and postfixed in the same fixative ON at 4C. The next day the brains were placed in PBS and sagittaly sliced at 100 µm. To visualize ChR-dtTomato expression, slices were mounted with Vectashield (Vector Laboratories) and visualized with a Leica SP5 X confocal microscope. For double labeling immunofluorescence, free floating section were washed twice in PBS and incubated with 10% donkey serum (Sigma Aldrich) in PBS-T for 2 hrs at RT. Slices were then incubated overnight at RT with one or more of the following primary antibodies prepared in PBS-T with 2.5% of donkey serum: mouse anti-GAD6 (1:300, developed by Dr. David Gottlieb was obtained from the Developmental Studies Hybridoma Bank developed under the auspices of the NICHD and maintained by The University of Iowa, Department of Biology, Iowa City, IA 52242), rabbit anti-GAD67 (1:100, Santa Cruz Biotechnology, Inc sc-5602), goat anti-CHAT(1:500, Millipore ab144),chicken-anti GFP (1:100, Abcam ab13970) or rabbit anti gephyrin (1:1000, Abcam ab32206). After the incubation with antibodies the samples were washed with PBS-T seven times for 5min and incubated for 2hrs at RT with the secondary antibodies: donkey anti-mouse Alexa-488 (Life Technologies, A-21202), donkey anti-rabbit Alexa-594 (Life Technologies, A-21207), goat anti-chicken Alexa-488 (Life Technologies, A-11039), donkey anti-goat Alexa-488(Life Technologies, A-11055) and donkey anti rabbit Alexa 488 (Life Technologies, A-21206), all diluted at 1:750 in PBS-T with 2.5% of donkey serum. The sections were then washed 3 times in PBS-T for

5 min and 4 times in PBS for 5 min. The samples were mounted with Vectashield and visualized with a Leica SP5 X confocal microscope.

GABA receptor cluster analysis. Confocal images in which slices were stained with antibodies against GFP and gephyrin were analyzed using the ImageJ software. The threshold for the green and red channel was manually set and a colocalization mask was obtained. Clusters were identified based on their round morphology and only clusters that laid within the mask were considered for further analysis. Each cluster was manually demarcated and the Person's coefficient measured. The Pearson's coefficient is a parameter that measures the degree of correlation between two channels, and it goes from +1 (positive correlation, 100% of colocalization) to -1 (negative correlation). For quantification only clusters exhibiting a positive Pearson's coefficient greater than 0.2, were considered.

Habitutaion/Dishabituation test. Control mice and animals previously injected with AAV8-hSyn-HA-hM4D(Gi)-IRES-mCitrine, received a single i.p. injection of either PBS (control group) or clozapine-N-Oxide (CNO 0.5mg/kg , treated group) and were tested one, two, three and four hours post-injection (h.p.i). Previous studies have shown that the maximal effect of CNO occurs at 1-4 hrs post injection (Krashes *et al.*, 2011; Sasaki *et al.*, 2011). A clean standard mouse cage (15cm x 30cm x 15cm, h x l x w) without bedding, was used as the test environment. Mice were placed in the cage and allowed to familiarize with the setup for 30 minutes. A wooden cube (2 cm^3) was placed in the cage with the mouse during the familiarization phase. At the conclusion of the familiarization

phase, the wooden block was removed for a one minute period. There was then three 2 minute exposures to a wooden block scented with water. These exposures serve to allow the mouse to familiarize to the experimental set-up. The second phase consisted of subsequent exposures to a wooden block that has been scented with 100 uL of the odor being tested. Exposures lasted 2 minutes with a 1 minute inter-trial interval. Each trial was videotaped and the time the mouse spent investigating the block was quantified offline. Investigation was defined as any time during which the mouse's nose is within a 2cm radius of the block. The order of odor presentation will be as follows: water 3x, ethy heptanoate (C7, 1:1000) 3X, ethyl octanoate (C8, 1:1000) 1X.

Odor threshold detection. Animals infected with the AAV8-hSyn-HA-hM4D(Gi)-IRES-mCitrine virus were tested using the same set up as described above. In this case the animals were presented with C7 at different dilutions. The sequence of odor went as follow: water 3x, C7 1:60000, C7 1:40000, C7 1:30000, C7 1:20000, C7 1:10000 and C7 1:1000.

To test for statistical significance, we used the Student's t-test. When the p values was less than 0.05, the null hypothesis (the means of two distributions are equal) was rejected.

3.3. Results

3.3.1. Granule cells receive inhibitory inputs mediated by $GABA_A$ receptors

To characterize inhibition onto GCs, we performed whole cell patch clamp recordings in sagittal slices of the OB of p20-p30 animals. GCs usually exhibit a hyperpolarized resting potential (–75.1±4mV, n=6, Smith et al 2009), therefore a suprathreshold depolarizing current was injected to elicit continuous firing (Fig 1A right; 3.9±1 Hz, n=8). Direct application of GABA (100 µM) in the vicinity of the GC soma produced a fast hyperpolarization (ΔVm= –16.4±0.9 mV, n=11), that completely abolished the firing, suggesting that GABA can inhibit GCs under physiological conditions. Firing in these cells quickly returned after the GABA washed out (Fig 1A). To further determine the type of receptor mediating these GABA responses, we conducted pharmacological experiments in the voltage clamp (VC) mode. The internal concentration of Cl^- in GCs is not known but it has been estimated to be about 11 mM (Belluzzi *et al.*, 2003), in which case the E_{Cl} should be close to –80 mV under our recording conditions. Therefore, we conducted our VC experiments at 0mV, while recording GABA currents using recording pipettes filled with Cs-Gluconate (Fig 1B). These conditions maximize the amplitude of GABAergic outward currents and enhance our ability to detect and quantify these responses without the contribution of excitatory currents, as the E_{rev} of glutamatergic currents is ~ 0 mV. Focal application of GABA (100µM) generated a large outward current (191±56 pA, n=8) and a consecutive application 10 s later, produced a response of similar amplitude (168±59 pA, n=6;

p>0.8), suggesting little or no desensitization of these responses within these short intervals (Fig 1B, top).

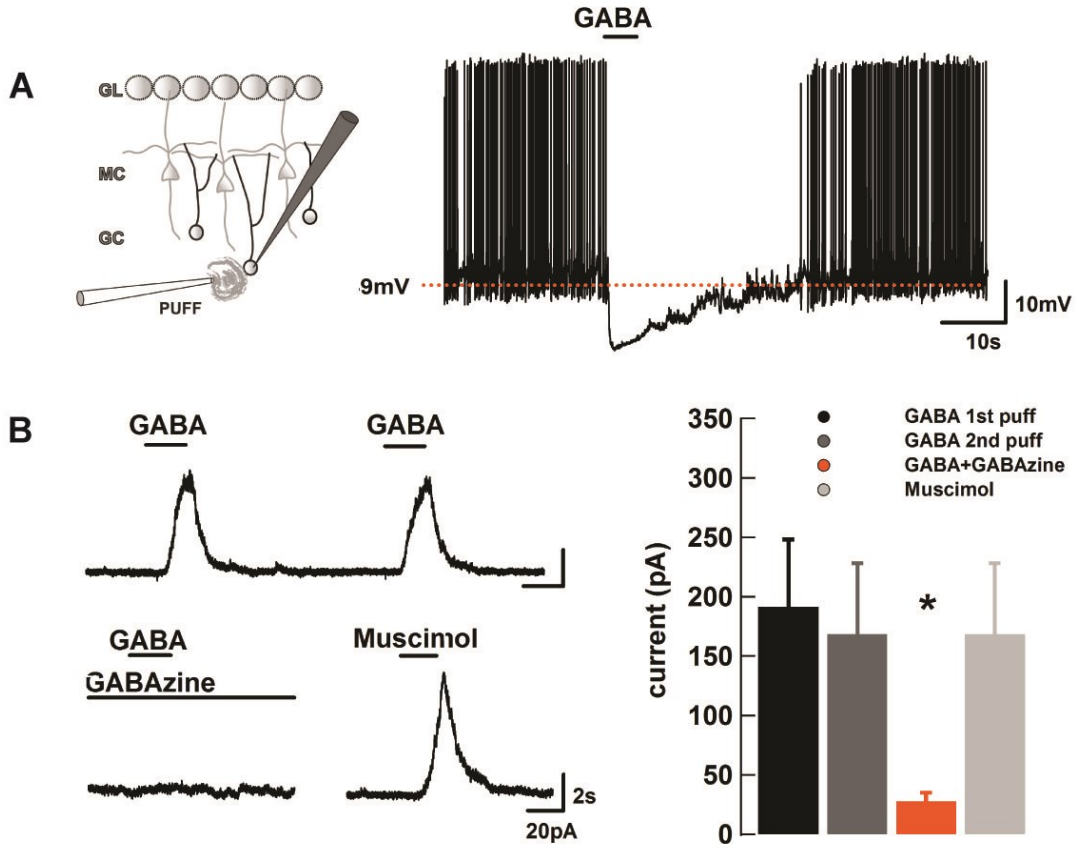

Fig1: **GABA inhibits GCs by activating $GABA_A$ receptors**. (**A**) Left, diagram depicting the cellular organization in the MOB and the recording arrangement. We performed whole cell recordings in GCs while drugs were delivered locally next to the soma using an automated perfusion system, in combination with bath perfusion (i.e. antagonists). Right, application of GABA (100μM) hyperpolarized and completely silenced the firing of a GC depolarized with a suprathreshold current stimulus. (**B**) Application of GABA (100μM) elicits an outward current in VC recordings of GCs. A second application of GABA, 10 s later, produced a response of similar amplitude. The GABA induced outward current was completely abolished in the presence of the selective $GABA_A$ receptor antagonist GABAzine (10 μM), while the selective $GABA_A$ receptor agonist muscimol (50 μM) mimicked the response to GABA. All VC recordings were done at 0mV. (**C**), graph bar summarizing the average amplitude of the responses elicited by the different pharmacological conditions. GABAzine significantly reduced GABA responses (**p*<0.004).

When GABA was applied in the presence of the selective $GABA_A$ antagonist, GABAzine (10 μM, Fig 1B, bottom), the outward current was completely abolished (27±7 pA, n=7; $p<0.01$). Moreover, application of the selective $GABA_A$ agonist, muscimol (50 μM) produced responses of similar amplitude and kinetics to those obtained with GABA applications (168±60 pA, n=6; Fig 1B). Together, these results indicate that GCs are inhibited by activation of ionotropic $GABA_A$ receptors.

Several factors, can alter the strength of synaptic connections such as variation on the vesicular neurotransmitter content and subunit composition of receptors in the postsynaptic membrane, among others (Nusser *et al.*, 2001). These synaptic parameters can be indirectly studied by analyzing the kinetic properties of spontaneous postsynaptic currents (sPSCs). Spontaneous excitatory or inhibitory postsynaptic currents (sEPSCs and sIPSCs, respectively) are the result of spontaneous release of neurotransmitter vesicles typically from presynaptic terminals. Similarly, evoked currents are produced by a presynaptic stimulus that gates a synchronous release of vesicles from a population of synapses. This synchronous release produces larger responses, and usually depend on Na-dependent action potentials invading the presynaptic terminal. Therefore, to gain a better insight into the nature and occurrence of inhibitory inputs onto GCs, we recorded sPSCs at –60 mV (Fig 2A). As mentioned above, GCs receive an abundant excitatory input from MCs, at dendrodendritic synapses and MC's axon collaterals, and from cortical feedback projections (Balu *et al.*, 2007); accordingly, GCs exhibited a high occurrence of sEPSCs (inward

currents) while a few sIPSCs (outward currents, orange dots) can also be observed, indicating a tonic GABAergic input onto GCs (Fig 2A).

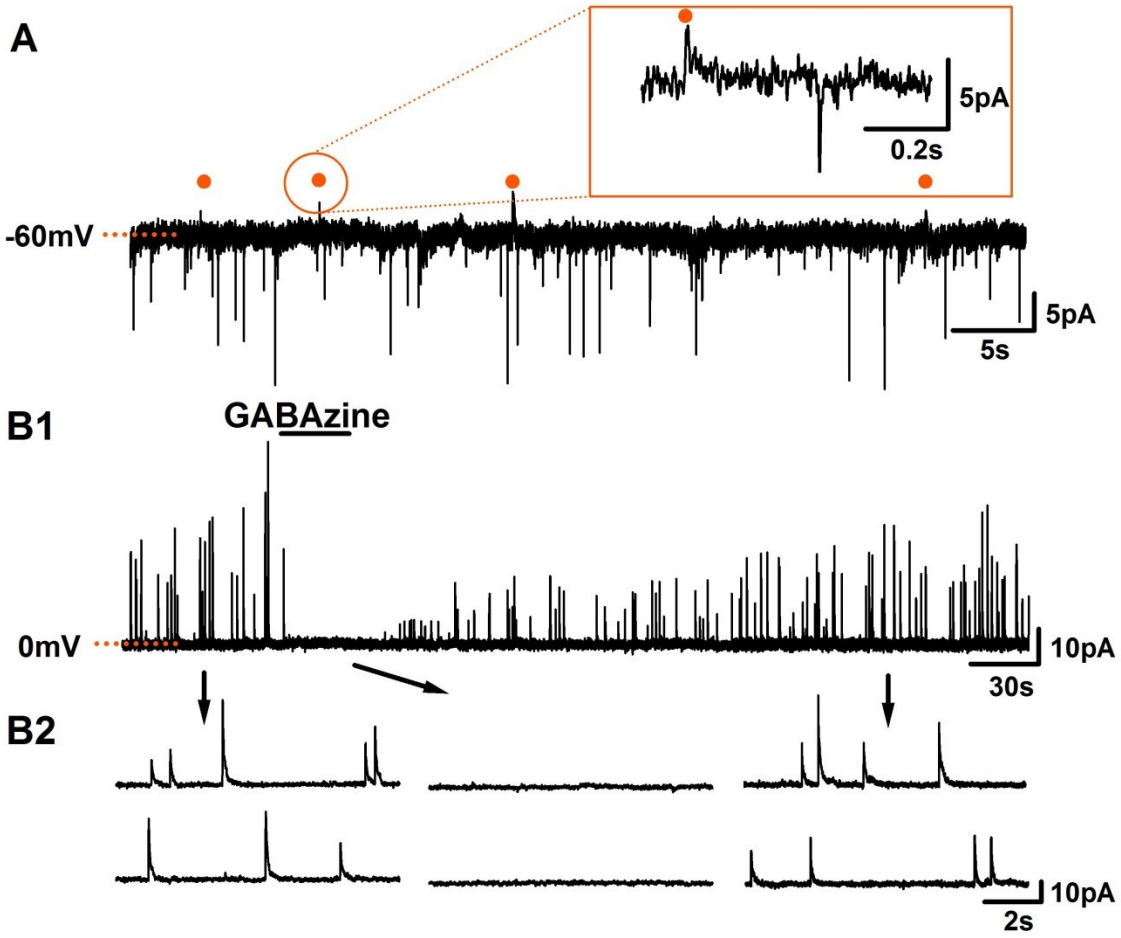

Fig 2: **Granule cells exhibit spontaneous inhibitory $GABA_A$ mediated currents**. (**A**) In recordings with a low Cl^- intracellular solution (see methods), GC show abundant sEPSCs, while a few sIPSCs are also present (orange dots; holding potential is –60 mV). One of these outward current events is magnified in the inset. (**B**) B1, to better isolate the sIPSCs we recorded GCs at 0mV, at this potential the occurrence of these outward currents is more evident and they are completely abolished in the presence of the selective $GABA_A$ receptor antagonist GABAzine (10μM). B2, selected expansions of the recording shown above.

In contrast, at 0 mV, we observed a larger occurrence of sIPSCs (0.7±0.1 Hz; n=4), which were presumably masked at –60 mV. Recall that 0 mV is the reversal potential for the sEPSCs, which allow us to study sIPSCs in isolation. In

agreement with our experiments with direct GABA application and indicating that the sIPSCs are mediated by $GABA_A$ receptor activation, GABAzine (10μM) completely abolished the sIPSCs (0.07±0.05Hz; n=4; $p<0.01$), (Fig 2B).

3.3.2. GABA IPSCs in GCs are not dependent on excitatory transmission

To examine the possibility that GABA inhibitory currents in GCs are dependent on glutamatergic transmission, for example through excitatory activation of local interneuorns, we recorded sIPSCs in the presence of the ionotropic glutamate receptors antagonists; the NMDA receptor blocker APV (100 μM), and the AMPA receptor antagonist (CNQX, 10μM). We also included TTX (0.5 μM) to determine the contribution of vesicular release mediated by Na-dependent action potentials. Under this pharmacological blockade the recorded events correspond to the miniature inhibitory synaptic currents (mIPSCs). Surprisingly, we found that the frequency of sIPSCs was not affected by the application of the glutamatergic blockers and TTX (0.34±0.05 Hz; n=34, vs. 0.41±0.1 Hz; n=21, $p>0.5$, Fig 3A, B1). This suggests that GABA inhibitory input onto GCs does not require a glutamatergic transmission, as is the case with vesicular release of GABA at DDS, or by activation of dSACs cells by cortical excitatory feedback (Schoppa & Urban, 2003; Boyd *et al.*, 2012). Moreover, the lack of effect of TTX indicates that Na^+ dependent action potentials are not necessary for GABA release. However we cannot rule out the possibility that GABA release from globally activated GCs, depends on the generation of Ca^{+2}

spikes. In fact, recent studies have indicated the presence of Ca^{+2} spikes in GCs (Pinato & Midtgaard, 2003; Egger *et al.*, 2005).

GCs extend a single apical dendrite to the EPL, where it branches extensively. This dendritic morphology creates a compartmentalized unit that can be divided into apical, proximal and basal/soma, each of which can receive synaptic inputs from different sources. We hypothesize that in the presence of the blockers inhibitory inputs from distal regions, previously electrotonically filtered, can now be recorded at the soma. IPSCs arising from distal regions of the GC are expected to exhibit slower kinetics compared to those originated closer to the recording site. To examine this possibility, we performed a detailed kinetic analysis of the sIPSCs. The amplitude probability distributions of the sIPSCs, showed a skewed distribution with a tail at larger amplitudes (Fig 3 B2, grey) and a mean amplitude of 23±0.4 pA. In the presence of the blockers, the mean amplitude of mIPSCs (orange) showed a small but significant decrease (Fig 3 B2 inset, 21.6±0.3 pA; $p<0.03$), while the mean decay time showed a small but significant increase (Fig 3 B3; sIPSC, 56.5±0.8 ms vs. mIPSC, 61.7±1.0 ms; $p<0.0002$). The small decrease in mean amplitude and the small increase in mean decay time, suggests that a small population of IPSCs is either unmasked or facilitated in the presence of the blockers. This possibility is supported by the changes on average rise time of these events. When we plotted the rise time probability histogram, a bimodal distribution was observed for both sIPSCs and mIPSCs, with medians centered at 1.6 ms and 2.3 ms (Fig 3 B4), and the average rise time had a small but significant increase after the drugs application

(Fig 3 B4, inset; sIPSC, 1.82±0.008 ms vs. mIPSCs, 1.93±0.10 ms; $p<0.0001$). To further distinguish between these two populations, we plotted the rise time of each event against its amplitude (Fig 3 B5, left). Two clusters can be observed, mimicking the bimodal distribution observed in the rise time probability plot. The cluster of events with the fastest rise time also exhibited higher amplitudes, while the IPSCs with slower rise times had in general smaller amplitudes. When the decay time was plotted against the rise time, two populations can also be observed (Fig 3B5 right).

Together, the magnitude and direction of the observed changes in kinetics suggest that the blockers could be affecting the electrotonic properties of GCs. For example, blocking glutamatergic conductances at dendrodendritic synapses is expected to increase the length constant in GCs by increasing the resistance of the membrane. Moreover, the existence of a rise time bimodal distribution, suggest that GCs also receive inhibitory inputs at more proximal regions and the soma (larger amplitude and faster kinetics).

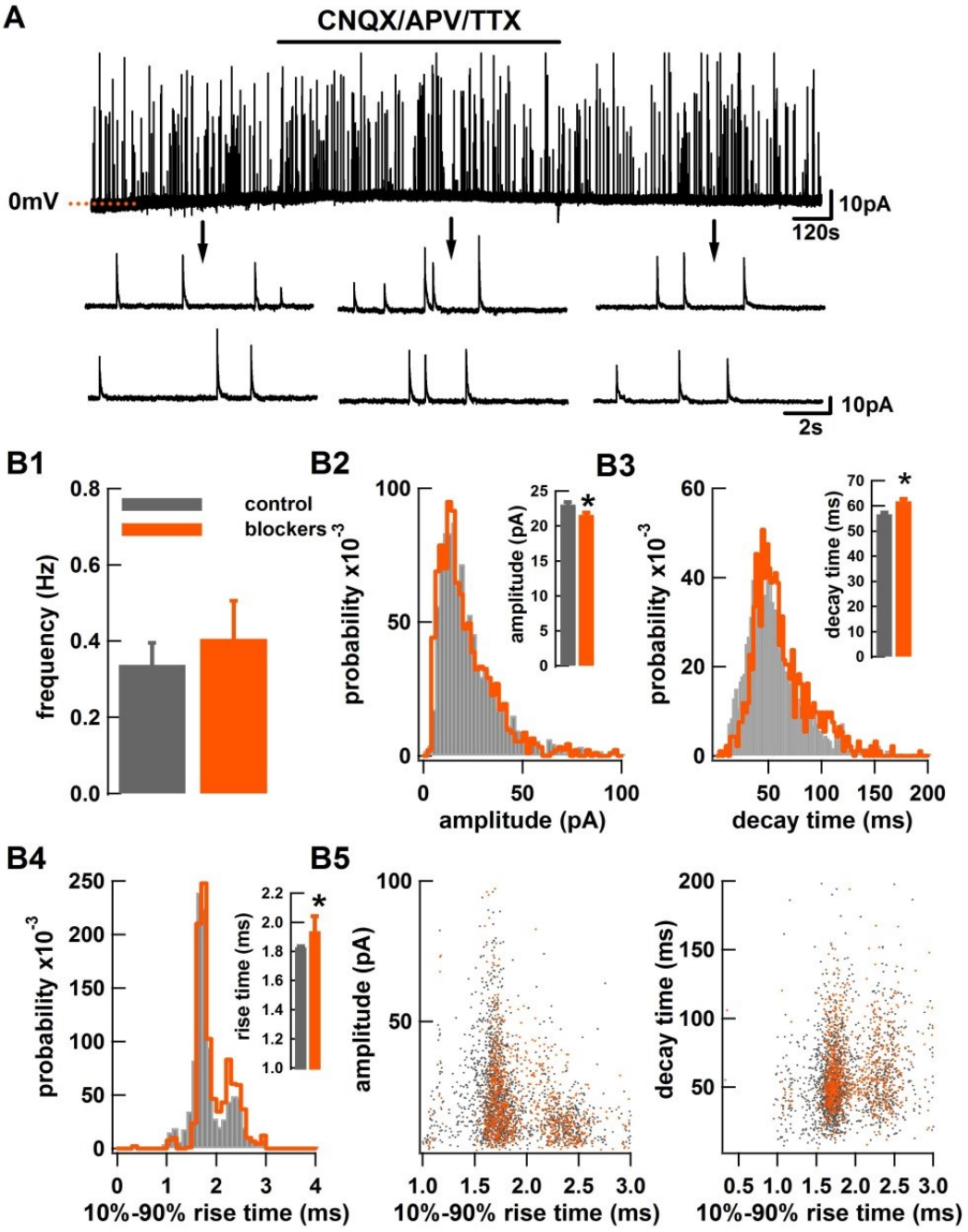

Fig 3: **The inhibitory input onto GCs is not affected by blockers of fast glutamatergic synaptic transmission and TTX**. (**A**) sIPSCs frequency is not affected by the application of blockers of fast glutamatergic synaptic transmission (CNQX, 10 μM; APV, 100 μM) and a blocker of Na-dependent action potentials (TTX, 0.5 μM). Traces below are sample recording at the times indicated by the arrows. (**B**) B1, summary bar graph showing that the frequency of sIPSCs (grey) is not significantly different from the events recorded in the presence of the application of the blockers (mIPSCs, orange, p>0.5). B2, probability histogram of amplitude of IPSCs (n=2710). The plot shows a skewed distribution with a mean amplitude of 23±0.4 pA that decreases after the

application of APV/CNQX and TTX (inset bar graph;*p<0.03). B3, analysis of the decay time shows a probability distribution slightly shifted to the right after the application of the blockers and a small increase in the mean decay time in the presence of blockers (inset bar graph;*p<0.0002). B4, the rise time distribution plot suggests the presence of two event populations with different rise times (see text). The mean rise time had a small but significant increase after the application of the drugs (inset bar graph;*p<0.0001). B5, graph showing the relationship between the rise time and amplitude (left) or decay time (right). Two clusters can be observed in both cases. The population with slower rise time exhibited smaller amplitudes, while faster events showed higher amplitudes. When the rise time of each event was plotted against its decay time, both clusters exhibited a similar distribution.

3.3.3 GABAergic neurons from the basal forebrain strongly regulate GCs' activity

Recent anatomical studies using anterograde tracing showed an extensive innervation of the OB by GABAergic fibers originating in the HDB/MCPO that targets preferentially the GCL (Gaykema *et al.*, 1990; Gracia-Llanes *et al.*, 2010). The existence of this afferent inhibitory input suggests the exciting possibility that GCs are regulated by centrifugal inhibition, which can regulate olfactory processing. Interestingly, the HDB/MCPO area is also the origin of cholinergic afferent fibers that target the OB (Zaborszky *et al.*, 1986) and this cholinergic input has been shown to have an important influence in olfactory mediated behaviors (Paolini & McKenzie, 1997; Mandairon *et al.*, 2006; Chaudhury *et al.*, 2009; Devore & Linster, 2012; Ma & Luo, 2012). Furthermore, studies in our lab have shown that cholinergic activation enhances the excitability of GCs (Smith & Araneda, 2010; Zimnik *et al.*, 2013).

The complex neuronal heterogeneity of the HDB/MCPO presents a challenge to the study of the contribution of the GABAergic output to GC

regulation. Therefore, we took advantage of molecular biology and optogenetic techniques to selectively express channelrhodopsin (ChR) in inhibitory neurons in the HDB/MCPO and precisely control GABA release from these GABAergic neurons. Adenoviral injections of flexed ChR were sterotactically made in the HDB/MCPO of mice expressing the Cre recombinase under the the control of the promoter of one of the isoforms of the enzyme glutamate decarboxylase (GAD65), which is responsible for the synthesis of GABA (GAD65-Cre mice). We first confirmed the presence of inhibitory neurons at the injection site by performing double immunofluorescence against the two isoforms of GAD (GAD65 and GAD67), (Fig 4A). We found that both proteins were expressed across the HDB/MCPO. Most of neurons were positive for either GAD65 or GAD67 (560 out of 612 total cell counted in 3 animals) with a small number of GABAergic neurons that were positive for both isoforms (52 cells). There was no significant differences in GAD expression between the medial (13±6 cells) and lateral regions of the HDB/MCPO (17±2 cells; $p>0.5$), therefore the AAV injection was performed between these two regions to enhance our ability to target GABAergic neurons (see methods). Three weeks post injection (w.p.i), neuronal somas in the HDB/MCPO abundantly expressed ChR (Fig 4 B1). Furthermore, as mentioned above, the HDB/MCPO also contains cholinergic neurons that project to the OB. As shown in Fig 4 B2, staining for choline acetyl tranferase (ChAT, green) shows ChR+ neurons (red) intermingled with ChAT positive cells, further corroborating that the virus injection is restricted to the HDB/MCPO (Fig 4 B2). Five w.p.i we observed extensive innervation of ChR positive fibers in the

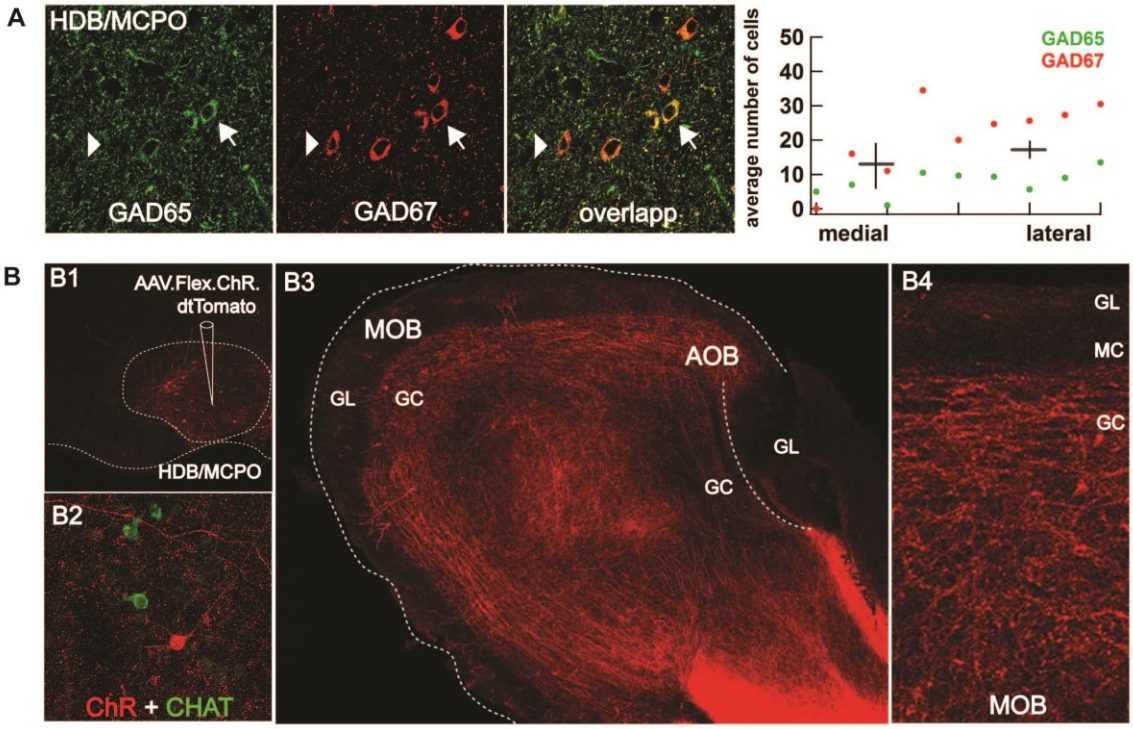

Fig 4: **Selective expression of Channelrhodopsin (ChR) in GABAergic neurons of the HDB/MCPO reveals a profuse feedback projection into the olfactory bulb.** (**A**) The optimal site of viral injection was determined using confocal imaging of the HDB/MCPO in a GAD2 Cre mouse immunostained against GAD65 (green) and GAD67 (red). The GABAergic neurons exclusively express one of the markers (white arrowhead), while a few cells are positive for GAD65 and GAD67 (white arrow, yellow). Right, the number of cells expressing the GAD protein was quantified and no significant difference was observed across the HDB/MCPO. **(B**) B1, confocal image showing abundant expression of ChR (red) in the HDB/MCPO of a GAD2 Cre mouse after targeted injection of AAV.Flex.ChR.dtTomato virus to this area. B2, the HDB/MCPO also is the site of projection of cholinergic projections to the forebrain, including the OB. GABAergic neurons expressing ChR (red) are intermingled with cholinergic neurons stained for choline acetyltransferase (CHAT). B3, confocal imaging of a sagittal section of the OB showing extensive labeling of GABAergic fibers expressing ChR projecting from the HDB/MCPO. B4, the afferents mostly innervate the GC layer with only sparse fibers reaching beyond the MC layer (to the EPL and GL

OB (Fig 4 B3). These afferents fibers targeted mostly the GCL, where the somas and proximal dendrite of GCs are found. No significant staining was observed in the EPL, suggesting that these GABAergic fibers target mostly the GC somata and proximal dendrites but not MCs or GL (Fig 4 B4). To determine

the physiological role of this GABAergic input onto GCs, we performed current clamp experiments while ChR+ terminals were stimulated with blue light (LightStim, Fig5A, right). As mentioned above different oscillatory frequencies in the OB network have been shown to play an important role in olfactory coding (Nusser *et al.*, 2001; Kay, 2005; Lagier *et al.*, 2007). Mice exhibit a basal respiration frequency of about 5Hz that increases to 10Hz when the animals are actively sniffing and exploring an odor.

We found that photo stimulation at these two frequencies reduced GC spiking induced by a depolarizing current stimulus (Fig 5A, middle). The effect was more pronounced at 10Hz, when the spiking rate decreased by 45.27±9.9 % (n=7; $p<0.003$ vs. at 5Hz, -27.93±3.3 %, $p<0.001$). In addition, VC experiments revealed that light stimulation (LightStim) of GABAergic fibers, produced a large outward current in the majority of the recorded cells (20 out of 22 GCs; Fig 5B, left). We reasoned that if inhibitory inputs from the HDB/MCPO act directly on GCs and do not require the activation of glutamatergic inputs, the responses obtained by LightStim should not be affected by blockers of excitatory transmission. For these experiments, in addtion to CNQX and APV we included the metabotropic glutamate receptor blocker (LY367385, 100 μM). Metabotropic glutamate receptors, mGLUR1 and mGLUR5, are found in MCs and GCs (Sahara *et al.*, 2001), and they have been shown to facilitate DDI in the MOB and AOB (Castro *et al.*, 2007; Dong *et al.*, 2009).In agreement with our analysis of spontanopeus currents the application of the antagonist cocktail did not alter the response to LightStim (Fig 5B). To better quantify these reponses we integrated

the currents produced by photo stimulation at 5 and 10 Hz, which corresponds to the charge transfer through GABA channels As shown in Fig 5B (right), the higher frequency of stimulation did not produce a larger charge influx, and although the average charge at 10 Hz was larger, it did not reach significance within the population analyzed (5Hz LightStim: 12.6±3 vs. 12±3 x 10^{-12} C; 10Hz LightStim: 19.1±4 vs. 15.9 ±4 x 10^{-12} C). Moreover, as expected (Petreanu *et al.*, 2009; Boyd *et al.*, 2012), the IPSCs evoked by ChR (eIPSCs) stimulation were completely abolished in the presence of TTX 0.5 µM (5Hz LightStim: 0.09±0.05 x 10^{-12} C, 10Hz LightStim: 0.6±0.2 x 10^{-12} C; $p<0.03$). In addition, the kinetic analysis of the eIPSCs indicated they were not affected by the presence of the blockers; amplitude (control, 43.6±2.9pA, n=12; in blockers, 46.9±3.3pA, n=10; p>0.4), rise time (3.02±0.04 ms;+blockers, 3.01±0.04 ms; p>0.9) and decay time (48.97±1.15;+blockers, 46.36±18 ms; p>0.2) (Fig 5C). This data suggest that evoked GABA release from HDB/MCPO neurons is not influenced by electrotonic conduction, similar to spontaneous release, and we propose that these fibers directly target the soma and/or proximal dendrite of GCs. Importantly, excitation of dSACs by cortical feedback projections is known to inhibit GCs. dSACs evoked inhibition onto GCs is, however, completely blocked in the presence of ionotropic glutamatergic blockers (Boyd *et al.*, 2012), ruling out the possibility that inhibition from dSACs could influence the inhibitory response observed in GCs after LightStim(Boyd *et al.*, 2012).

As expected, the amplitude from eIPSCs (blue) were larger than the sIPSCs amplitude (Fig5 C, grey, sIPSC 28.3±0.9 pA; $p<0.0001$), while the rise

time was slightly slower (sIPSC, 2.7±0.02; $p<0.0001$) and the decay time slightly faster (sIPSC, 55.94±1.36 ms; t-test $p<0.009$). This small difference in kinetics between evoked and spontaneous IPSCs recorded from the same cells, could reflect the increase in occurrence of a specific inhibitory synapses (more distal) evoked by GABAergic fibers stimulation, which could have GABA receptor of different composition.

3.3.4 Inhibitory neurons born in the adult brain contributes to GCs' inhibition

Another possible source of inhibition in GCs, are neighboring GCs. To examine this possibility, we selectively expressed ChR in GCs by AAV injections performed in the RMS (Fig 6A). GCs are constantly born in the adult brain (adult neurogenesis); cells born in the SVZ migrate through the RMS to the OB where they integrate in the olfactory network. More than 95% of adult born neurons differentiate into GCs and can form functional synaptic connections with MCs and other cellular components of the bulb, including PGs and neighboring GCs (Bardy *et al.*, 2010). As shown in Fig 6A, four w.p.i., the OB is extensively labeled with ChR+ GCs. ChR is expressed throughout the GC axis including soma and dendritic tree (Fig 6A, middle). LightStim onto these ChR+ GCs elicit a large desensitizing inward current (Fig 6A, right), in agreement with the characteristics of ChR mediated currents previously described (Boyden *et al.*, 2005).

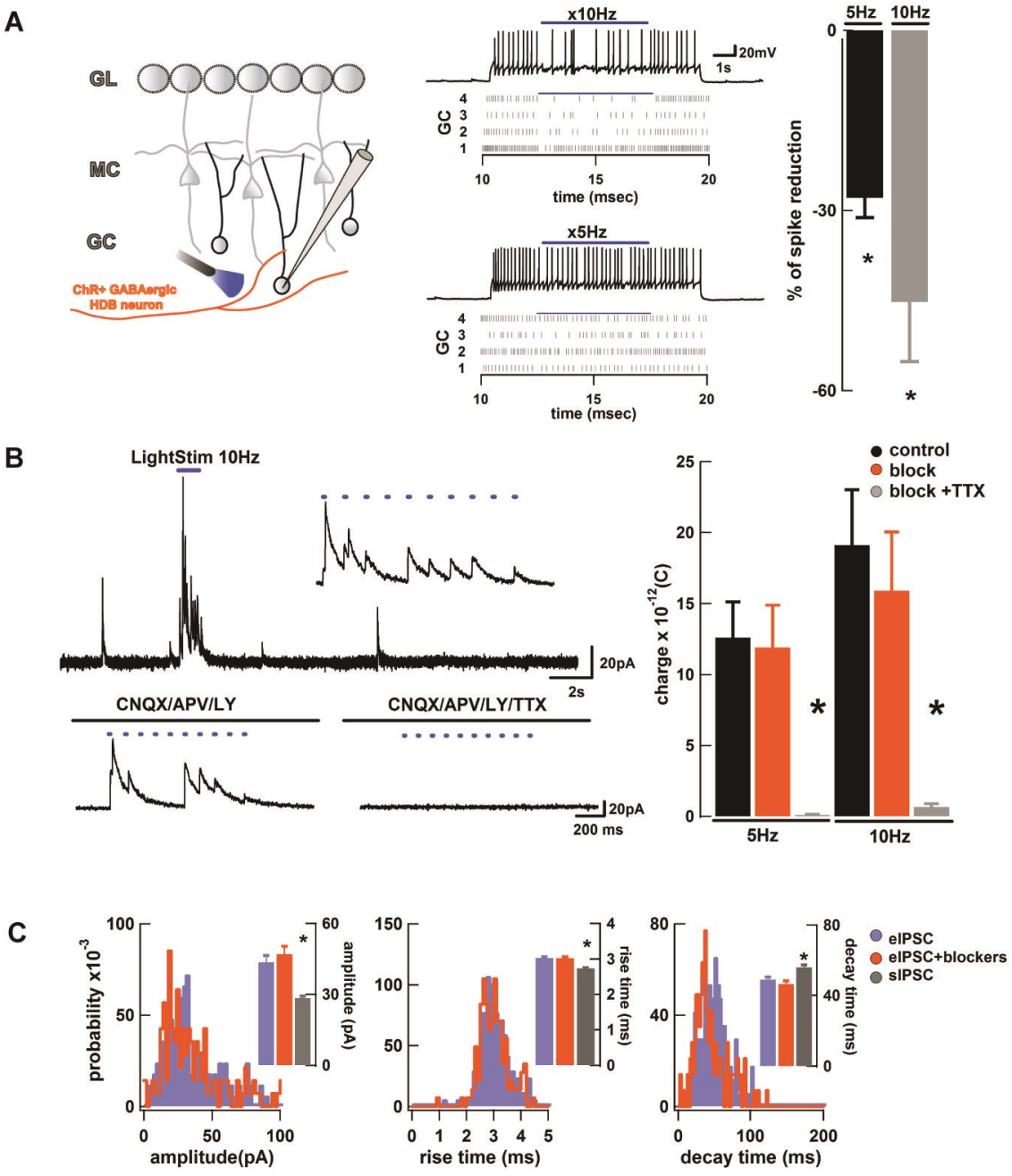

Fig 5: **Stimulation of ChR expressing HDB/MCPO GABAergic afferents inhibits GCs**. *(***A**) Left, diagram showing the typical recording arrangement used for these experiments; we recorded from GC surrounded by ChR+ GABAergic fibers and stimulated with pulses of blue light (LightStim). Middle, stimulation of GABAergic fibers with pulses of blue light (LightStim, 10 kHz) in the vicinity of a recorded GC, decreases the frequency of firing elicited by a depolarizing current stimulus (top traces). Lower traces show raster plots of 3 different GCs showing a fast and reversible change in action potential frequency induced by the LightStim. Right, summary bar graph showing that increasing the LightStim frequency produces larger increase in inhibition of firing in GCs (*p<0.004). (**B**) Left, representative trace of a GC with showing the occurrence of

sIPSCs at a low frequency. In this GC LightStim at 10 Hz elicits robust evoked IPSCs (eIPSCs). The inset shows a magnification of the eIPSCs induced by the LightStim. Bottom left, in the same cell, the LightStim eIPSCs were not affected by the addition of ionotropic and metabotropic glutamatergic transmission blockers (CNQX, 10 μM; APV, 100 μM; LY 100 μM) but were completely abolished by the addition of TTX (0.5 μM). Right, bar graph showing that the charge transfer, calculated from the integral of the eIPSCs, induced by LightStim at 5 and 10Hz, was not different in the presence of blockers (*p<0.03). (**C**) The amplitude probability distribution of eIPSCs (blue) and eIPSCs when the blockers were applied (orange) was not significantly different. Similarly, there was no difference in rise time or decay time. The kinetic analysis of the sIPCs, indicated that they exhibited slight differences compared to the eIPSCs with smaller amplitudes (*p<0.0001), faster rise times (*p<0.0001) and slower decay times (*p<0.009).

We performed VC recordings from ChR negative GCs located in the proximity of ChR+ cells to increase the possibility of finding connected pairs. LightStim under these conditions elicit inhibitory currents in 12 out of 38 cells (Fig6 B). Interestingly, kinetic analysis revealed that the amplitude of the eIPSCs (n=8) by ChR+ GCs, was larger compared to eIPCs elicited by HDB/MCPO stimulation (57.91±1.7 pA vs. 43.6±3; p<0.003). However, there was no difference in the rise and decay time, between the eIPSCs elicited by stimulation of ChR+GCs or GABAergic HDB/MCPO fibers (rise time 2.99±0.05ms vs. 3.01±0.04ms; p>0.06); decay time (47.72±2.1ms vs 48.9±1.5ms; p>0.6). The lack of difference in the kinetic parameters suggests that inhibition originating in neighboring GCs and basal forebrain GABAergic neurons is mediated by inhibitory synpases with overlapping distribution or GABA receptors with similar composition.

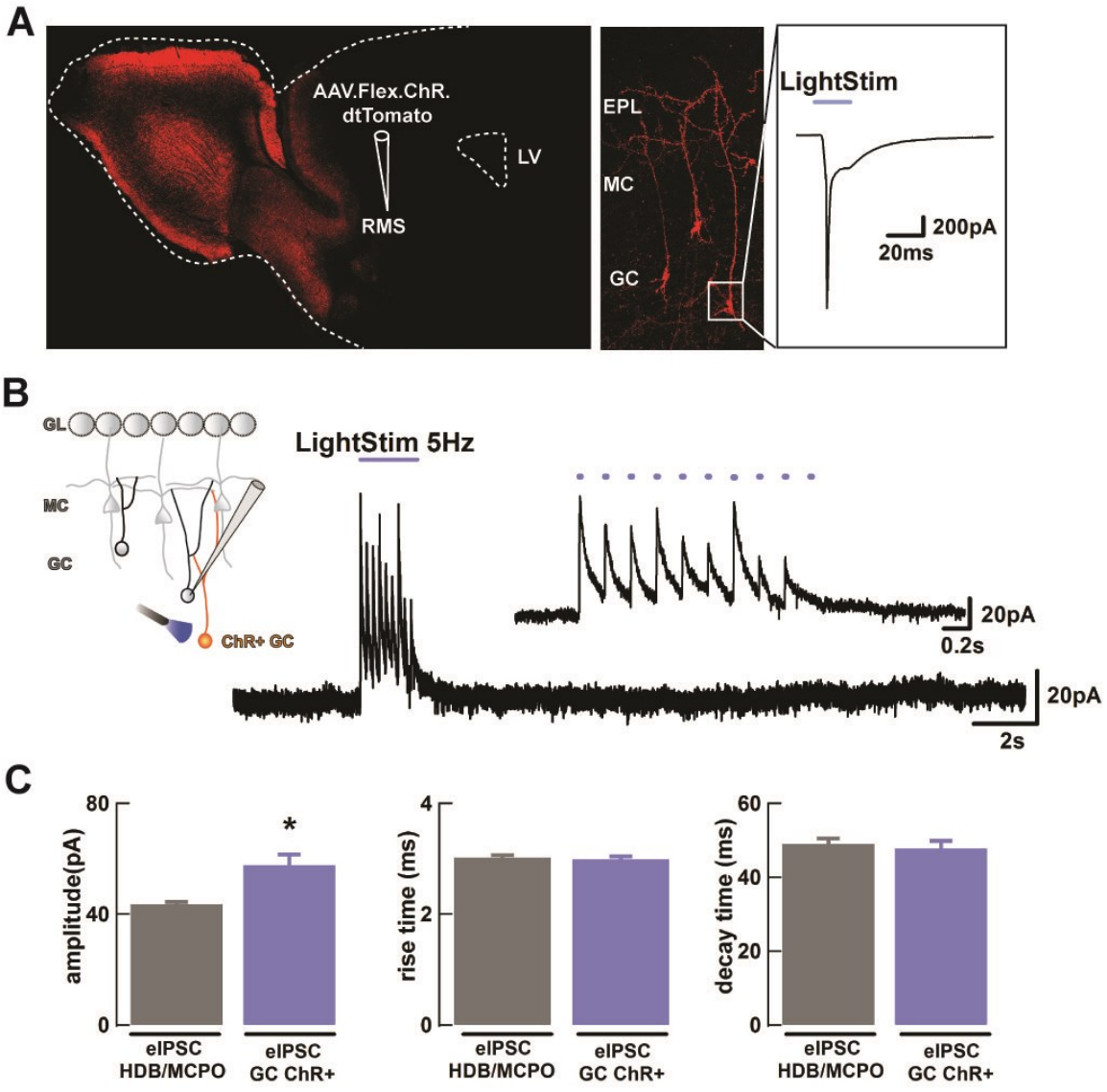

Fig6: **Selective stimulation of adult born GCs expressing ChR inhibits neighboring GCs**.(**A**) Left, Sagittal section of the OB of a GAD65-Cre mouse injected with AAV.Flex.ChR.dtTomato virus in the RMS to selectively express ChR in adult born, and migrating, GCs. Abundant labeling is present throughout the GC layer of the MOB and AOB. Middle, higher magnification of GC layer in the MOB, showing extensive labeling of the soma and dendritic tree in a few ChR+ GCs. Right, recording from a ChR+ GC, in this cell, a 100ms LightStim produces a fast desensitizing inward current. (**B**) Upper left, diagram showing the typical recording arrangement used for these experiments; we recorded from unlabeled GCs (no change elicited by LightStim) surrounded by ChR+ GCs.Right, a 5 Hz LightStim evoked inhibitory responses in a GC surrounded by adult born ChR+ GCs. (**C**) Left, bar graph showing that the LightStim eIPSCs had a larger mean amplitude compared to HDB/MCPO mediated eIPSC (t-test, *p<0.0003). There is no change in the kinetic parameters rise time or decay time.

The larger amplitude obtained when ChR+ cells were stimulated suggests that despite the low connectivity level found between GCs (31.6%), more GABA is being released by neighboring GCs than by HDB/MCPO neurons, that more synaptic contacts are made between GCs than between GABAergic fibers and/or that in connected GC-GC pairs, GABA release can occur in close proximity to the synaptic contact allowing it to reach a higher concentration in the synaptic cleft. Another possibility is that the inhibitory responses elicited by activation of ChR+ GCs activate $GABA_A$ receptors of different subunit composition, which could allow different amount of currents (i.e. channels with longer open times). However, the amount of charge tranfered in both conditions was no significantly different ruling out this possibility (ChR+ GCs stimulation: 12.8 ±4 x 10^{-12} C; HDB/MCPO stimulation: 12.6 ± 3 x 10^{-12} C; p>0.6).

We propose that basal forebrain GABAergic fibers innervates mostly GCs soma and proximal dendrites (see Fig 4A), whereas GABA release from neighboring GCs could be occurring at distal regions, where GABA release at DDS have been broadly documented, and/or at GCs' proximal dendrite and soma. In our experimental conditions the spatial source of the IPSCs cannot be identified performing a kinetic analysis of the evoked responses, since we are promoting a massive GABA release from these sources, masking the small changes in IPSC kinetics that could reflect their distal or proximal origin. Therefore, to further corroborate our physiological findings, we determined the expression and location of postsynaptic GABA receptors clusters using antibodies against gephyrin, an anchoring protein known to be essential to form

postsynaptic clusters of GABA receptors (Craig *et al.*, 1996; Sassoe-Pognetto, 2011) (Fig 7). GCs were labeled by electroporation of the green fluorescent protein (GFP) in the SVZ. Thirty days post injection, GFP+ cells born postnatally can be found in the OB exhibiting morphology of mature neurons (Fig 7, right). Confocal analysis of immunostaining against GFP and gephyrin indicated that GABA receptor clusters (red) can be found throughout the GCs' soma, proximal and apical dendrites (Fig 7; n=15 cells from 3 animals). More importantly, colocalization analysis of the Person's coefficient was performed to quantify clusters that were localized on the cell and not on its proximity. Only clusters exhibiting a positive correlation of the Pearson coefficient greater than 0.2 were considered for quantification (see methods). As shown in Fig 7C, we found cluster through the axis of the GC, however more cluster are found in the soma ($2.96\pm0.5/\mu m^2$), than in the proximal ($1.84\pm0.5/\mu m^2$) or apical dendrites ($1.22\pm0.4/\mu m^2$; t-test $p<0.02$).

We hypothesize that GABA inhibitory inputs onto the apical dendrite could have an important role modulating DDS between GCs and MCs. On the other hand, GABA inhibition into the soma, and mostly from the HDB, is necessary to globally maintain the excitatory/inhibitory balance onto GCs, and consequently regulate recurrent and lateral inhibition with MCs.

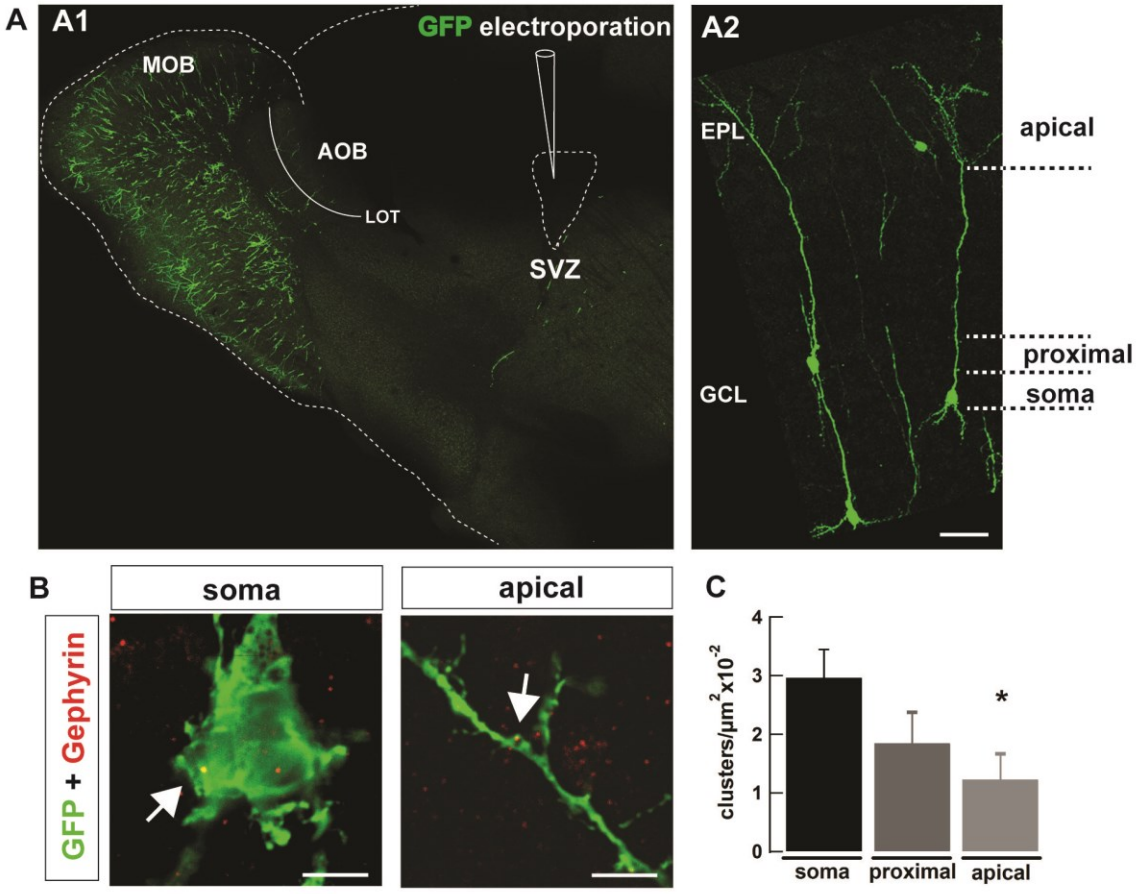

Fig7: **GABA receptor clusters can be found throughout the soma and dendritic extension of GCs**.(**A**) A1,Confocal reconstruction of the olfactory bulb showing postnatally born GCs labeled with the green fluorescent protein (GFP) using electroporation (see methods).A2, higher magnification confocal imaging showing GFP+ GCs with mature neuronal morphology as evidenced by the dendritic branching pattern and position; somata and proximal dendrites in the GC layer and apical dendrites extending their arborization into the external plexiform layer. Scale bar 50μm. (**B**) confocal imaging of a GC stained against GFP (green) and gephyrin, a postsynaptic GABA receptor clustering marker (red). White arrows show co-localization of GABA receptor clusters and GFP (yellow) in the soma and the apical dendrite of a GC. Scale bar 5μm. (**C**) Quantification of the number of clusters per area throughout the GC (n=15) shows that the soma exhibited the highest number of clusters (2.96±0.5/μm^2), followed by the proximal dendrite (1.84±0.5/μm^2). The apical dendrite exhibits a significantly lower number of GABA receptor clusters compared to the soma (1.22±0.4/μm^2; p<0.02).

3.3.5 GABA release from the basal forebrain is required for olfactory discrimination

Lateral inhibition mediated by GC-MC synaptic connectivity is thought to be an important mechanism for olfactory discrimination; in particular, the ability to discriminate between perceptually similar odorants or odor mixtures is thought to depend on lateral inhibition (Yokoi *et al.*, 1995). Moreover, changes in GC's activity, and therefore in their regulation of MCs function, have been shown to produce profound changes in olfactory mediated behaviors.

To determine the impact of HDB/MCPO inhibition in olfactory processing, we used Designer Receptors Exclusively Activated by a Designer Drug (DREADD) technology to selectively silence GABAergic neurons. DREADDs are muscarinic receptors that have been mutated to selectively respond to the exogenous compound clozapine-N-oxide (CNO) but not to the endogenous ligand acetylcholine (Armbruster *et al.*, 2007). We injected a Cre-dependent expression virus encoding the inhibitory DREADD (hM4Di) into the HDB/MCPO of GAD65-Cre mice. Four w.p.i, animals previously injected with DREADD in the HDB/MCPO were tested for olfactory discrimination, after PBS (control) or CNO injections (treated, Fig 8A). We used the habituation/dishabituation paradigm (see methods) using odors structurally similar (esters differing in one carbon). Animals presented three consecutive times to the "habituated" odor, ethyl heptanoate (C7), show a reduction in the sniffing time; in Fig 8, the normalized investigation time against the first odor presentation is graphed. Under control conditions (PBS), presentation of the novel odor (C8) resulted in a significant

increase in investigation time indicating that they are able to discriminate between the C7 and C8 esters (27.4±14 vs. 73.6±7, n=5, $p<0.01$). More importantly, the same animals were unable to discriminate the odor pair two hours after injection of CNO (0.5 mg/kg; C7, 14.6±9 vs. C8, 15.9±14, $p<0.4$). Previous behavioral studies have shown that maximal effects of CNO, acting on the DREADDs occurs within a short window of time (Krashes *et al.*, 2011; Sasaki *et al.*, 2011). Accordingly, 4 hours post CNO injection, mice begin to recover the ability to discriminate C7 and C8 (C7, 13.7±10 vs. C8, 73.5±36.6, $p<0.09$), indicating that the effect of CNO is reversible. A deficit in olfactory discrimination could be due to disruptions in odor detection thresholds. However, as shown in Fig 8C, the detection threshold of mice presented with various dilutions of the C7 ester was not different when injected with PBS or CNO (Fig 8C). In both conditions, animals habituated to a wooden block with water increased their investigation time when C7 was presented at a 1:30,000 dilution compared with the odor presented at a lower dilution of 1:40,000 (PBS: 2.96±1.3 vs. 1.28±0.7; CNO: 4.3±0.7 vs. 0.22±0.2 s). A similar detection threshold for C7 (1:30,000) was found in a control group of mice, injected with PBS or CNO (not shown). Our results indicate that afferent inhibition from the HDB onto GCs is also required for proper olfactory discrimination.

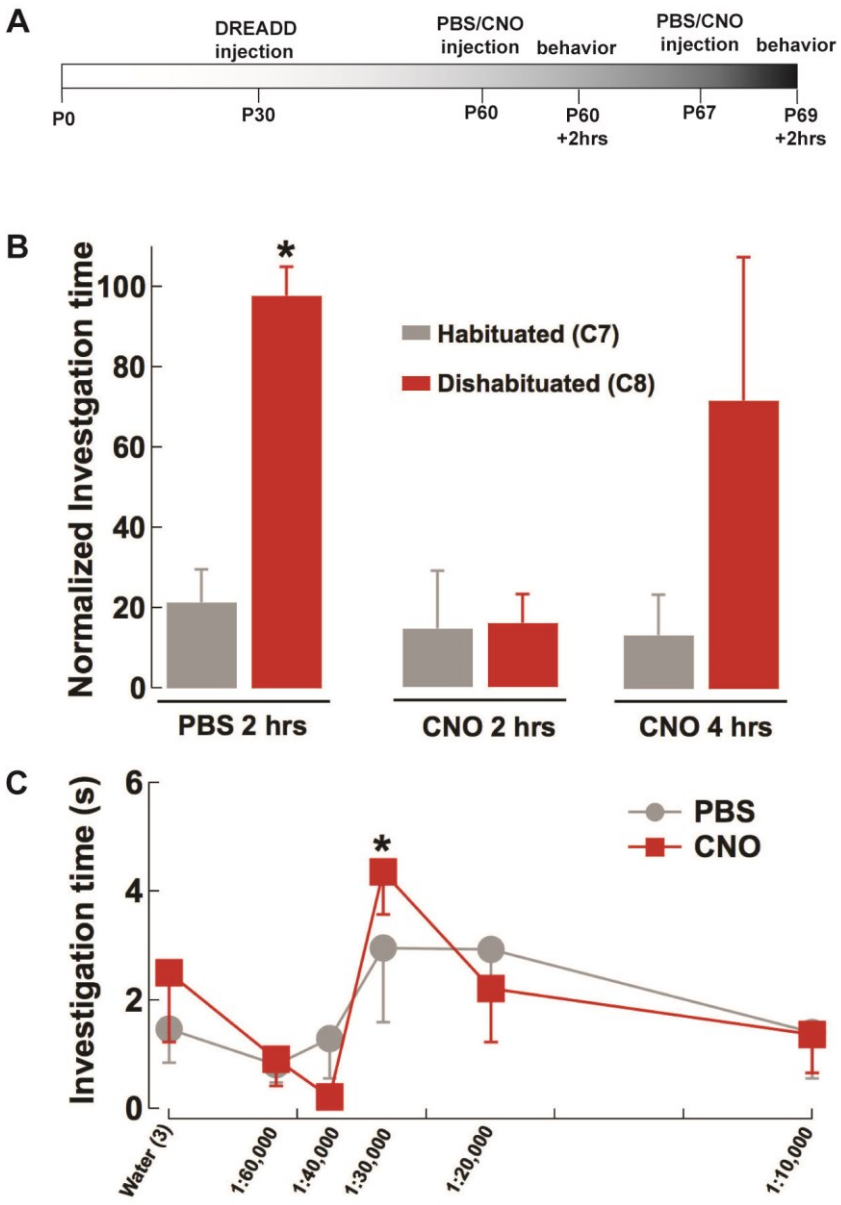

Fig8: **Inhibitory inputs from the HDB/MCPO are required for odor discrimination**. (**A**) Animals were injected with a virus encoding for hM4Di into the HDB/MCPO. 4 weeks later, animals received either a PBS (control condition) or a CNO (treated condition) intraperitoneal (i.p.) injection and tested for odor discrimination using the habituation/dishabitaution paradigm. Two days later the same animals are exposed to the reversed condition. (**B**) animals are presented three times with ethyl heptanoate (C7) followed by one presentation of ethyl octanoate (C8). Mice injected with PBS habituate to C7 and then dishabituate/discriminate when exposed C8. In the treated condition, animals failed to display the behavior 2 h.p.i. Four h.p.i the inability to discriminate between C7 and C8 was completely recovered. (**C**) odor threshold detection paradigm. The animals were injected with PBS or CNO and tested 2 hours later. Three water presentations were followed by C7 at different concentrations (from 1:60000 to 1:10000). Under both conditions animals recognized the odor at a dilution of 1:30000.

3.3.6 HDB/MCPO mediated inhibition of GCs is larger in the AOB

The AOB is the first relay station for pheromonal information process through sensory neurons in the VNO. Pheromonal cues are relevant to elicit proper social and reproductive behaviors in member of the same species and play a complementary role with the MOS in the processing of olfactory information (see Chapter 1). GABAergic afferent from the HDB/MCPO extensively innervates the GC layer of OB, including the AOB (Fig 4B3), suggesting that GCs in the AOB are also regulated by inhibition of the HDB/MCPO. As shown in Fig 9 LightStim of HDB/MCPO fibers largely reduced GCs firing rate during a depolarizing current stimulus at 5 (-55.2±9Hz, n=6, $p<0.002$) and 10Hz (-70.1±12Hz, n=4, $p<0.02$) (Fig 9A). Interestingly, LightStim at 5Hz in the AOB produced a significantly larger reduction in firing in GCs, when compared to the spike reduction produced in the MOB at the same frequency of stimulation ($p<0.02$). Similar to GCs in the MOB, LightStim produced a large outward current in cells of the AOB (20 out of 20 cells). The quantification of charge inlflux in these cells indicated that, like in the MOB, the addition of glutamatergic synaptic blockers (CNXQ, APV, LY) did not affect the inhibitory responses (Fig 9B). Similarly, the responses were completely blocked by the addition of TTX (control, 12.7±3; +blockers, 18.5±5 x 10^{-12} C; +blockers and TTX, 0.2±0.1 x 10^{-12} C; $p<0.02$). One possible explanation for the higher inhibition observed in GCs of the AOB, might be related to different $GABA_A$ receptor subunit compositions, with different kinetic properties. However, the charge flux in GCs produced by LightStim in the AOB, was not, significantly different to the

charge flux upon stimulation in the MOB. One possibility is that the same amount of charge has a bigger impact on GCs on the AOB, due to differences in the electrophysiological properties of the cell.

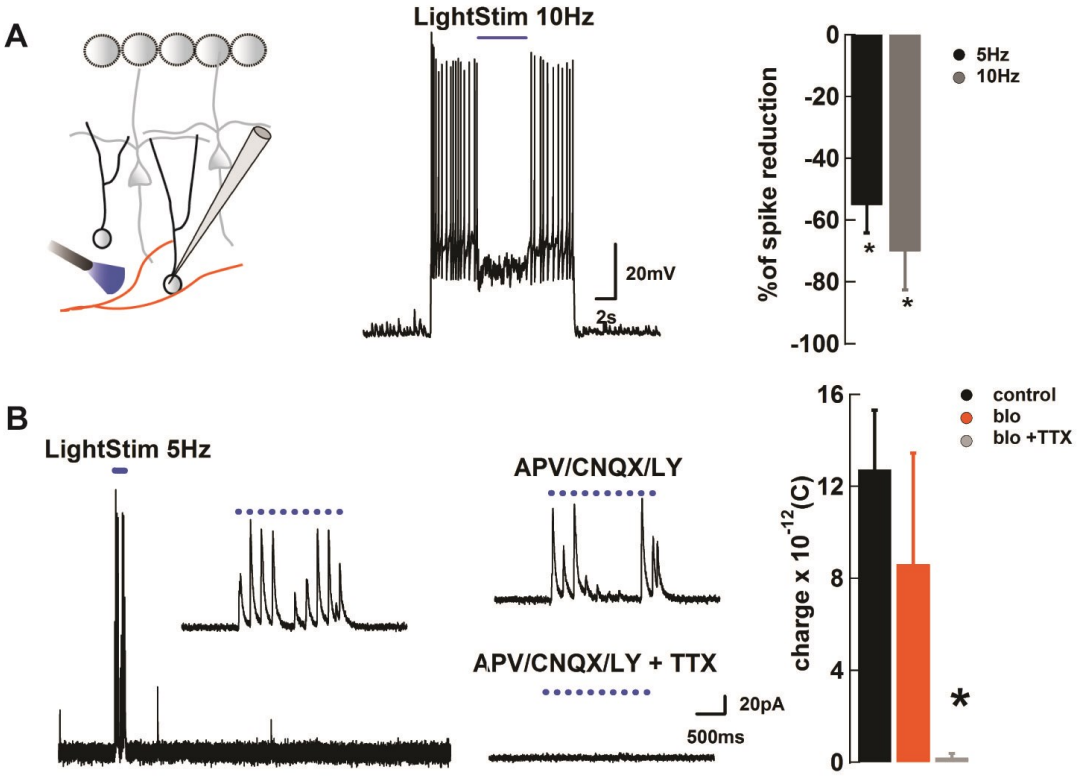

Fig9: **Optogenetic stimulation of GABAergic neurons in the HDB produces inhibitory responses in AOB.** (**A**) Middle, LightStim of the HDB fibers at 10Hz produces inhibition of stimulus-induced firing in GCs. Right, bar graph showing a significant decrease in the firing rate produced by LightStim at 5 and 10Hz (5Hz, ,*p< 0.002; 10Hz,*p< 0.02). (**B**) Left, representative trace of a GC in LightStim at 5 Hz elicits an evoked inhibitory response. This response was not affected by the addition of glutamatergic blockers but was completely abolished by the addition of TTX. Right, the charge flow induced by LightStim was not different in the presence of blockers, but completely abolished in the presence of TTX (*p<0.02).

Taken together, our results suggest that inhibition greatly affects GC excitability in the MOB and AOB. Furthermore, inhibitory regulation onto GCs arises from different sources suggesting that inhibition of GCs is compartmentalized, given the circuit a great flexibility to regulate the inhibitory tone in the OB under different behavioral demands. Moreover, we showed that this inhibition is required to elicit proper olfactory discrimination. We hypothesize that the inhibitory input, like excitatory input, act to maintain a proper balance for the strength of lateral inhibition in the OB, which is necessary for fine discrimination.

3.4. Discussion

We found that GCs receive abundant inhibition which decreases excitability and that this inhibtion arises from at least two different sources: the HDB/MCPO and neighboring GCs. Moreover, we found GABA receptor clusters in the soma, proximal and apical dendrites of GCs, suggesting that inhibition can affect different compartments of the GCs, where different types of computation occur. In addition, our results show, for the first time, that inhibition from the basal forebrain is required for olfactory discrimination, an olfactory ability essential for individuals' survival and reproduction.

3.4.1 Characterization of Inhibitory inputs onto GCs

Electrophysiological recordings in GCs, showed that GABA can hyperpolarize actively spiking GCs by eliciting an outward current mediated by

$GABA_A$ receptors as it was completely blocked by the $GABA_A$ antagonist GABAzine, and mimicked by the $GABA_A$ agonist muscimol. Other studies have shown that $GABA_A$ receptors are ubiquitously expressed in the OB in particular on MCs, where they mediate DDI, and also in GCs (Barnard *et al.*, 1998; Panzanelli *et al.*, 2004; Panzanelli *et al.*, 2005). $GABA_A$ receptors are pentameric structures composed by a wide arrange of subunits encoded by different genes (α, β, γ, δ, ε, π, ρ). In the central nervous systems combinations of two α and two β subunits with one or more γ, δ or ε can be found (Barnard *et al.*, 1998). MCs and GCs express $GABA_A$ receptors with different subunit composition; α1, α3, β2 are found in MCs, while α2 and β3 are predominantly expressed in GCs (Laurie *et al.*, 1992; Barnard *et al.*, 1998; Panzanelli *et al.*, 2005). Differences in subunit composition of GABA receptors have been shown to affect channel kinetics and GABA affinity, and therefore the kinetics of responses elicited by GABA in the cells where these synapses are present (Mortensen *et al.*, 2011). Thus, the difference in subunit composition of GABA receptors in different neuronal types in the OB suggests that GABA inhibition may have a different role in these cell types.

Distinct sources of GABAergic inputs regulate GCs activity: neighboring GCs, or other local inhibitory neurons, and GABAergic afferents from the basal forebrain. One aim of our study was to produce a detailed kinetic analysis of IPSCs in GCs, which could uncover, and perhaps distinguish, between different populations of inhibitory responses. The kinetic properties of the currents caused by spontaneous vesicle release depend on several factors. For instance, at the

presynaptic site, the probability of multiquantal release, variation on the vesicular neurotransmitter content and clearance of neurotransmitters in the postsynaptic cleft could all affect the efficacy of a neurotransmitter in the postsynaptic cell. Similarly, in the postsynaptic membrane, subunit composition of receptors and number and density of receptors in the synaptic specializations, can also affect synaptic strength (Nusser *et al.*, 2001; Mortensen *et al.*, 2011). Comparison o of sIPCSs and mIPSCs revealed slight differences in the kinetic parameters; the mean amplitude decreased and the rise time and decay time increased in the mIPSCs. A likely explanation is that application of the blockers, in which the mIPSCs are recorded, increased GC resistance, improving clamping of distal regions, and increasing the length constant of the cells, allowing the detection of events that occur in distal regions from the soma. Therefore, we propose the existence of a population of IPSCs that result from GABA release onto distal regions of GCs (i.e. apical dendrite). This can have important consequences in olfactory processing, since most of DDI occurs in the distal dendrites (Shepherd *et al.*, 2007; Sassoe-Pognetto, 2011). This possibility is also supported by work from the Strowbridge group (Balu *et al.*, 2007), in which they stimulated excitatory inputs onto the apical dendrite or the soma of GCs. They found that both populations of EPSCs exhibited different kinetic properties: EPSCs originated in the apical dendrite had slower rise time and smaller amplitudes compared to the EPSCs originated in the soma. In addition, the frequency of IPSCs did not change in TTX. These results indicate that neurons releasing GABA are mostly in a non-spiking state, or that their spiking is independent on

TTX sensitive channels. For example, in the MOB it has been shown that Ca^{+2} influx through voltage gated calcium channels can generate low threshold calcium spikes insensitive to TTX in GCs (Pinato & Midtgaard, 2003; Egger *et al.*, 2005). Addressing, this issue is challenging, as most available Ca^{+2} channel blockers could not distinguish between block Ca^{+2} spikes and block of vesicular release. More importantly, the lack of effect on IPSCs frequency in the presence of glutamatergic blockers indicates that the inhibitory currents recorded in GCs do not depend on excitatory transmission and that they correspond to direct activation of GCs. Evidence have indicated local inhibition of GCs is produced by the activaton of local interneurons activated by excitatory afferent fibers (Boyd *et al.*, 2012). Importantly, the site of inhibition can have different consequences affecting GC excitability and information processing. Inhibitory inputs targeting the apical dendrite might have a great incidence regulating DDI in the EPL while somatic inputs could exert a more global effect on GCs activity, regulating not only local DDI, but also lateral inhibition.

3.4.2 GABA released from neurons in the HDB/MCPO and neighbor GCs inhibit GCs

The HDB/MCPO receives inputs from several regions of the brain including the OB, amygdala, hypothalamus and brainstem (Linster & Hasselmo, 2000; Wang & Swann, 2006). At the same time, it projects cholinergic and GABAergic afferents to the OB (Zaborszky *et al.*, 1986; Gaykema *et al.*, 1990; Gracia-Llanes *et al.*, 2010), suggesting that activation of this nuclei could impact olfactory processing. Early experiments in which the HDB/MCPO was electrically

stimulated elicited conflicting results. For instance some groups reported that activation of this forebrain nucleus elicited GC excitation and MC inhibition (Kunze *et al.*, 1992a; Kunze *et al.*, 1992b), while others showed that electrical stimulation of this nucleus had a dual effect on MCs, an excitation followed by inhibition (Nickell & Shipley, 1988). Due to the technical constraints of electrical stimulation it has not been possible to isolate the effects of any particular neuronal population until only recently (Ma & Luo, 2012). We also note that most of these previous studies have addressed the role of the HDB from the perspective of cholinergic modulation in the OB. Here, for the first time, we expressed ChR in GABAergic neurons of the HDB/MCPO to selectively stimulate GABA release from these cells. In agreement with studies using anterograde tracing (Gracia-Llanes *et al.*, 2010), we found that ChR+ fibers mostly innervate the GC layer. Some fibers also reached the GL and almost no ChR+ fibers were observed in the MC layer or EPL. These results suggest that HDB/MCPO exert its inhibitory action primarily onto GC soma, which could have an important global effect in GCs' activity.

Olfactory network oscillations at different frequencies are associated with MC's firing synchronization and olfactory processing. Specifically, oscillations in the theta rhythm (4-12 Hz) follow the respiratory cycle frequency and are proposed to mediate olfactory learning in go-no go tasks (Kay, 2005). Therefore, we used two different frequencies of LightStim, 5Hz and 10Hz. The first one has been associated with animal passive sniffing, while the latter has been measured when the animal is actively localizing or sniffing an odor. Both frequencies

decreased GCs' spiking, with a larger response occurring at LightStim of 10Hz. Importantly, 91% of recorded GCs exhibited outward currents upon LightStim, suggesting that most of GCs receive inhibitory inputs from the basal forebrain.

Since ChR+ fibers were concentrated in the GCL, it is safe to speculate that HDB/MCPO-GCs synaptic connections occur preferentially in GCs' soma and/or proximal dendrite. Accordingly, blocking excitatory inputs did not have an effect in the kinetic properties of the eIPSCs, that is, they are not affected by changes in the electrotonic properties of the cells. Also, in agreement with the synchronous and larger release of GABA from GABAergic terminals induced by LightStim the eIPSCs exhibit a larger amplitude than the sIPSCs.

GCs are the most abundant cells in the OB; they are tightly packed in one thick layer of the bulb extending their dendrite apical to the EPL, where dendritic spines form DDS with MCs. Therefore, GABA release by one GC could reach neighboring GCs promoting inhibition. GC-GC inhibition can be produced by at least two different stimuli: localized overspill of GABA at DDS in the EPL or by GABA released in the EPL and GC layer after a global depolarization of GCs. Recently, it has been shown that GCs born postnatally, once properly integrated in the bulbar network, can inhibit other GCs (Bardy *et al.*, 2010). Ablation of adult neurogenesis decreases inhibition onto MCs and surprisingly, selective stimulation of newborn neurons facilitates olfactory learning and memory (Nissant & Pallotto, 2011; Alonso *et al.*, 2012). To study the role of GABA release from neighboring GCs, we selectively expressed ChR in GCs born in the adult brain. We found that contrary to the abundant response to LightStim when we

stimulated GABAergic axon from the HDB, responses to LightStim were sparser, with only ~ 30% of the GC exhibiting inhibitory responses, despite our abundant labeling of GCs. It has been estimated that ~50% newborn cells arriving into the OB die before integration (Petreanu & Alvarez-Buylla, 2002). Nevertheless, the activity in GCs upon LightStim is larger that the previously reported by the Lledo group that found only a ~17% of GC-GC synaptic connectivity using a similar experimental approach (Bardy *et al.*, 2010). Interestingly, the kinetic analysis of the eIPSCs by stimulation of neighboring GCs, indicated no difference in rise and decay time when compared to the eIPSCs elicited by stimulation of HDB/MCPO GABAergic terminals. One possibility is that inhibition in GCs, regardless of the input, is mediated by the same type of $GABA_A$ receptors (i.e. subunit composition). It has been shown that at least two types of alpha subunits are expressed in GCs: α1 and α3. Superficial GCs mainly express α3, while deep GCs mainly express α1 (Panzanelli *et al.*, 2005; Lagier *et al.*, 2007; Sassoe-Pognetto, 2011). All our recordings were performed in deep GCs, suggesting that the inhibitory currents in these GCs correspond to the activation of only one receptor type. On the other hand, the eIPSCs elicited from neighboring GCs was larger compared to the eIPSC elicited by HDB/MCPO stimulation. This difference might arise from a larger release of GABA from ChR+ cells or from a higher number of inhibitory connections between GC-GC than GC-HDB/MCPO. To elucidate this question additional experiments need to be performed in which LightStim could be localized to a smaller area (i.e. two-photon stimulation) to

elicit GABA release from a single terminal, for example a dendritic spine, an compared with that of stimulation of GABAergic fibers.

The morphology and synaptic connectivity of GCs within the OB network dictates their functional involvement in shaping MC output, in fact the only output of GCs is to MCs. As mentioned above, spatially restricted excitation of GC dendrites can produce localized inhibition of MC through recurrent inhibition, while a global activation of GCs (i.e. somatic excitation) can affect a larger number of MCs through lateral inhibition (Isaacson & Strowbridge, 1998). Similarly, GABAergic inhibitory inputs can potentially exert actions locally or globally. As predicted by our results, we found that GCs expressed GABA receptors clusters in their soma, proximal and apical dendrites, suggesting that GCs inhibition can regulate GCs' activity at different levels, and as argued, with different physiological effect on GC excitability. Similarly, in the hippocampus a great variety of interneurons affect pyramidal cells activity (Freund & Buzsaki, 1996). Some interneurons produce perisomatic inhibition, while others make synaptic contact preferentially in the dendritic branches of pyramidal cells (dendritic targeting interneurons). Perisomatic targeting interneurons are known to strongly affect Na+ mediated action potential initiation and network oscillations (Freund & Katona, 2007). Dendritic targeting interneurons, on the other hand, affect local synaptic integration and filtering of input information (Miles *et al.*, 1996). Moreover, abnormal perisomatic inhibition onto cortical pyramidal cells is suggested to produce activity dysfunctions that lead to epileptic foci (Freund & Katona, 2007). In the MOB, we found that GCs express a greater number of

GABA receptors clusters in the soma, suggesting that inhibition onto GCs can have important consequences for olfactory processing. Inputs in this area will produce global inhibition of GCs, as opposed to the local inhibition produced when GABA is release onto the apical dendrite, which could produce different effects on recurrent and later inhibition of MCs.

3.4.3 Basal forebrain mediated inhibition onto GCs is required for olfactory discrimination.

Proper olfactory coding depends on several circuitry properties, such as local synaptic connectivity but also network properties. Oscillations in the MOB are known to be particularly important for information processing. As mentioned above theta rhythm or the respiratory frequency between 4-12 Hz, mediates some aspects of learning through MC cell spiking synchronization (Ravel *et al.*, 2003). Other frequencies, such as the γ oscillations (40-70Hz) are also known to mediate olfactory behaviors, such as olfactory discrimination (Nusser *et al.*, 2001). There is evidence that γ oscillations, initially thought to be an intrinsic property of the bulbar circuitry (Neville & Haberly, 2003), arise from the interaction between cortical structures and bulbar components (Boyd *et al.*, 2012) and that GABA inhibition onto GCs is required to maintain proper levels of γ oscillations (Nusser *et al.*, 2001). In terms of local synaptic connectivity, cortical axo-somatic inputs onto GCs are believed to globally affect GCs excitability. This excitatory connection could depolarize GCs releasing the Mg+2 block in NMDA receptors facilitating DDI and lateral inhibition (Balu *et al.*, 2007). We propose an opposite function for the somatic inhibitory input form the HDB/MCPO.

Our results suggest that GABA released from the HDB/MCPO could act primarily through axo-somatic interaction onto GCs. Therefore, we hypothesize that disrupting basal forebrain inhibition onto GCs, could have a negative impact on olfactory discrimination. We used the habituation/dishabituation test, a paradigm used to evaluate odor discrimination and short term memory in mice (Yang & Crawley, 2009). This test evaluates the ability to discern two odor stimuli as well as short-term memory as the mouse has to remember the previously exposed subsequent odors. Silencing the HDB/MCPO inhibitory drive onto the OB completely disrupted the discrimination between two structurally similar odorants, measured by a lack of dishabituation when the animal was exposed to the novel odor. Others studies have shown that lesions in the HDB, impair the animals ability to habituate to consecutive presentations of an odor (Paolini & McKenzie, 1993) our behavioral test showed that these mice had no deficit in habituation. Acetylcholine has been involved in memory formation in several brain regions (Dani & Bertrand, 2007), suggesting that its release from the HDB could play a role in short-term memory formation required for olfactory habituation. Therefore, by lesioning the HDB, GABAergic as well as cholinergic neurons projections are disrupted. This situation is bypassed in our experimental setup, where the effect observed correspond solely to GABAergic neurons inactivation. Other groups, on the other hand, have shown no disruption in olfactory memory formation when acetylcholine concentration is manipulated in the bulb (Devore & Linster, 2012). Therefore, inhibitory inputs from this area can

have an unexpected and important role in olfactory discrimination, attributed to acetylcholine in the past.

3.4.4 Inhibition from the HDB/MCPO inhibit GCs in the AOB

The AOS play an important complimentary role in social olfactory cues processing. In mammals, it is critical to elicit behaviors such as aggression, motivational approach toward receptive females and pregnancy block, when a recently mated female is expose to an unfamiliar male (for review see Dulac & Torello, 2003; Keller *et al.*, 2009). Interestingly, stimulation of ChR+ fibers, as in the MOB, inhibited AOB GCs spiking. Importantly, the degree of inhibition was larger in the GCs of the AOB when compared to the MOB. AOS mediated behavior are gated by a direct connection from MCs in the AOB to the Vomeronasal Amygdala and to the hypothalamus (Bartoshuk & Beauchamp, 1994; Dulac & Torello, 2003; Keverne, 2004). Rely of information then, unlike in the MOB, bypasses cortical structures and elicit fast endocrine changes that regulate behavioral output. Therefore, the AOS relies even more for extensive odor processing by fine tuning MCs output through GC-MC DDS in the AOB. Despite the larger inhibitory effect on spiking in the AOB, the magnitude of inhibitory currents was not different (as assessed by the charge) compared to stimulation of the HDB/MCPO fibers in the MOB. Therefore, GCs in the AOB could have different electrophysiological properties that make them more sensitive to inhibition (i.e. less excitatory inputs that shunts inhibition). We are currently studying this possibility.

GCs are one of the main components of olfactory processing in the OB. They are thought to integrate bottom-up and top-down information to properly regulate the MCs output. Here, we showed that GCs receive extensive inhibition from different sources that could affect GCs activity. Inhibition from neighboring GCs and global inhibition from HDB/MCPO afferent fibers could affect the OB inhibitory tone locally or in extensive regions of the bulb. Indeed for the first time we showed that inhibition onto GCs is required for proper olfactory discrimination.

Future experiments need to be performed in order to determine the role that GC-GC and dSAC-GC inhibition have in olfactory processing. Finally, inhibition onto GCs could also have an impact decoding information about social cues, since the GCs in the AOB are also inhibitory control

CHAPTER 4: CONCLUDING REMARKS AND FUTURE EXPERIMENTS

4.1 Concluding Remarks

Tight control of odor processing is an important determinant of an individual's survival, including a high-risk situation (i.e. predator proximity). Among the cellular components of the OB circuit, output by MCs is importantly regulated by the activity of GCs, which are in turn highly regulated by local and extrinsic neurons. Here, we showed that new inhibitory cells, in particular GCs are recruited by olfactory stimuli (Chapter 2) and that proper regulation of GCs by inhibition is required for the maintenance of olfactory behaviors that rely in odor discrimination (Chapter 3). Inhibition of GCs is a novel mechanism by which olfactory output can be regulated, and therefore odor processing. There are several questions, however, that remain to be answered. Among them, how does GABA released from adult generated neurons affect olfactory coding? How does inhibition arising from centrifugal fibers affect GCs synaptic processing? How is excitation and inhibition integrated in GCs and how is the balance excitation/inhibition maintained? What are the behavioral states that lead to GCs get exited or inhibited? Considering all the evidence presented in this work, we propose the following model for the role of inhibition of GCs in the MOB (Fig 1):

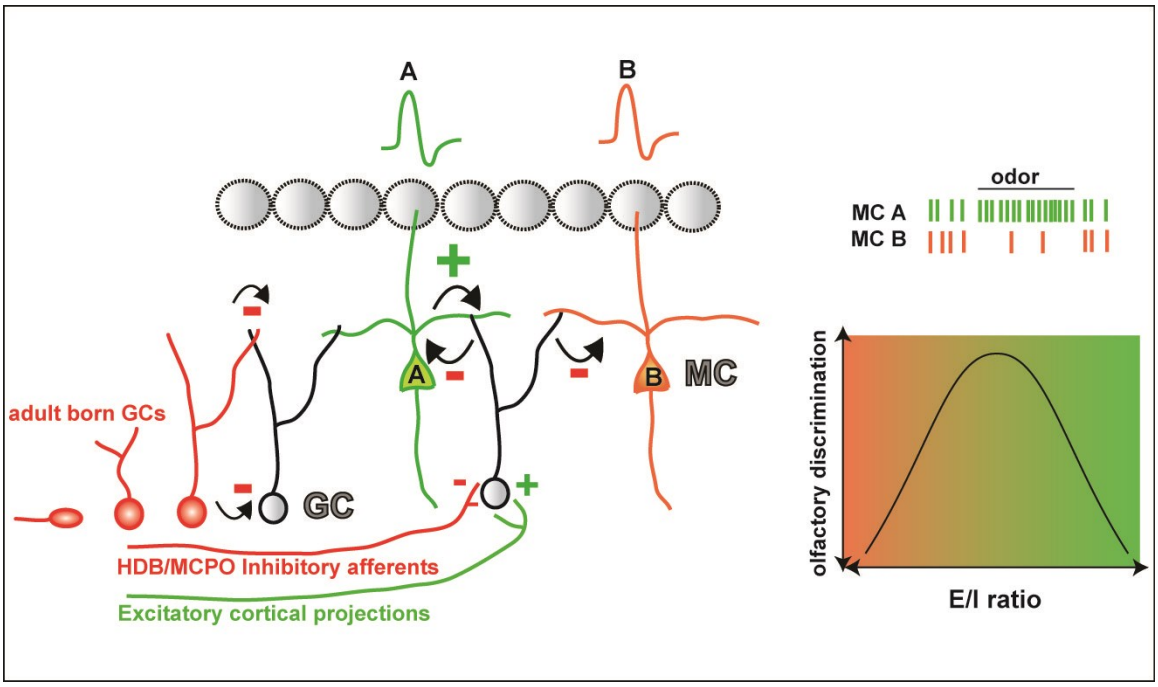

Fig1: **Inhibition onto GCs is required for proper olfactory discrimination**. GCs receive excitatory inputs from DDS and from cortical projections. Inhibition from GABAergic neurons in the HDB/MCPO or by other local inhibitory neurons can offset this excitation. A strong odor (A), stimulates MC A (green), which will excite a GC through DDS. When the weaker odor (B) is presented, MC B is excited. GC excitation by MC A can reach suprathreshold potential and produce extensive GABA release from this GC and inhibit a neighboring MC (MC B). Inhibition or excitation in the soma of GC can affect GC excitability and its ability to perform DDI. An adequate excitation/inhibition balance onto GCs is required to exert adequate MC induced lateral inhibition (graph, bottom right). Too much inhibition (or absence of excitation) in GCs will reduce lateral inhibition, while too much excitation is expected to increase inhibition regardless of the input to MC. Hypothetical MCs' output after the presentation of odor A and B is shown on the right. The inhibitory tone in the OB is in addition modified by the constant supply of inhibitory neurons.

Due to the anatomy and synaptic connectivity of the olfactory system, information is processed in the MOB in "column-like" functional units and in "region-like" columns in the AOB (see Chapter 1). It has been shown that excitation of a MC by an olfactory stimulus can inhibit neighboring MCs, increasing the output of more salient stimuli to higher brain areas. This lateral inhibition is mediated by GCs; specifically, activation of MC A by odor A, will

excite GCs through DDS. GCs will in turn release GABA locally (reciprocal inhibition), however, a stronger stimulus would produce a larger activation of MC A, leading to a suprathreshold excitation on GCs, causing GCs to inhibit neighboring MCs. If a weaker odor (odor B) is presented at the same time that odor A, MC A will enhance lateral inhibition and strongly inhibit the output of MC B. This computation has been shown to mediate olfactory discrimination by enhancing odor contrast and decreasing background noise. In this general view, events that modify GC excitability other than activation of DDS, (i.e. excitatory feedback from cortex) should promote lateral inhibition. On, the other hand, events that lead to global inhibition of the GCs (work presented here) would have the opposite effect on lateral inhibition, decreasing it. However, we found that olfactory discrimination was impaired in the absence of inhibition onto GCs. This unexpected finding lead us to propose that normal lateral inhibition occurs only at a set balance of excitation/inhibition (E/I) onto GCs. Extreme GC excitation will increase lateral inhibition regardless of the value of the olfactory stimulus and therefore reduce odor discrimination (Fig 1, right diagram). Similarly, too much inhibition onto GCs on the other hand, will decrease lateral inhibition impairing the ability of an animal to discriminate between two odors. Therefore as mentioned above, we propose the need of a proper balance between excitation/inhibition of GCs. In our model, a moderate level of excitation favors lateral inhibition, more than inhibition does; hence, the peak of the curve for odor discrimination is not centered at a ratio of 1. As shown in the diagram the inhibitory input onto GCs can be activated locally, that is from neighboring GCs,

and more globally from the HDB. However, the inhibition despicted in the curve on the right represent the effect of global inhibition.

In some situations, animals need to quickly distinguish between different odors (i.e. predator vs. conspecific urine) and quickly react; while in others situations they need to finely discriminate between odors blends emitted by a conspecific (i.e. female urine in estrous vs. anestrous state). In the former case, the olfactory cue needs to quickly trigger an escape behavior. In this situation, where no fine perceptual discrimination is needed, global inhibition or an imbalance of the excitation/inhibition ratio of GCs can be important to increase the salience of the output of a few MCs, those cells activated by odor predator. In fact, some single odor molecules, like TMZ, can induce an intense fear response in rodents. On the other hand when animals need to extract precise information (through discrimination) global excitation of GCs may be more important. Nevertheless, as explained above a ratio that is too large or low decreases odor discrimination. In summary, we propose that inhibition from GABAergic fibers of the basal forebrain participates maintaining a proper inhibition/excitation balance for adequate olfactory processing.

How can adult generated neurons affect lateral inhibition? Our laboratory and others have demonstrated that newborn GCs recruitment is induced by olfactory stimuli. Thus, specific activation of bulbar columns or regions could selectively promote the integration of GCs, augmenting the possibility of sharpening responses by increasing the inhibition of DDS associated with those columns (i.e. associated with the salient odor stimuli that activated the MCs).

Indeed our work in the AOB showed that there was a differential increase in neurogenesis across the anterior-posterior axis depending on the type of olfactory stimuli the animals were exposed to, further supporting this hypothesis.

Under what circumstances is inhibiton from the basal forebrain or neighboring GCs recruited? The OB sends excitatory projection to the HDB/MCPO and this area in turn project afferents back to the OB. This loop of connectivity could mediate fast changes in olfactory coding by the OB, depending on rapid changes in environmental context. The recruitment of adult generated neurons is on the other hand, regulated by chronic exposure to different behavioral contexts (mating, aggression, etc). The integration of newborn neurons is thought to be important to maintain the plasticity in the olfactory system, required for long-term learning and memory.

In summary, we found that inhibition in the OB is tightly regulated by a constant addition of inhibitory interneurons, and this addition can be regulated by behavior. More importantly, these inhibitory neurons are regulated by inhibitory inputs originated from local and extrinsic circuits and this inhibitory control is crucial for adequate olfactory information processing.

4.2 Future experiments

As discussed in Chapter 2, integration newly born neurons in the adult OB is stimulated by several physiological conditions and behaviors, including odor enrichment, mate choice and pregnancy (Gheusi *et al.*, 2009). We showed that

there is a region-specific increase in neurogenesis in the AOB, which correlated with the type of pheromonal stimulation the animals were exposed to. Although there is strong evidence supporting the role of neurogenesis iin olfactory memory and learning in the MOB (Mak *et al.*, 2007; Moreno *et al.*, 2009; Alonso *et al.*, 2012), little is known about the role of neuronal integration in social behaviors, such as mating and aggression. To further gain insight on the functional role of adult generated GCs, adult born neurons can be selectively stimulated while measuring the animals' behavioral output. For instance, ChR can be selectively expressed in adult born neurons, as shown in chapter 2. Then stimulation can be performed *in vivo* through an optic fiber inserted with cannula directly into the AOB or MOB. On the other hand, ablation of adult neurogenesis can be achieved by perfussing the mitotic blocker cytosine arabinoside (AraC) directly into the SVZ. These type of experiments can help to answer the question whether inhibition coming from newborn neurons in sufficient to elicit behavioral changes.

At the cellular level, the integration of new neurons into an already existing network is an intriguing process, of which very little is known. One possible mechanism involved in this process is the proposed regulation of excitation/inhibition ratio of GCs. This ratio changes dramatically as migrating neuroblasts form into mature neurons (Lledo *et al.*, 2006). Notoriously, inhibitory inputs mature quicker than excitatory inputs and recent evidence has shown that GABA signaling have a critical role influencing newborn neurons structural maturation and integration in the MOB in response to sensory stimulation

(Nissant & Pallotto, 2011; Pallotto *et al.*, 2012). Despite the importance that GABAergic signaling has in the integration of newly born neurons, we do not know what are the sources of GABA that promote these changes. A further future goal is to study the effect of basal forebrain GABA release onto newborn neurons and study how it can affect their survival and integration. Electrophysiologically, adult born neurons can be selectively labeled with GFP by viral injection in the RMS. At the same time a viral injection of ChR can be expressed in GABAergic neurons of the HDB/MCPO. Four weeks later, GFP+cells (adult generated neurons) and HDB/MCPO fibers positive for ChR, will be found in the OB. At this time, recordings will be made from green adult generated neurons at the same time that GABAergic afferents from the basal forebrain are stimulated. Behaviorally, one possible approach is to selectively silence the HCB/MCPO GABAergic fibers (with viral DREADD injections, chapter3) for a determined period of time and measure the impact of reducing GABA release from this source in the number of neurons that reach and integrate in the bulb. Newborn neurons in this case will be labeled with BrdU to quantify neurogenesis.

We showed that synaptic inhibition from neighboring GCs and HDB/MCPO fibers affect GC activity and we concluded that inhibition from the HDB/MCPO is mostly axo-somatic. Our experiments, however, did not allow us to determine the location of inhibition onto GCs, when GABA was released from neighboring GCs. In these experiments, to elicit GABA release from ChR+cells we used a blue light stimulus that affected a large area of the slice. A more

precise stimulation can be achieved by using a laser source for blue light. This affords more spatial control, and local stimulation can be selectively performed in different regions of the recorded GCs (apical dendrite vs. soma).

Finally, we proposed that a correct balance between excitation and inhibition onto GCs is necessary to establish a proper inhibitory tone in the OB. To further test this hypothesis we will independently control excitatory and inhibitory pathways. One way to approach this could be by studying the effect of selective optogenetic stimulation of the HDB/MCPO and the piriform cortex at the same time. A new version of ChR that can induce depolarization with green light has become recently available (Yizhar *et al.*, 2011). Thus, each neuronal population (excitatory pyramidal cells in the piriform cortex and GABAergic neurons in the HDB/MCPO) could be infected with ChR responsive to either blue or green light in the same animal. Then, the degree of stimulation of each pathway can be independently modified at the same time. It has been suggested that proper olfactory processing depends on the relative timing between dendrodendritic excitation and GLU release from cortical pyramidal neurons onto GCs (Balu *et al.*, 2007). Therefore, *in vivo* stimulation of cortical neurons and GABAergic HDB/MCPO neurons, will help us to elucidate the effect of GCs excitation/inhibition balance onto olfactory processing and perception, in particular how these systems affect time dependent processing.

BIBLIOGRAPHY

Ahlenius, H., Visan, V., Kokaia, M., Lindvall, O. & Kokaia, Z. (2009) Neural stem and progenitor cells retain their potential for proliferation and differentiation into functional neurons despite lower number in aged brain. *J Neurosci*, **29**, 4408-4419.

Alonso, M., Lepousez, G., Sebastien, W., Bardy, C., Gabellec, M.M., Torquet, N. & Lledo, P.M. (2012) Activation of adult-born neurons facilitates learning and memory. *Nat Neurosci*, **15**, 897-904.

Alonso, M., Viollet, C., Gabellec, M.M., Meas-Yedid, V., Olivo-Marin, J.C. & Lledo, P.M. (2006) Olfactory discrimination learning increases the survival of adult-born neurons in the olfactory bulb. *J Neurosci*, **26**, 10508-10513.

Altman, J. & Das, G.D. (1965a) Autoradiographic and histological evidence of postnatal hippocampal neurogenesis in rats. *J Comp Neurol*, **124**, 319-335.

Altman, J. & Das, G.D. (1965b) Post-natal origin of microneurones in the rat brain. *Nature*, **207**, 953-956.

Araneda, R.C. & Firestein, S. (2006) Adrenergic enhancement of inhibitory transmission in the accessory olfactory bulb. *J Neurosci*, **26**, 3292-3298.

Arevian, A.C., Kapoor, V. & Urban, N.N. (2008) Activity-dependent gating of lateral inhibition in the mouse olfactory bulb. *Nat Neurosci*, **11**, 80-87.

Armbruster, B.N., Li, X., Pausch, M.H., Herlitze, S. & Roth, B.L. (2007) Evolving the lock to fit the key to create a family of G protein-coupled receptors potently activated by an inert ligand. *Proc Natl Acad Sci U S A*, **104**, 5163-5168.

Balu, R., Pressler, R.T. & Strowbridge, B.W. (2007) Multiple modes of synaptic excitation of olfactory bulb granule cells. *J Neurosci*, **27**, 5621-5632.

Bardy, C., Alonso, M., Bouthour, W. & Lledo, P.M. (2010) How, when, and where new inhibitory neurons release neurotransmitters in the adult olfactory bulb. *J Neurosci*, **30**, 17023-17034.

Barnard, E.A., Skolnick, P., Olsen, R.W., Mohler, H., Sieghart, W., Biggio, G., Braestrup, C., Bateson, A.N. & Langer, S.Z. (1998) International Union of Pharmacology. XV. Subtypes of gamma-aminobutyric acidA receptors: classification on the basis of subunit structure and receptor function. *Pharmacol Rev*, **50**, 291-313.

Bartoshuk, L.M. & Beauchamp, G.K. (1994) Chemical senses. *Annu Rev Psychol*, **45**, 419-449.

Baum, M.J. & Kelliher, K.R. (2009) Complementary roles of the main and accessory olfactory systems in mammalian mate recognition. *Annu Rev Physiol*, **71**, 141-160.

Bean, N.J. (1982) Olfactory and vomeronasal mediation of ultrasonic vocalizations in male mice. *Physiol Behav*, **28**, 31-37.

Belluscio, L., Koentges, G., Axel, R. & Dulac, C. (1999) A map of pheromone receptor activation in the mammalian brain. *Cell*, **97**, 209-220.

Belluzzi, O., Benedusi, M., Ackman, J. & LoTurco, J.J. (2003) Electrophysiological differentiation of new neurons in the olfactory bulb. *J Neurosci*, **23**, 10411-10418.

Beshel, J., Kopell, N. & Kay, L.M. (2007) Olfactory bulb gamma oscillations are enhanced with task demands. *J Neurosci*, **27**, 8358-8365.

Bovetti, S., Veyrac, A., Peretto, P., Fasolo, A. & De Marchis, S. (2009) Olfactory enrichment influences adult neurogenesis modulating GAD67 and plasticity-related molecules expression in newborn cells of the olfactory bulb. *PLoS One*, **4**, e6359.

Boyd, A.M., Sturgill, J.F., Poo, C. & Isaacson, J.S. (2012) Cortical feedback control of olfactory bulb circuits. *Neuron*, **76**, 1161-1174.

Boyden, E.S., Zhang, F., Bamberg, E., Nagel, G. & Deisseroth, K. (2005) Millisecond-timescale, genetically targeted optical control of neural activity. *Nat Neurosci*, **8**, 1263-1268.

Brennan, P.A., Kendrick, K.M. & Keverne, E.B. (1995) Neurotransmitter release in the accessory olfactory bulb during and after the formation of an olfactory memory in mice. *Neuroscience*, **69**, 1075-1086.

Brennan, P.A. & Keverne, E.B. (1997) Neural mechanisms of mammalian olfactory learning. *Prog Neurobiol*, **51**, 457-481.

Brennan, P.A., Schellinck, H.M. & Keverne, E.B. (1999) Patterns of expression of the immediate-early gene egr-1 in the accessory olfactory bulb of female mice

exposed to pheromonal constituents of male urine. *Neuroscience*, **90**, 1463-1470.

Brill, M.S., Ninkovic, J., Winpenny, E., Hodge, R.D., Ozen, I., Yang, R., Lepier, A., Gascon, S., Erdelyi, F., Szabo, G., Parras, C., Guillemot, F., Frotscher, M., Berninger, B., Hevner, R.F., Raineteau, O. & Gotz, M. (2009) Adult generation of glutamatergic olfactory bulb interneurons. *Nat Neurosci*, **12**, 1524-1533.

Bruce, H.M. (1959) An exteroceptive block to pregnancy in the mouse. *Nature*, **184**, 105.

Buck, L. & Axel, R. (1991) A novel multigene family may encode odorant receptors: a molecular basis for odor recognition. *Cell*, **65**, 175-187.

Buck, L.B. (1996) Information coding in the vertebrate olfactory system. *Annu Rev Neurosci*, **19**, 517-544.

Carleton, A., Petreanu, L.T., Lansford, R., Alvarez-Buylla, A. & Lledo, P.M. (2003) Becoming a new neuron in the adult olfactory bulb. *Nat Neurosci*, **6**, 507-518.

Castro, J.B., Hovis, K.R. & Urban, N.N. (2007) Recurrent dendrodendritic inhibition of accessory olfactory bulb mitral cells requires activation of group I metabotropic glutamate receptors. *J Neurosci*, **27**, 5664-5671.

Chamero, P., Marton, T.F., Logan, D.W., Flanagan, K., Cruz, J.R., Saghatelian, A., Cravatt, B.F. & Stowers, L. (2007) Identification of protein pheromones that promote aggressive behaviour. *Nature*, **450**, 899-902.

Chaudhury, D., Escanilla, O. & Linster, C. (2009) Bulbar acetylcholine enhances neural and perceptual odor discrimination. *J Neurosci*, **29**, 52-60.

Chen, W.R., Xiong, W. & Shepherd, G.M. (2000) Analysis of relations between NMDA receptors and GABA release at olfactory bulb reciprocal synapses. *Neuron*, **25**, 625-633.

Clancy, A.N., Coquelin, A., Macrides, F., Gorski, R.A. & Noble, E.P. (1984) Sexual behavior and aggression in male mice: involvement of the vomeronasal system. *J Neurosci*, **4**, 2222-2229.

Colom, L.V. (2006) Septal networks: relevance to theta rhythm, epilepsy and Alzheimer's disease. *J Neurochem*, **96**, 609-623.

Craig, A.M., Banker, G., Chang, W., McGrath, M.E. & Serpinskaya, A.S. (1996) Clustering of gephyrin at GABAergic but not glutamatergic synapses in cultured rat hippocampal neurons. *J Neurosci*, **16**, 3166-3177.

Dani, J.A. & Bertrand, D. (2007) Nicotinic acetylcholine receptors and nicotinic cholinergic mechanisms of the central nervous system. *Annu Rev Pharmacol Toxicol*, **47**, 699-729.

Dawley, E.M. & Crowder, J. (1995) Sexual and seasonal differences in the vomeronasal epithelium of the red-backed salamander (Plethodon cinereus). *J Comp Neurol*, **359**, 382-390.

Devore, S. & Linster, C. (2012) Noradrenergic and cholinergic modulation of olfactory bulb sensory processing. *Front Behav Neurosci*, **6**, 52.

Dong, H.W., Heinbockel, T., Hamilton, K.A., Hayar, A. & Ennis, M. (2009) Metabotropic glutamate receptors and dendrodendritic synapses in the main olfactory bulb. *Ann N Y Acad Sci*, **1170**, 224-238.

Dorries, K.M., Adkins-Regan, E. & Halpern, B.P. (1997) Sensitivity and behavioral responses to the pheromone androstenone are not mediated by the vomeronasal organ in domestic pigs. *Brain Behav Evol*, **49**, 53-62.

Dudley, C.A. & Moss, R.L. (1999) Activation of an anatomically distinct subpopulation of accessory olfactory bulb neurons by chemosensory stimulation. *Neuroscience*, **91**, 1549-1556.

Dulac, C. (2000) Sensory coding of pheromone signals in mammals. *Curr Opin Neurobiol*, **10**, 511-518.

Dulac, C. & Axel, R. (1995) A novel family of genes encoding putative pheromone receptors in mammals. *Cell*, **83**, 195-206.

Dulac, C. & Torello, A.T. (2003) Molecular detection of pheromone signals in mammals: from genes to behaviour. *Nat Rev Neurosci*, **4**, 551-562.

Easaw, J.C., Petrov, T. & Jhamandas, J.H. (1997) An electrophysiological study of neurons in the horizontal limb of the diagonal band of Broca. *Am J Physiol*, **272**, C163-172.

Egger, V., Svoboda, K. & Mainen, Z.F. (2005) Dendrodendritic synaptic signals in olfactory bulb granule cells: local spine boost and global low-threshold spike. *J Neurosci*, **25**, 3521-3530.

Enwere, E., Shingo, T., Gregg, C., Fujikawa, H., Ohta, S. & Weiss, S. (2004) Aging results in reduced epidermal growth factor receptor signaling, diminished olfactory neurogenesis, and deficits in fine olfactory discrimination. *J Neurosci*, **24**, 8354-8365.

Escanilla, O., Arrellanos, A., Karnow, A., Ennis, M. & Linster, C. (2010) Noradrenergic modulation of behavioral odor detection and discrimination thresholds in the olfactory bulb. *Eur J Neurosci*, **32**, 458-468.

Eyre, M.D., Antal, M. & Nusser, Z. (2008) Distinct deep short-axon cell subtypes of the main olfactory bulb provide novel intrabulbar and extrabulbar GABAergic connections. *J Neurosci*, **28**, 8217-8229.

Farbman, A.I. (1992) *Cell biology of olfaction*. Cambridge University Press, Cambridge ; New York, N.Y., USA.

Fiber, J.M. & Swann, J.M. (1996) Testosterone differentially influences sex-specific pheromone-stimulated Fos expression in limbic regions of Syrian hamsters. *Horm Behav*, **30**, 455-473.

Fowler, C.D., Liu, Y., Ouimet, C. & Wang, Z. (2002) The effects of social environment on adult neurogenesis in the female prairie vole. *J Neurobiol*, **51**, 115-128.

Freund, T.F. & Buzsaki, G. (1996) Interneurons of the hippocampus. *Hippocampus*, **6**, 347-470.

Freund, T.F. & Katona, I. (2007) Perisomatic inhibition. *Neuron*, **56**, 33-42.

Gaykema, R.P., Luiten, P.G., Nyakas, C. & Traber, J. (1990) Cortical projection patterns of the medial septum-diagonal band complex. *J Comp Neurol*, **293**, 103-124.

Gheusi, G., Ortega-Perez, I., Murray, K. & Lledo, P.M. (2009) A niche for adult neurogenesis in social behavior. *Behav Brain Res*, **200**, 315-322.

Gracia-Llanes, F.J., Crespo, C., Blasco-Ibanez, J.M., Nacher, J., Varea, E., Rovira-Esteban, L. & Martinez-Guijarro, F.J. (2010) GABAergic basal forebrain afferents innervate selectively GABAergic targets in the main olfactory bulb. *Neuroscience*, **170**, 913-922.

Gritti, I., Henny, P., Galloni, F., Mainville, L., Mariotti, M. & Jones, B.E. (2006) Stereological estimates of the basal forebrain cell population in the rat, including neurons containing choline acetyltransferase, glutamic acid decarboxylase or phosphate-activated glutaminase and colocalizing vesicular glutamate transporters. *Neuroscience*, **143**, 1051-1064.

Guerin, D., Peace, S.T., Didier, A., Linster, C. & Cleland, T.A. (2008) Noradrenergic neuromodulation in the olfactory bulb modulates odor habituation and spontaneous discrimination. *Behav Neurosci*, **122**, 816-826.

Guo, J., Zhou, A. & Moss, R.L. (1997) Urine and urine-derived compounds induce c-fos mRNA expression in accessory olfactory bulb. *Neuroreport*, **8**, 1679-1683.

Halabisky, B., Friedman, D., Radojicic, M. & Strowbridge, B.W. (2000) Calcium influx through NMDA receptors directly evokes GABA release in olfactory bulb granule cells. *J Neurosci*, **20**, 5124-5134.

Halem, H.A., Baum, M.J. & Cherry, J.A. (2001) Sex difference and steroid modulation of pheromone-induced immediate early genes in the two zones of the mouse accessory olfactory system. *J Neurosci*, **21**, 2474-2480.

Halpern, M., Shapiro, L.S. & Jia, C. (1995) Differential localization of G proteins in the opossum vomeronasal system. *Brain Res*, **677**, 157-161.

Hasselmo, M.E. & Sarter, M. (2011) Modes and models of forebrain cholinergic neuromodulation of cognition. *Neuropsychopharmacology*, **36**, 52-73.

Heinrichs, S.C. & Koob, G.F. (2006) Application of experimental stressors in laboratory rodents. *Curr Protoc Neurosci*, **Chapter 8**, Unit8 4.

Hellier, J.L., Arevalo, N.L., Blatner, M.J., Dang, A.K., Clevenger, A.C., Adams, C.E. & Restrepo, D. (2010) Olfactory discrimination varies in mice with different levels of alpha7-nicotinic acetylcholine receptor expression. *Brain Res*, **1358**, 140-150.

Herrada, G. & Dulac, C. (1997) A novel family of putative pheromone receptors in mammals with a topographically organized and sexually dimorphic distribution. *Cell*, **90**, 763-773.

Huang, L. & Bittman, E.L. (2002) Olfactory bulb cells generated in adult male golden hamsters are specifically activated by exposure to estrous females. *Horm Behav*, **41**, 343-350.

Hudson, R. & Distel, H. (1986) Pheromonal release of suckling in rabbits does not depend on the vomeronasal organ. *Physiol Behav*, **37**, 123-128.

Hurst, J.L. & Beynon, R.J. (2004) Scent wars: the chemobiology of competitive signalling in mice. *Bioessays*, **26**, 1288-1298.

Imamura, K., Mataga, N. & Mori, K. (1992) Coding of odor molecules by mitral/tufted cells in rabbit olfactory bulb. I. Aliphatic compounds. *J Neurophysiol*, **68**, 1986-2002.

Inamura, K., Kashiwayanagi, M. & Kurihara, K. (1999) Regionalization of Fos immunostaining in rat accessory olfactory bulb when the vomeronasal organ was exposed to urine. *Eur J Neurosci*, **11**, 2254-2260.

Isaacson, J.S. & Strowbridge, B.W. (1998) Olfactory reciprocal synapses: dendritic signaling in the CNS. *Neuron*, **20**, 749-761.

Jahr, C.E. & Nicoll, R.A. (1982) An intracellular analysis of dendrodendritic inhibition in the turtle in vitro olfactory bulb. *J Physiol*, **326**, 213-234.

Jakupovic, J., Kang, N. & Baum, M.J. (2008) Effect of bilateral accessory olfactory bulb lesions on volatile urinary odor discrimination and investigation as well as mating behavior in male mice. *Physiol Behav*, **93**, 467-473.

Jia, C. & Halpern, M. (1996) Subclasses of vomeronasal receptor neurons: differential expression of G proteins (Gi alpha 2 and G(o alpha)) and segregated projections to the accessory olfactory bulb. *Brain Res*, **719**, 117-128.

Jia, C. & Halpern, M. (1997) Segregated populations of mitral/tufted cells in the accessory olfactory bulb. *Neuroreport*, **8**, 1887-1890.

Kalinchuk, A.V., McCarley, R.W., Stenberg, D., Porkka-Heiskanen, T. & Basheer, R. (2008) The role of cholinergic basal forebrain neurons in adenosine-mediated homeostatic control of sleep: lessons from 192 IgG-saporin lesions. *Neuroscience*, **157**, 238-253.

Kaneko, N., Okano, H. & Sawamoto, K. (2006) Role of the cholinergic system in regulating survival of newborn neurons in the adult mouse dentate gyrus and olfactory bulb. *Genes Cells*, **11**, 1145-1159.

Kang, N., Baum, M.J. & Cherry, J.A. (2009) A direct main olfactory bulb projection to the 'vomeronasal' amygdala in female mice selectively responds to volatile pheromones from males. *Eur J Neurosci*, **29**, 624-634.

Kay, L.M. (2005) Theta oscillations and sensorimotor performance. *Proc Natl Acad Sci U S A*, **102**, 3863-3868.

Kay, L.M. & Sherman, S.M. (2007) An argument for an olfactory thalamus. *Trends Neurosci*, **30**, 47-53.

Keller, M., Baum, M.J., Brock, O., Brennan, P.A. & Bakker, J. (2009) The main and the accessory olfactory systems interact in the control of mate recognition and sexual behavior. *Behav Brain Res*, **200**, 268-276.

Keller, M., Douhard, Q., Baum, M.J. & Bakker, J. (2006) Destruction of the main olfactory epithelium reduces female sexual behavior and olfactory investigation in female mice. *Chem Senses*, **31**, 315-323.

Kelliher, K.R., Spehr, M., Li, X.H., Zufall, F. & Leinders-Zufall, T. (2006) Pheromonal recognition memory induced by TRPC2-independent vomeronasal sensing. *Eur J Neurosci*, **23**, 3385-3390.

Kempermann, G. & Gage, F.H. (2002) Genetic determinants of adult hippocampal neurogenesis correlate with acquisition, but not probe trial performance, in the water maze task. *Eur J Neurosci*, **16**, 129-136.

Keverne, E.B. (1995) Olfactory learning. *Curr Opin Neurobiol*, **5**, 482-488.

Keverne, E.B. (2004) Importance of olfactory and vomeronasal systems for male sexual function. *Physiol Behav*, **83**, 177-187.

Kimoto, H. & Touhara, K. (2005) Induction of c-Fos expression in mouse vomeronasal neurons by sex-specific non-volatile pheromone(s). *Chem Senses*, **30 Suppl 1**, i146-147.

Koolhaas, J.M., De Boer, S.F., De Rutter, A.J., Meerlo, P. & Sgoifo, A. (1997) Social stress in rats and mice. *Acta Physiol Scand Suppl*, **640**, 69-72.

Kovacs, T. (2004) Mechanisms of olfactory dysfunction in aging and neurodegenerative disorders. *Ageing Res Rev*, **3**, 215-232.

Krashes, M.J., Koda, S., Ye, C., Rogan, S.C., Adams, A.C., Cusher, D.S., Maratos-Flier, E., Roth, B.L. & Lowell, B.B. (2011) Rapid, reversible activation of AgRP neurons drives feeding behavior in mice. *J Clin Invest*, **121**, 1424-1428.

Kumar, A., Dudley, C.A. & Moss, R.L. (1999) Functional dichotomy within the vomeronasal system: distinct zones of neuronal activity in the accessory olfactory bulb correlate with sex-specific behaviors. *J Neurosci*, **19**, RC32.

Kunze, W.A., Shafton, A.D., Kem, R.E. & McKenzie, J.S. (1992a) Intracellular responses of olfactory bulb granule cells to stimulating the horizontal diagonal band nucleus. *Neuroscience*, **48**, 363-369.

Kunze, W.A., Shafton, A.D., Kemm, R.E. & McKenzie, J.S. (1992b) Olfactory bulb output neurons excited from a basal forebrain magnocellular nucleus. *Brain Res*, **583**, 327-331.

Lagier, S., Panzanelli, P., Russo, R.E., Nissant, A., Bathellier, B., Sassoe-Pognetto, M., Fritschy, J.M. & Lledo, P.M. (2007) GABAergic inhibition at dendrodendritic synapses tunes gamma oscillations in the olfactory bulb. *Proc Natl Acad Sci U S A*, **104**, 7259-7264.

Larsen, C.M., Kokay, I.C. & Grattan, D.R. (2008) Male pheromones initiate prolactin-induced neurogenesis and advance maternal behavior in female mice. *Horm Behav*, **53**, 509-517.

Laurie, D.J., Seeburg, P.H. & Wisden, W. (1992) The distribution of 13 GABAA receptor subunit mRNAs in the rat brain. II. Olfactory bulb and cerebellum. *J Neurosci*, **12**, 1063-1076.

Lee, S.H. & Dan, Y. (2012) Neuromodulation of brain states. *Neuron*, **76**, 209-222.

Lemasson, M., Saghatelyan, A., Olivo-Marin, J.C. & Lledo, P.M. (2005) Neonatal and adult neurogenesis provide two distinct populations of newborn neurons to the mouse olfactory bulb. *J Neurosci*, **25**, 6816-6825.

Levine, C. & Marcillo, A. (2008) Origin and endpoint of the olfactory nerve fibers: as described by Santiago Ramon y Cajal. *Anat Rec (Hoboken)*, **291**, 741-750.

Leypold, B.G., Yu, C.R., Leinders-Zufall, T., Kim, M.M., Zufall, F. & Axel, R. (2002) Altered sexual and social behaviors in trp2 mutant mice. *Proc Natl Acad Sci U S A*, **99**, 6376-6381.

Lin, D.Y., Zhang, S.Z., Block, E. & Katz, L.C. (2005) Encoding social signals in the mouse main olfactory bulb. *Nature*, **434**, 470-477.

Linster, C. & Hasselmo, M.E. (2000) Neural activity in the horizontal limb of the diagonal band of broca can be modulated by electrical stimulation of the olfactory bulb and cortex in rats. *Neurosci Lett*, **282**, 157-160.

Lledo, P.M., Alonso, M. & Grubb, M.S. (2006) Adult neurogenesis and functional plasticity in neuronal circuits. *Nat Rev Neurosci*, **7**, 179-193.

Lledo, P.M. & Lazarini, F. (2007) Neuronal replacement in microcircuits of the adult olfactory system. *C R Biol*, **330**, 510-520.

Lledo, P.M., Merkle, F.T. & Alvarez-Buylla, A. (2008) Origin and function of olfactory bulb interneuron diversity. *Trends Neurosci*, **31**, 392-400.

Lledo, P.M. & Saghatelyan, A. (2005) Integrating new neurons into the adult olfactory bulb: joining the network, life-death decisions, and the effects of sensory experience. *Trends Neurosci*, **28**, 248-254.

Loebel, D., Scaloni, A., Paolini, S., Fini, C., Ferrara, L., Breer, H. & Pelosi, P. (2000) Cloning, post-translational modifications, heterologous expression and ligand-binding of boar salivary lipocalin. *Biochem J*, **350 Pt 2**, 369-379.

Lois, C. & Alvarez-Buylla, A. (1993) Proliferating subventricular zone cells in the adult mammalian forebrain can differentiate into neurons and glia. *Proc Natl Acad Sci U S A*, **90**, 2074-2077.

Lois, C. & Alvarez-Buylla, A. (1994) Long-distance neuronal migration in the adult mammalian brain. *Science*, **264**, 1145-1148.

Lomas, D.E. & Keverne, E.B. (1982) Role of the vomeronasal organ and prolactin in the acceleration of puberty in female mice. *J Reprod Fertil*, **66**, 101-107.

Louie, K. & Glimcher, P.W. (2012) Efficient coding and the neural representation of value. *Ann N Y Acad Sci*, **1251**, 13-32.

Luo, M., Fee, M.S. & Katz, L.C. (2003) Encoding pheromonal signals in the accessory olfactory bulb of behaving mice. *Science*, **299**, 1196-1201.

Ma, M. & Luo, M. (2012) Optogenetic activation of basal forebrain cholinergic neurons modulates neuronal excitability and sensory responses in the main olfactory bulb. *J Neurosci*, **32**, 10105-10116.

Magavi, S.S., Mitchell, B.D., Szentirmai, O., Carter, B.S. & Macklis, J.D. (2005) Adult-born and preexisting olfactory granule neurons undergo distinct experience-dependent modifications of their olfactory responses in vivo. *J Neurosci*, **25**, 10729-10739.

Mak, G.K., Enwere, E.K., Gregg, C., Pakarainen, T., Poutanen, M., Huhtaniemi, I. & Weiss, S. (2007) Male pheromone-stimulated neurogenesis in the adult female brain: possible role in mating behavior. *Nat Neurosci*, **10**, 1003-1011.

Mandairon, N., Ferretti, C.J., Stack, C.M., Rubin, D.B., Cleland, T.A. & Linster, C. (2006) Cholinergic modulation in the olfactory bulb influences spontaneous olfactory discrimination in adult rats. *Eur J Neurosci*, **24**, 3234-3244.

Mandarim-de-Lacerda, C.A. (2003) Stereological tools in biomedical research. *An Acad Bras Cienc*, **75**, 469-486.

Mandiyan, V.S., Coats, J.K. & Shah, N.M. (2005) Deficits in sexual and aggressive behaviors in Cnga2 mutant mice. *Nat Neurosci*, **8**, 1660-1662.

Markopoulos, F., Rokni, D., Gire, D.H. & Murthy, V.N. (2012) Functional properties of cortical feedback projections to the olfactory bulb. *Neuron*, **76**, 1175-1188.

Martel, K.L. & Baum, M.J. (2007) Sexually dimorphic activation of the accessory, but not the main, olfactory bulb in mice by urinary volatiles. *Eur J Neurosci*, **26**, 463-475.

Martel, K.L. & Baum, M.J. (2009) A centrifugal pathway to the mouse accessory olfactory bulb from the medial amygdala conveys gender-specific volatile pheromonal signals. *Eur J Neurosci*, **29**, 368-376.

Maruniak, J.A., Wysocki, C.J. & Taylor, J.A. (1986) Mediation of male mouse urine marking and aggression by the vomeronasal organ. *Physiol Behav*, **37**, 655-657.

Matsutani, S. & Yamamoto, N. (2008) Centrifugal innervation of the mammalian olfactory bulb. *Anat Sci Int*, **83**, 218-227.

Mayhew, T.M. & Gundersen, H.J. (1996) If you assume, you can make an ass out of u and me': a decade of the disector for stereological counting of particles in 3D space. *J Anat*, **188 (Pt 1)**, 1-15.

Merkle, F.T., Mirzadeh, Z. & Alvarez-Buylla, A. (2007) Mosaic organization of neural stem cells in the adult brain. *Science*, **317**, 381-384.

Miles, R., Toth, K., Gulyas, A.I., Hajos, N. & Freund, T.F. (1996) Differences between somatic and dendritic inhibition in the hippocampus. *Neuron*, **16**, 815-823.

Ming, G.L. & Song, H. (2005) Adult neurogenesis in the mammalian central nervous system. *Annu Rev Neurosci*, **28**, 223-250.

Mirich, J.M., Williams, N.C., Berlau, D.J. & Brunjes, P.C. (2002) Comparative study of aging in the mouse olfactory bulb. *J Comp Neurol*, **454**, 361-372.

Mitra, R., Sundlass, K., Parker, K.J., Schatzberg, A.F. & Lyons, D.M. (2006) Social stress-related behavior affects hippocampal cell proliferation in mice. *Physiol Behav*, **89**, 123-127.

Mombaerts, P., Wang, F., Dulac, C., Chao, S.K., Nemes, A., Mendelsohn, M., Edmondson, J. & Axel, R. (1996) Visualizing an olfactory sensory map. *Cell*, **87**, 675-686.

Moreno, M.M., Linster, C., Escanilla, O., Sacquet, J., Didier, A. & Mandairon, N. (2009) Olfactory perceptual learning requires adult neurogenesis. *Proc Natl Acad Sci U S A*, **106**, 17980-17985.

Mortensen, M., Patel, B. & Smart, T.G. (2011) GABA Potency at GABA(A) Receptors Found in Synaptic and Extrasynaptic Zones. *Front Cell Neurosci*, **6**, 1.

Mouret, A., Gheusi, G., Gabellec, M.M., de Chaumont, F., Olivo-Marin, J.C. & Lledo, P.M. (2008) Learning and survival of newly generated neurons: when time matters. *J Neurosci*, **28**, 11511-11516.

Mouret, A., Lepousez, G., Gras, J., Gabellec, M.M. & Lledo, P.M. (2009) Turnover of newborn olfactory bulb neurons optimizes olfaction. *J Neurosci*, **29**, 12302-12314.

Mugford, R.A. & Nowell, N.W. (1970) Pheromones and their effect on aggression in mice. *Nature*, **226**, 967-968.

Mullen, R.J., Buck, C.R. & Smith, A.M. (1992) NeuN, a neuronal specific nuclear protein in vertebrates. *Development*, **116**, 201-211.

Neville, K.R. & Haberly, L.B. (2003) Beta and gamma oscillations in the olfactory system of the urethane-anesthetized rat. *J Neurophysiol*, **90**, 3921-3930.

Nickell, W.T. & Shipley, M.T. (1988) Neurophysiology of magnocellular forebrain inputs to the olfactory bulb in the rat: frequency potentiation of field potentials and inhibition of output neurons. *J Neurosci*, **8**, 4492-4502.

Nissant, A. & Pallotto, M. (2011) Integration and maturation of newborn neurons in the adult olfactory bulb--from synapses to function. *Eur J Neurosci*, **33**, 1069-1077.

Norlin, E.M., Gussing, F. & Berghard, A. (2003) Vomeronasal phenotype and behavioral alterations in G alpha i2 mutant mice. *Curr Biol*, **13**, 1214-1219.

Nusser, Z., Kay, L.M., Laurent, G., Homanics, G.E. & Mody, I. (2001) Disruption of GABA(A) receptors on GABAergic interneurons leads to increased oscillatory power in the olfactory bulb network. *J Neurophysiol*, **86**, 2823-2833.

Oboti, L., Savalli, G., Giachino, C., De Marchis, S., Panzica, G.C., Fasolo, A. & Peretto, P. (2009) Integration and sensory experience-dependent survival of newly-generated neurons in the accessory olfactory bulb of female mice. *Eur J Neurosci*, **29**, 679-692.

Oliva, A.M., Salcedo, E., Hellier, J.L., Ly, X., Koka, K., Tollin, D.J. & Restrepo, D. (2010) Toward a mouse neuroethology in the laboratory environment. *PLoS One*, **5**, e11359.

Pallotto, M., Nissant, A., Fritschy, J.M., Rudolph, U., Sassoe-Pognetto, M., Panzanelli, P. & Lledo, P.M. (2012) Early formation of GABAergic synapses governs the development of adult-born neurons in the olfactory bulb. *J Neurosci*, **32**, 9103-9115.

Palmer, C.R. & Kristan, W.B., Jr. (2011) Contextual modulation of behavioral choice. *Curr Opin Neurobiol*, **21**, 520-526.

Pankevich, D.E., Baum, M.J. & Cherry, J.A. (2004) Olfactory sex discrimination persists, whereas the preference for urinary odorants from estrous females disappears in male mice after vomeronasal organ removal. *J Neurosci*, **24**, 9451-9457.

Panzanelli, P., Homanics, G.E., Ottersen, O.P., Fritschy, J.M. & Sassoe-Pognetto, M. (2004) Pre- and postsynaptic GABA receptors at reciprocal dendrodendritic synapses in the olfactory bulb. *Eur J Neurosci*, **20**, 2945-2952.

Panzanelli, P., Perazzini, A.Z., Fritschy, J.M. & Sassoe-Pognetto, M. (2005) Heterogeneity of gamma-aminobutyric acid type A receptors in mitral and tufted cells of the rat main olfactory bulb. *J Comp Neurol*, **484**, 121-131.

Paolini, A.G. & McKenzie, J.S. (1993) Effects of lesions in the horizontal diagonal band nucleus on olfactory habituation in the rat. *Neuroscience*, **57**, 717-724.

Paolini, A.G. & McKenzie, J.S. (1997) Effects of inactivation of the magnocellular preoptic nucleus of olfactory bulb processing. *Neuroreport*, **8**, 929-935.

Papes, F., Logan, D.W. & Stowers, L. (2010) The vomeronasal organ mediates interspecies defensive behaviors through detection of protein pheromone homologs. *Cell*, **141**, 692-703.

Peretto, P., Giachino, C., Panzica, G.C. & Fasolo, A. (2001) Sexually dimorphic neurogenesis is topographically matched with the anterior accessory olfactory bulb of the adult rat. *Cell Tissue Res*, **306**, 385-389.

Petreanu, L. & Alvarez-Buylla, A. (2002) Maturation and death of adult-born olfactory bulb granule neurons: role of olfaction. *J Neurosci*, **22**, 6106-6113.

Petreanu, L., Mao, T., Sternson, S.M. & Svoboda, K. (2009) The subcellular organization of neocortical excitatory connections. *Nature*, **457**, 1142-1145.

Pinato, G. & Midtgaard, J. (2003) Regulation of granule cell excitability by a low-threshold calcium spike in turtle olfactory bulb. *J Neurophysiol*, **90**, 3341-3351.

Pressler, R.T. & Strowbridge, B.W. (2006) Blanes cells mediate persistent feedforward inhibition onto granule cells in the olfactory bulb. *Neuron*, **49**, 889-904.

Raineki, C., Pickenhagen, A., Roth, T.L., Babstock, D.M., McLean, J.H., Harley, C.W., Lucion, A.B. & Sullivan, R.M. (2010) The neurobiology of infant maternal odor learning. *Braz J Med Biol Res*, **43**, 914-919.

Rajendren, G. & Dominic, C.J. (1985) Effect of transection of the vomeronasal nerve on the male-induced implantation failure (the Bruce effect) in mice. *Indian J Exp Biol*, **23**, 635-637.

Rajendren, G., Dudley, C.A. & Moss, R.L. (1990) Role of the vomeronasal organ in the male-induced enhancement of sexual receptivity in female rats. *Neuroendocrinology*, **52**, 368-372.

Rall, W. & Shepherd, G.M. (1968) Theoretical reconstruction of field potentials and dendrodendritic synaptic interactions in olfactory bulb. *J Neurophysiol*, **31**, 884-915.

Ravel, N., Chabaud, P., Martin, C., Gaveau, V., Hugues, E., Tallon-Baudry, C., Bertrand, O. & Gervais, R. (2003) Olfactory learning modifies the expression of odour-induced oscillatory responses in the gamma (60-90 Hz) and beta (15-40 Hz) bands in the rat olfactory bulb. *Eur J Neurosci*, **17**, 350-358.

Ressler, K.J., Sullivan, S.L. & Buck, L.B. (1994) Information coding in the olfactory system: evidence for a stereotyped and highly organized epitope map in the olfactory bulb. *Cell*, **79**, 1245-1255.

Rochefort, C., Gheusi, G., Vincent, J.D. & Lledo, P.M. (2002) Enriched odor exposure increases the number of newborn neurons in the adult olfactory bulb and improves odor memory. *J Neurosci*, **22**, 2679-2689.

Rodriguez-Alarcon, G., Canales, J.J. & Salvador, A. (2007) Rewarding effects of 3,4-methylenedioxymethamphetamine ("Ecstasy") in dominant and subordinate OF-1 mice in the place preference conditioning paradigm. *Prog Neuropsychopharmacol Biol Psychiatry*, **31**, 191-199.

Rodriguez, I., Feinstein, P. & Mombaerts, P. (1999) Variable patterns of axonal projections of sensory neurons in the mouse vomeronasal system. *Cell*, **97**, 199-208.

Sahara, Y., Kubota, T. & Ichikawa, M. (2001) Cellular localization of metabotropic glutamate receptors mGluR1, 2/3, 5 and 7 in the main and accessory olfactory bulb of the rat. *Neurosci Lett*, **312**, 59-62.

Sasaki, K., Suzuki, M., Mieda, M., Tsujino, N., Roth, B. & Sakurai, T. (2011) Pharmacogenetic modulation of orexin neurons alters sleep/wakefulness states in mice. *PLoS One*, **6**, e20360.

Sassoe-Pognetto, M. (2011) Molecular and functional heterogeneity of neural circuits: an example from the olfactory bulb. *Brain Res Rev*, **66**, 35-42.

Schoppa, N.E., Kinzie, J.M., Sahara, Y., Segerson, T.P. & Westbrook, G.L. (1998) Dendrodendritic inhibition in the olfactory bulb is driven by NMDA receptors. *J Neurosci*, **18**, 6790-6802.

Schoppa, N.E. & Urban, N.N. (2003) Dendritic processing within olfactory bulb circuits. *Trends Neurosci*, **26**, 501-506.

Segovia, S., Garcia-Falgueras, A., Carrillo, B., Collado, P., Pinos, H., Perez-Laso, C., Vinader-Caerols, C., Beyer, C. & Guillamon, A. (2006) Sexual dimorphism in the vomeronasal system of the rabbit. *Brain Res*, **1102**, 52-62.

Segovia, S., Guillamon, A., del Cerro, M.C., Ortega, E., Perez-Laso, C., Rodriguez-Zafra, M. & Beyer, C. (1999) The development of brain sex differences: a multisignaling process. *Behav Brain Res*, **105**, 69-80.

Shepherd, G.M. (1972) Synaptic organization of the mammalian olfactory bulb. *Physiol Rev*, **52**, 864-917.

Shepherd, G.M., Chen, W.R., Willhite, D., Migliore, M. & Greer, C.A. (2007) The olfactory granule cell: from classical enigma to central role in olfactory processing. *Brain Res Rev*, **55**, 373-382.

Shingo, T., Gregg, C., Enwere, E., Fujikawa, H., Hassam, R., Geary, C., Cross, J.C. & Weiss, S. (2003) Pregnancy-stimulated neurogenesis in the adult female forebrain mediated by prolactin. *Science*, **299**, 117-120.

Smith, M.T., Pencea, V., Wang, Z., Luskin, M.B. & Insel, T.R. (2001) Increased number of BrdU-labeled neurons in the rostral migratory stream of the estrous prairie vole. *Horm Behav*, **39**, 11-21.

Smith, R.S. & Araneda, R.C. (2010) Cholinergic modulation of neuronal excitability in the accessory olfactory bulb. *J Neurophysiol*, **104**, 2963-2974.

Smith, R.S., Weitz, C.J. & Araneda, R.C. (2009) Excitatory actions of noradrenaline and metabotropic glutamate receptor activation in granule cells of the accessory olfactory bulb. *J Neurophysiol*, **102**, 1103-1114.

Sotty, F., Danik, M., Manseau, F., Laplante, F., Quirion, R. & Williams, S. (2003) Distinct electrophysiological properties of glutamatergic, cholinergic and GABAergic rat septohippocampal neurons: novel implications for hippocampal rhythmicity. *J Physiol*, **551**, 927-943.

Spehr, M., Spehr, J., Ukhanov, K., Kelliher, K.R., Leinders-Zufall, T. & Zufall, F. (2006) Parallel processing of social signals by the mammalian main and accessory olfactory systems. *Cell Mol Life Sci*, **63**, 1476-1484.

Stowers, L., Holy, T.E., Meister, M., Dulac, C. & Koentges, G. (2002) Loss of sex discrimination and male-male aggression in mice deficient for TRP2. *Science*, **295**, 1493-1500.

Su, C.Y., Menuz, K. & Carlson, J.R. (2009) Olfactory perception: receptors, cells, and circuits. *Cell*, **139**, 45-59.

Suarez, R. & Mpodozis, J. (2009) Heterogeneities of size and sexual dimorphism between the subdomains of the lateral-innervated accessory olfactory bulb (AOB) of Octodon degus (Rodentia: Hystricognathi). *Behav Brain Res*, **198**, 306-312.

Sugai, T., Yoshimura, H., Kato, N. & Onoda, N. (2006) Component-dependent urine responses in the rat accessory olfactory bulb. *Neuroreport*, **17**, 1663-1667.

Sullivan, R.M. (2001) Unique Characteristics of Neonatal Classical Conditioning: The Role of the Amygdala and Locus Coeruleus. *Integr Physiol Behav Sci*, **36**, 293-307.

Takami, S. & Graziadei, P.P. (1990) Morphological complexity of the glomerulus in the rat accessory olfactory bulb--a Golgi study. *Brain Res*, **510**, 339-342.

Thompson, R.N., Napier, A. & Wekesa, K.S. (2007) Chemosensory cues from the lacrimal and preputial glands stimulate production of IP3 in the vomeronasal organ and aggression in male mice. *Physiol Behav*, **90**, 797-802.

Tirindelli, R., Dibattista, M., Pifferi, S. & Menini, A. (2009) From pheromones to behavior. *Physiol Rev*, **89**, 921-956.

Vandenbergh, J.G. (1973) Acceleration and inhibition of puberty in female mice by pheromones. *J Reprod Fertil Suppl*, **19**, 411-419.

Vandenbergh, J.G. (1975) Proceedings: Pheromonal stimulation of puberty in female mice. *J Endocrinol*, **64**, 38P.

Veyrac, A., Sacquet, J., Nguyen, V., Marien, M., Jourdan, F. & Didier, A. (2009) Novelty determines the effects of olfactory enrichment on memory and neurogenesis through noradrenergic mechanisms. *Neuropsychopharmacology*, **34**, 786-795.

Wagner, S., Gresser, A.L., Torello, A.T. & Dulac, C. (2006) A multireceptor genetic approach uncovers an ordered integration of VNO sensory inputs in the accessory olfactory bulb. *Neuron*, **50**, 697-709.

Wang, J. & Swann, J.M. (2006) The magnocellular medial preoptic nucleus I. Sources of afferent input. *Neuroscience*, **141**, 1437-1456.

Wang, Z., Balet Sindreu, C., Li, V., Nudelman, A., Chan, G.C. & Storm, D.R. (2006) Pheromone detection in male mice depends on signaling through the type 3 adenylyl cyclase in the main olfactory epithelium. *J Neurosci*, **26**, 7375-7379.

Whitten, W.K. (1959) Occurrence of anoestrus in mice caged in groups. *J Endocrinol*, **18**, 102-107.

Xu, F., Schaefer, M., Kida, I., Schafer, J., Liu, N., Rothman, D.L., Hyder, F., Restrepo, D. & Shepherd, G.M. (2005) Simultaneous activation of mouse main and accessory olfactory bulbs by odors or pheromones. *J Comp Neurol*, **489**, 491-500.

Yamaguchi, T., Inamura, K. & Kashiwayanagi, M. (2000) Increases in Fos-immunoreactivity after exposure to a combination of two male urinary components in the accessory olfactory bulb of the female rat. *Brain Res*, **876**, 211-214.

Yang, M. & Crawley, J.N. (2009) Simple behavioral assessment of mouse olfaction. *Curr Protoc Neurosci*, **Chapter 8**, Unit 8 24.

Yap, J.J., Takase, L.F., Kochman, L.J., Fornal, C.A., Miczek, K.A. & Jacobs, B.L. (2006) Repeated brief social defeat episodes in mice: effects on cell proliferation in the dentate gyrus. *Behav Brain Res*, **172**, 344-350.

Yizhar, O., Fenno, L.E., Prigge, M., Schneider, F., Davidson, T.J., O'Shea, D.J., Sohal, V.S., Goshen, I., Finkelstein, J., Paz, J.T., Stehfest, K., Fudim, R., Ramakrishnan, C., Huguenard, J.R., Hegemann, P. & Deisseroth, K. (2011) Neocortical excitation/inhibition balance in information processing and social dysfunction. *Nature*, **477**, 171-178.

Yokoi, M., Mori, K. & Nakanishi, S. (1995) Refinement of odor molecule tuning by dendrodendritic synaptic inhibition in the olfactory bulb. *Proc Natl Acad Sci U S A*, **92**, 3371-3375.

Yoshikage, M., Toshiaki, I., Seiichi, K., Nobuo, K. & Nishimura, M. (2007) Sex steroids modulate the signals from volatile female odors in the accessory olfactory bulb of male mice. *Neurosci Lett*, **413**, 11-15.

Zaborszky, L., Carlsen, J., Brashear, H.R. & Heimer, L. (1986) Cholinergic and GABAergic afferents to the olfactory bulb in the rat with special emphasis on the

projection neurons in the nucleus of the horizontal limb of the diagonal band. *J Comp Neurol*, **243**, 488-509.

Zhang, H., Lin, S.C. & Nicolelis, M.A. (2010) Spatiotemporal coupling between hippocampal acetylcholine release and theta oscillations in vivo. *J Neurosci*, **30**, 13431-13440.

Zhao, C., Deng, W. & Gage, F.H. (2008) Mechanisms and functional implications of adult neurogenesis. *Cell*, **132**, 645-660.

Zimnik, N.C., Treadway, T., Smith, R.S. & Araneda, R.C. (2013) 1A-Adrenergic regulation of inhibition in the olfactory bulb. *J Physiol*, **591**, 1631-1643.